Role of miR-1305 in Regulating Pluripotency, Cell Cycle and Apoptosis in Human Embryonic Stem Cells

Shibo Jin

Bachelor of Medicine

Thesis submitted to Newcastle University in candidature for the Degree of Doctor of Philosophy

2015

ABSTRACT

Human embryonic stem cells and human induced pluripotent stem cells are defined as pluripotent in view of their ability to maintain self-renewal and differentiation to cells of all three germ layers. So far the mechanism underlying the cell cycle regulation, self-renewal and pluripotency of human pluripotent stem cells are not fully understood. In this study, we first screened for candidate miRNAs which might play important roles in regulating pluripotency and cell cycle by using a microarray based approach. miR-1305 was chosen as a target, as its expression profile changed during human embryonic stem cell differentiation and cell cycle. We also revealed the role of miR-1305 in regulating differentiation in human embryonic stem cells as well as cell cycle and apoptosis in human embryonic and induced pluripotent stem cells. Our results provide evidence that overexpression of miR-1305 induces significant human embryonic stem cell differentiation and downregulation of miR-1305 maintains human embryonic stem cell pluripotency. Furthermore, *POLR3G* was identified as a downstream target by which miR-1305 regulates human embryonic stem cell differentiation. Together our data corroborate previous findings indicating an intrinsic link between miRNA and maintenance of pluripotency in human embryonic stem cells.

ACKNOWLEDGMENT

First and foremost, I would like to express my special appreciation and thanks to my supervisors, Professor Majlinda Lako, Dr. Irina Neganova and Professor Lyle Armstrong for giving me this opportunity to undertake this PhD project. I am appreciating for the time they spent on this project and their kindness guidance and support, their priceless advices on this project and many insightful discussions over the past four years. It was a great honour for me to join in this group. I also would like to thanks Linda and Irina for understanding and helping to complete this thesis, and go through my drafts again and again. I am grateful for all our discussions and the helpful feedbacks on the drafts of this thesis.

I also want to thank all the colleagues in Stem cell group for their kindness help and friendship. The group has been a source of good advice and collaboration. I would like to thanks Dr. Joseph Collin and Dr. Irina Neganova for providing me the initial microarray data and their support and teaching on my lab work, also Dr. Yan Jiang help me a lot with PCR experiment . Also to Dr. David Montaner for helping us analyses the microarray data and Dr. Carmen Martin-Ruiz helping me on real-time PCR and Dr. Maria Ledran for help me read the thesis and offered important advices. Many thanks to Ian Dimmick, for his help on all the flow cytometry experiment.

I would also like to take this opportunity to thank Professor Hanns Lochmüller and Professor Ioakim Spyridopoulos for their valuable advices on my PhD project.

A special thanks to my family and friends. Words cannot express how grateful I am for their support in all these year. At the end I would like express appreciation to my beloved wife Lili, for your support and understanding on my PhD study and my life. These past several years have not been an easy ride, especially the last few months during my thesis writing, but you always sticking by my side. I can't finish my study without you. You love me like no one else has and has changed me for the better. Thank you with all my heart and soul.

TABLE OF CONTENTS

LIST OF FIGURES

LIST OF TABLES

ABBREVIATIONS

Abbreviation	Full nomenclature
°C	Degress centigrade
µg	Microgram
2i	dual inhibition
3'UTR	Three prime untranslated regions
5'UTR	Five prime untranslated regions
Ago2	Argonaute
APC	Axin/adenomatous polyposis coli
ATM	Ataxia-telangiectasia mutated
ATR	ATM and Rad 3-related
bFGF	Basic fibroblast growth factor
BIO	6-bromoindirubin-3'-oxime
BMPs	Bone morphogenetic proteins
CAK	Cyclin activating kinase
Cdk	Cyclin-dependent kinase
cip/kip	CDK interacting protein/Kinase inhibitory protein
cm^2	Square centimetre
c-Myc	v-myc avian myelocytomatosis viral oncogene homolog
CO_2	Carbon dioxide
EB	Embryoid body
ECM	Extracellular matrix
EMT	epithelial-to-mesenchymal transition

ERK1/2	Extracellular signal-regulated protein kinases ½
ESCC miRNAs	Embryonic Stem cell specific Cell Cycle regulating miRNAs
FBS	Fetal Bovine Serum
GDFs	Growth differentiation factors
GSK3β	Glycogen synthase kinase 3 beta
hES cell	Human embryonic stem cell
hiPS cell	Human induced pluripotent stem cell
ICM	Inner cell mass
IGFs	Insulin like growth factors
INK4	Inhibitor of Kinase 4
iPS cell	induced pluripotent stem cell
KLF4	Kruppel-like factor 4
KO-SR	knock Out-Serum Replacement
LIF	Leukemia inhibitory factor
M phase	Mitosis phase
MDM2	Mouse double minute 2 homolog
MEF	Mouse embryonic fibroblast
miRNAs	MicroRNAs
ml	Millilitre
mol	Mole
NEAA	Non-Essential Amino Acids
Oct-3/4	POU class 5 homeobox 1
PBS	Phosphate Buffered Saline
PDGF	Platelet derived growth factor

PDLSC	periodontal ligament-derived stem cell
PH	Pleckstrin –homology
PI3K	Phosphoinositide-3-kinase
PIKK	Phosphatidylinositol 3-kinase-related kinase
POLR3G	Polymerase (RNA) III (DNA directed) polypeptide G (32kD)
Rb	Retinoblastoma
RISC	RNA-induced silencing complex
RTKs	Receptor tyrosine kinases
RT-PCR	Reverse transcription polymerase chain reaction
S phase	Synthesis phase
S1P	Sphinigosine-1-phsphate
SDS 2.4	Sequence Detection System 2.4
Sox2	SRY (sex determining region Y)-box 2
TCF/LEF	T cell fator/lymphoid enhancer
TGF-β	Transforming growth factor-β
PGD	preimplantation genetic diagnosis
HD	Huntington's disease
ALS	amyotrophic lateral sclerosis
RPE	retina pigment epithelium
RCS	Royal College of Surgeons
SDS	Sodium dodecyl sulfate
Na-doc	Na-deoxycholate

DECLARATION

This thesis is submitted to the degree of Doctor of Philosophy in University of Newcastle upon Tyne. The research detailed within was performed in the Stem Cell Group laboratories under the supervision of Professor Majlinda Lako, Dr. Irina Neganova and Professor Lyle Armstrong between September 2011 and September 2015 and in my own work unless otherwise stated.

I certify that no part of the material offered in this thesis has previously been submitted by me for a degree in this or any other University.

This copy has been supplied in the understanding that it is copyright material and that no quotation form the thesis may be made without proper acknowledgement.

Shibo Jin

CHAPTER 1 INTRODUCTION

Chapter 1. Introduction

1.1 Human Pluripotent Stem Cells

1.1.1 Human Embryonic Stem Cells

Human embryonic stem cells (hES cells), which are derived from the inner cell mass (ICM) of early preimplantation human embryos, have two unique properties: unlimited self-renewal (ability to divide symmetrically to generate many undifferentiated cells under proper culture condition) and pluripotency (potential to give rise to any cell type of the adult organism) (Figure 1) [1,2].
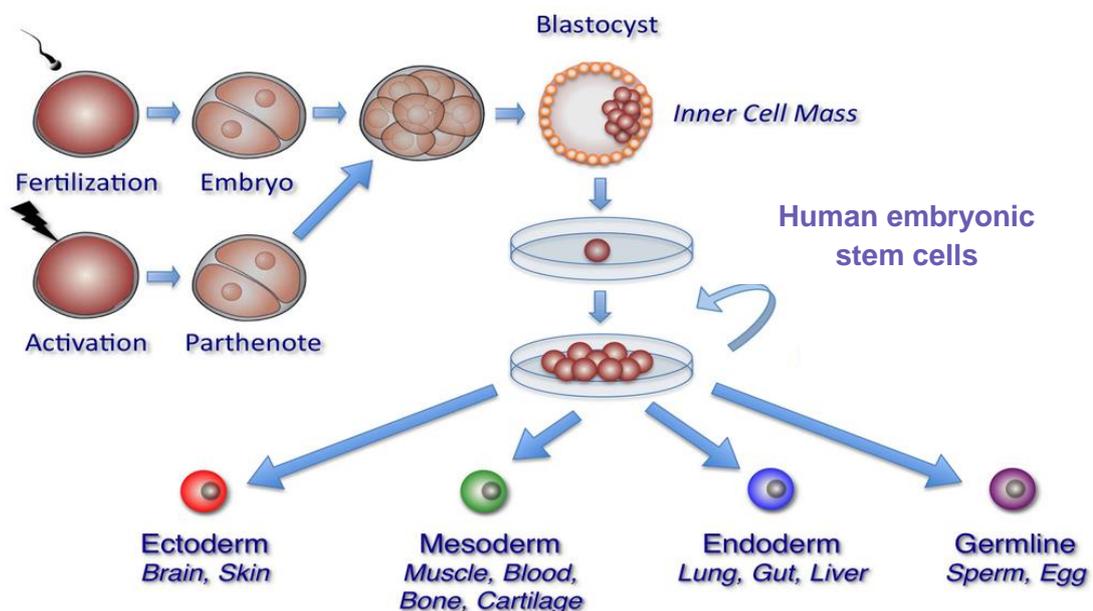
Figure 1. Generation of hES cell lines.

hES cells are derived from the inner cell mass (ICM) of early preimplantation human embryos. They can maintain self-renewal and generate all cell types from all three embryonic germ layers and the germline (Adapted from Yabut O et al, 2011) [3].

The first hES cell lines was derived in 1998 by James A. Thomson at University of Wisconsin [4]. Thereafter, many hES cell lines have been produced and characterized in a number of independent laboratories [5-7]. In culture, hES cells grow in colonies; the cells have a high nuclear/cytoplasm ratio and expression of pluripotency markers, such as *OCT4* (*POU4F1*), *NANOG, SOX2, LIN28* and *POLR3G* (Polymerase (RNA) III (DNA directed) polypeptide G (32kD)) et al [8-10]. The undifferentiated state of hES cells could

be maintained by culturing hES cells on feeder cells (mouse embryonic fibroblast cells (MEF), human feeder cells) with hES media which contains bFGF, or on extracellular matrix (ECM, like matrigel or vitronectin) in medium which contains both bFGF and TGFβ1 (Figure 2).
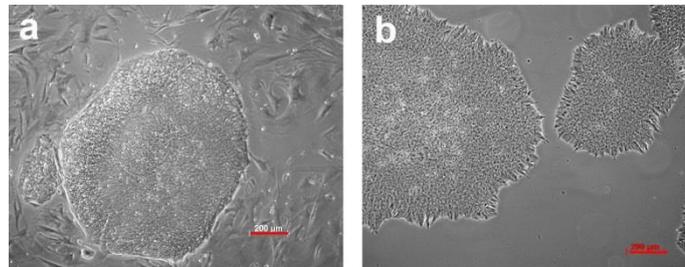
Figure 2. The morphology of hES cells cultured under (a) MEF or (b) feeder free condition.

There are two discrete pluripotent states recently termed as *naïve* and *primed* [11]. Naïve pluripotent stem cells, represented by ICM-derived mouse ES cells [12], can efficiently contribute to chimeric embryos, maintain both X chromosomes in an active state in female cells, can be cloned with high efficiency, grow as packed dome colonies and require the growth factor LIF and 2i (dual inhibition of extracellular signal-regulated protein kinases ½ (ERK1/2) and glycogen synthase kinase 3 beta (GSK3β)) to maintain pluripotency [13-15]. Primed pluripotent stem cells (such as mouse epiblast stem cells), are derived from the post-implantation epiblast of embryos. The ICM of an embryo will develop into hypoblast and epiblast. Hypoblast cells will develop into primitive endoderm, while the epiblast cells are progenitors of definitive endoderm, mesoderm and ectoderm. The epiblast stem cells are pluripotent and can give rise to differentiated teratomaes, and are highly inefficient in repopulating the ICM upon aggregation or injection into host blastocysts [16-18]. These are characterized by a flattened morphology, intolerance to passaging as single cells, and dependent on bFGF and TGFβ/ Activin signalling [16-18]. Although not identical, hES cells share several defining features with primed mouse epiblast stem cells, such as a flattened morphology, intolerance to passaging as single cells, dependence on bFGF and TGFβ/ Activin signalling [4,19-21].

There are many similarities and differences between mouse and human ES cells. They are both pluripotent stem cells, which can maintain unlimited self-renewal and

pluripotency. Both mouse and human ES cells express pluripotent markers Oct4, Sox2, and Nanog, as the foundation of mammalian pluripotency [22]. Mouse ES cells are positive for SSEA-1 while negative for SSEA-3, SSEA-4. However hES cells express SSEA-3 and SSEA-4 but not SSEA-1 [23].

Leukaemia inhibitory factor (LIF) and bone morphogenetic protein (BMP) are required for efficient maintenance of mES cells in culture [14]. In contrast, LIF is insufficient to inhibit the differentiation of hES cells, instead FGF and TGF-β pathways are central mediators in the maintenance of undifferentiated hESCs [24].

Both mouse and human ES cells have short cell cycle compared with their differentiation counterparts, but the cell cycle of hES cells is longer than mouse ES cells. Unlike mouse ES cells, hES cells exists both G1/S and G2/M checkpoint [25,26]. In mouse ES cells, the G1/S transition of cell cycle is mainly regulated by miR-290-295 cluster and four members of the miR-302 cluster, while hES cells, cell cycle is regulated by miR-302/372 cluster, miR-195 and miR-92b [27].

Property	Ground State	Primed State
Embryonic tissue	early epiblast	egg cylinder or embryonic disc
Culture stem cell	rodent ESCs	rodent EpiSCs; primate "ESCs"
Blastocyst chimaeras	yes	no[a]
Teratomas	yes	yes
Differentiation bias	none	variable
Pluripotency factors	Oct4, Nanog, Sox2, Klf2, Klf4	Oct4, Sox2, Nanog
Naive markers[b]	Rex1, NrOb1, Fgf4	absent
Response to Lif/Stat3	self-renewal	none
Response to Fgf/Erk	differentiation	self-renewal
Clonogenicity	high	low
XX status	XaXa	XaXi
Response to 2i	self-renewal	differentiation/death

[a]   Not applied to primate cells.

[b]   Representative examples.

Table 1. Comparison of Naïve and Primed Pluripotent States.
(Adapted from Nicholes et al. 2009) [11].

The conversion of hES cells to a naïve state is desirable as their features should facilitate techniques such as gene editing and more efficient differentiation. Several groups have tried to derive the naïve state hES cells by transgene expression [28-32] or the use of media containing small molecular and growth factors [33-41]. Maintenance of these ground state cells is possible using a combination of bFGF and LIF, together with 2i [33-41]. There remain many challenges in generating naïve pluripotency, for all protocol yield slightly different cellular states. It is still unclear which state is closest to its *in vivo* counterpart. Clearly additional research on regulation of hES cell pluripotency is needed for better understanding of the true naïve state.

1.1.2 Human Induced Pluripotent Stem Cells

By screening 24 pluripotency factors, in 2006, Takahashi and Yamanaka identified a small number of key factors (*Oct-3/4, Sox2, c-Myc*, and *Klf4*) that can cause adult skin fibroblasts to reprogram to a pluripotent state akin to embryonic stem cells[42,43]. These reprogrammed cells are called induced pluripotent stem cells (iPS cells). The iPS cells also have unlimited self-renewal and pluripotency [44](Figure 3). This study opened a completely new area in this field. It is now possible to reprogram differentiated somatic

cells into pluripotent cells that have the capacity to generate all the cell type of adult tissues [45]. The iPS technology has the potential to ease the controversy and ethical dilemmas associated with hES cells and to effectively bypass the problem of immune rejection[46].
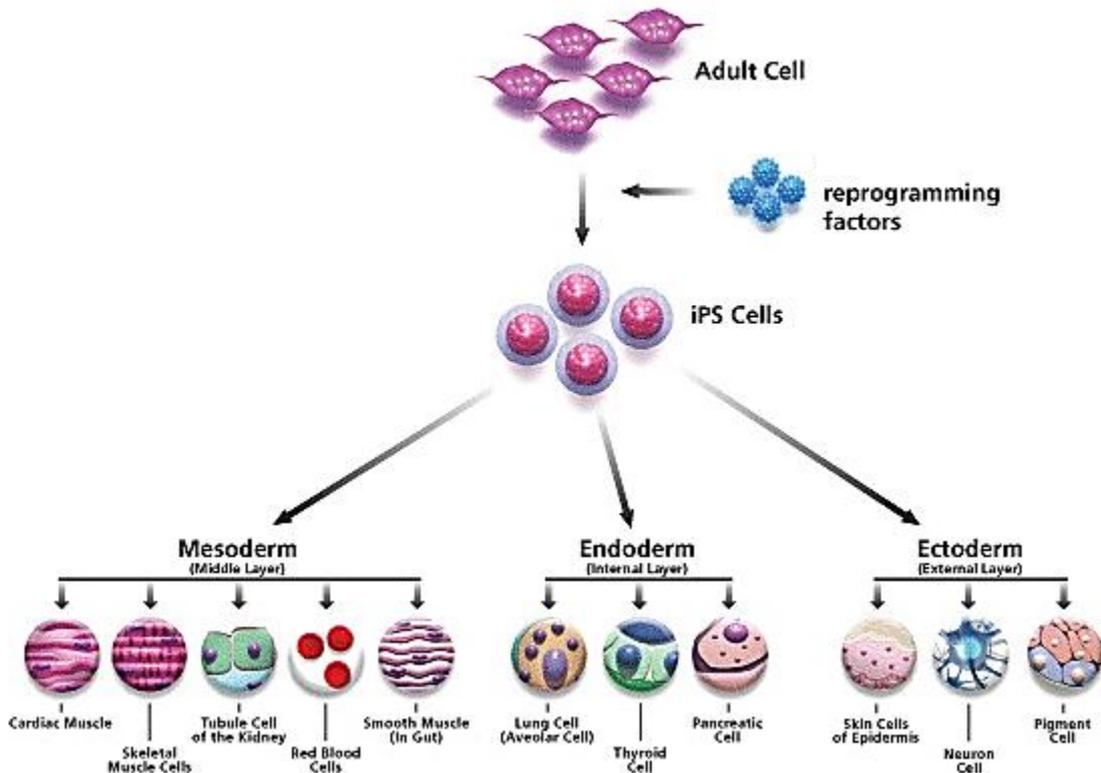
Figure 3. Induced Pluripotent Stem (iPS) Cells.

Adult cell could be reprogrammed to the pluripotent state by reprogramming factors. The iPS cells also have unlimited self-renewal and pluripotency (Adapted from http://liveaction.org/blog/stem-cell-research-the-basics-types-of-research-medical-status-and-ethical-drawbacks/).

Thereafter, many other somatic cell types including blood, keratinocytes were reprogrammed into iPS cells by forcing expression of different combination of genes or treating with chemicals [47-50]. The early delivery methods used for reprogramming were integrating methods (retrovirus, lentivirus, or non-virus based transposons), which have the risk of tumour formation [45]. Later the researchers developed integration-free strategies by employing adenovirus, Sendai virus, plasmids, mRNA, miRNA, and the protein-based protocols [51-56]. Among all these non-integration methods, synthetic mRNA-based protocols have maximum efficiency over the original retrovirus-mediated system for delivering reprogramming factors [54]. But the stability of RNA and the induction of innate antiviral defence pathways remain a barrier to their further clinical

use [54]. For better clinical prospects, small molecules alone have been successfully employed in the generation of iPS cells, which represents significant progress in cell reprogramming technology [50]. Currently available reprogramming protocols with their induction efficiency and time frame advantages and disadvantages are summarized in Table 2.

	Methods	Cell Type	Efficiency (%)	Advantages	Disadvantages
Integrating	Retrovirus	Fibroblasts, neural stem cells, stomach cells, liver cells, keratinocytes, amniotic cells, blood cells and adipose cells	~0.001-0.1	Reasonable efficient	Genomic intergration, incomplete provirus silencing
	Lentivirus	Fibroblasts and keratinocytes	~0.001-0.1	Reasonable efficient	Genomic intergration, incomplete provirus silencing
	Transposon	Fibroblasts	~0.01	Reasonable efficient	Labour-intensive screening of excised lines
Non-integrating	Adenovirus	Fibroblasts and liver cells	~0.0001	No genomic integration	Low efficiency
	Sendai virus	CB cells and fibroblasts	~0.001	No genomic integration	Difficulty in purging cells of replicating virus
	Protein	Fibroblasts	~0.001	No genomic integration, no DNA-related complications	Short half-life, and requirement for large quantities of proteins muliple application
	mRNA	Fibroblasts	~1	No genomic integration, high efficiency	Multiple rounds of transfection
	miRNA	Stromal cells and dermal fibroblasts	~0.02-1	No genomic integration, efficient	possiblity of subfragments
	Episomal Plasmids	Fibroblasts	~0.01-1	only occasional genomic integration	Occasionla genomic integration
Combined factors with Chemicals	OSKM+PD0325901 + CHIR99021	Neural stem cells	0.11	Increase the efficiency	The presense of retrovirus
	O+NaB+ PS48+ A-83-01+PD0325901	Keratinocytes	0.00004		
	O+A-83-01+AMI-5	Fibroblasts	0.02		
	OS+ VPA	Fibroblasts	0.5		
Chemical alone		Fibrolabsts	0.2	No DNA/RNA related complications	Not determined

CB, core blood; O, OCT4; S, SOX2; K, KLF4; M, C-MYC; VPA, valproic acid.

Table 2. Methods for reprogramming somatic cells to iPS cells [50-64].

Both hES cells and human induced pluripotent stem (hiPS) cells share the important properties of self-renewal and pluripotency, however accumulating reports suggest the difference of transcriptome [65,66], histone code differences [67], DNA methylation [68] and variation of differentiation propensity [69,70] between hES cells and hiPS cells. These studies have led to many questions of the equivalence of these two promising cell types.

Although global gene expression profiles of hES cells and hiPS cells are largely similar, subtle differences in the expression of mRNAs and miRNAs have been reported [67,71,72].

The researchers applied genome-wide methods to compare hES cells with hiPS cells by array CGH (uncover subkaryotypic genome alterations); coding RNA profiling (uncover gene expression changes); miRNA profiling (to determine changes in miRNAs) and histone modification profiling (epigenetic changes). These analyses found gene expression that is different from hES cells and shared among hiPS cells generated in different reprogramming experiments, indicating that hiPS cells should be considered a unique subtype of pluripotent cell [72].

The DNA methylation patterns in hiPS cells are not identical with hES cells. Some of the differences appear to be related to the origin of somatic cells as an epigenetic memory [73,74]. Notably, continuous passaging [75] or chromatin modifying drug treatments [74] could abrogate the epigenetic memory induced transcriptional differences in murine iPS cells, indicating the epigenetic memory may affect the differentiation propensity only transiently. In one recent work, researchers have identified a panel of 82 CpG methylation sites that can distinguish hiPS cells from hES cells with high accuracy by comparing a large number of hES cells (n=155) and hiPS cells (n=114) generated in different lab from different somatic cells by various methods [76].

Despite similarities between hES cells and hiPS cells at general features of self-renewal and pluripotency, reports of variability in the *in vitro* differentiation potential of hiPS cells with respect to hES cells have frustrated investigator in this field. For instance, a reduced and more variable yield of neural and cardiovascular cells has been observed in hiPS cells [69,70]. In addition, hiPS cell derived early blood progenitor and endothelial cells appear to undergo premature senescence [77]. What underlies these differences in yield of useful differentiated cell types is still far from clear.

1.1.3 Application of hES Cells and hiPS Cells

hES cells and hiPS cells share the important properties of self-renewal and pluripotency; that is, they are theoretically capable of generating unlimited amounts of any differentiated cell in the human body. These unique features have made hES cells and hiPS cells extremely important in basic and applied research. They may serve as attractive tools for human early development research, disease modelling, drug screening and cell replacement.

Research into human embryonic development

The early human development process is still unclear due to limited sources of human embryos and ethical issues. Apart from the very early preimplantation stage, human embryos are inaccessible for research. One approach to overcome this obstacle is to use animal models. But despite the similarity between human and mouse, there are still major differences between species in size, growth and anatomy [78]. While hES cells can recapitulate embryogenesis by expression developmentally regulated genes and by activating molecular pathways as they occur *in vivo*. Moreover they could be used to study the function of specific gene on particular developmental events, such as cell lineage commitment and differentiation.

Under suspension condition, hES cells tend to aggregate, forming a special structure termed EBs (embryoid bodies). EBs are dynamic structures that undergo extensive changes. While the EBs grow, differentiation take places, resulting in the production of many different cell types including cells from all three germ layers [79]. There are some evidences show that the development of EB correlate with embryogenesis. One such example is the study of the Nodal signalling pathway, which plays a major role in the determination of embryonic axes (right-left, dorsal-ventral, and anterior-posterior) as well as in mesoderm induction during early gastrulation. By comparing the expression of NODAL and its targets LEFTYA, LEFTYB, PITX2, between early, mid- and fully matured hES generated EBs, a transient expression pattern was observed. All four genes are expressed at different time points during differentiation, in keeping with the conserved pathway as it occurs in the embryo [79].

Disease modelling, Drug Screening

Another potential use of hES cells and hiPS cells is for disease modelling and drug screening.

There are different approaches for adopting hES cells in models of genetic diseases.

1) Screening hES cells from embryos using preimplantation genetic diagnosis (PGD). PGD is mainly used to screen embryos from patients with and carriers of diseases that are caused by highly penetrant and well-characterized genetic mutations. Embryos carrying these mutations can be used to derive hES cells, and the ensuing phenotypes following differentiation are assumed to be similar to those of the affected family members. This approach has been successfully used to derive hES cells and model disorders such as Huntington's disease (HD) [80,81].

HD is characterized by the degeneration of striatal projection neurons and is caused by an expansion of CAG repeats in the *huntingtin* (*HTT*) gene that is inherited an autosomal dominant manner. hES cells were derived from embryos diagnosed with mutant *HTT*, and forebrain neurons differentiated from these mutant hES cells showed greater glutamate sensitivity than healthy controls [81]. This is the first time that such an early development event was experimentally assessable for HD and it enables the dissection of disease mechanisms.

The derivation of hES cells from PGD embryos has been reported for a range of additional diseases, including FXS [80], Patau, Down, Triple X and Turner syndromes [82], as well as cystic fibrosis [83]. However, only a few diseases are caused by mutations that can be diagnosed by PGD. Disease without a known genetic cause cannot be obtained in this way. Furthermore, the derivation of such cells relies on access to embryos and on parental consent for embryo donation.

2) Co-culturing differentiated cells derived from hES cells with pathogenic primary cells. This is another approach to use hES cells for disease modelling. For example, for modelling amyotrophic lateral sclerosis (ALS), in which astrocytes are implicated in causing motor neuron death, several research groups have generated hES cell-derived motor neurons that had been co-cultured with primary astrocytes with mutant SOD1, which causes ALS [84,85]. These motor neurons were found more susceptible to degeneration [84,85]. This model was used to assess compounds with neuroprotective

effects. MK0524, Apocynin and PTGDR2 were identified as putative therapeutic agents for ALS [79].

3) Another method involves using gene editing to introduce disease–causing mutations into hES cells from healthy donors. Recent advances in genome engineering with zinc finger nucleases (ZFNs) [86], transcription activator like effector nucleases (TALENs) [87,], and CRISPR/Cas systems [88,89] which can modify the genome with precision will potentially allow the modification of hES cell genomes more rountinely. One study recently provided proof of generating mutations in 15 different genes what are linked to multiple disorders, including dyslipidemia, insulin resistance, hypoglycaemia, lipodystrophy, motor neuron death, which was sufficient to induce disease –associated phenotypes [87].

One promising potential of reprogramming is the ability of generation patient specific iPS cells. These disease-specific iPS cells can then be differentiated into specific cell types. This is very helpful to study the initiation and progression of disease, and to study how therapeutic interventions would affect the disease cells. Recently, hiPS cells have been applied to study cardiac disease (e.g. long QT syndrome), neurodegenerative disease (e.g. Alzheimer disease), and other disorders [90-94]. This application is especially useful for some diseases that were extremely difficult to generate animal models. hiPS cells can represent the corresponding disease and allow identification of drug targets and understanding of effects of treatment (Figure 4).

Recently, Lee and colleagues successfully derived hiPS cells from patient with familial dysautonomia, a rare genetic disorder of the peripheral nervous system [95]. Investigators produced central and peripheral neural precursors and subsequently found three disease-related phenotypes, thus providing evidence that disease-related cell types could reflect disease pathogenesis *in vitro*. After screening with multiple compounds, they showed that the disease phenotype could be partially normalized by a plant hormone-kinetin [95]. This study demonstrated how iPS cells can model the disease and facilitate the discovery of drug. This platform could use to generate predictive tests to determine differences in the clinical manifestation of the disorder (Figure 4).
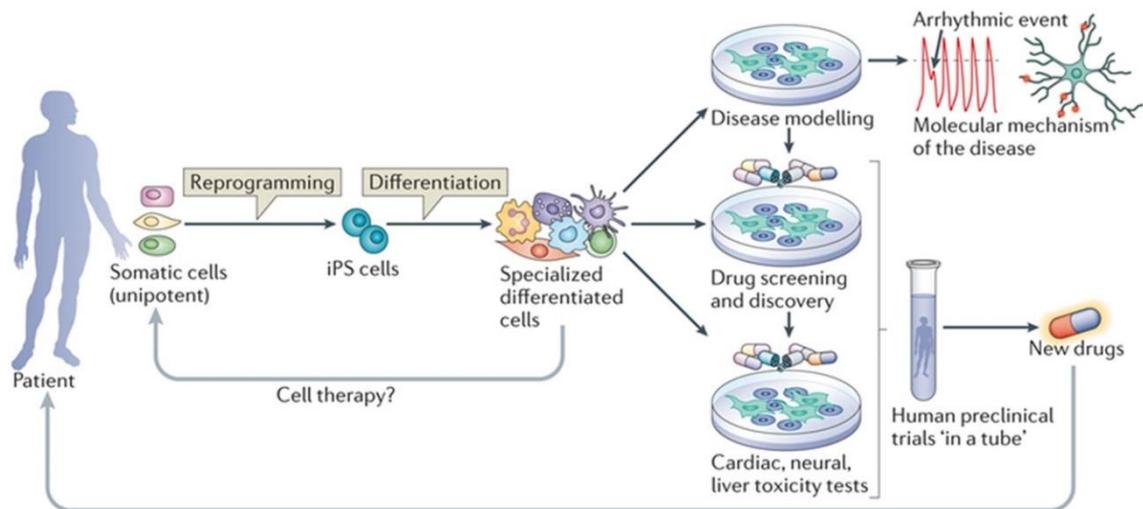
Figure 4 . hiPS cells derivation, differentiation and application.

Patient somatic cells can be reprogrammed into iPS cells. After inducing differentiation in vitro, hiPS cells can be used in disease modelling, drug screening and discovery and testing cellular toxic responses (Adapted from Milena Bellin et al, 2012) [90].

Cell Replacement

The most important potential of hES and hiPS cells is they could be used clinically to develop replacement cells for transplantation medicine for diseases caused by loss of cell function or loss of one or several types of cells, like Parkinson's disease, stroke, diabetes, heart failures [96-98].

hES cells can be maintained indefinitely under defined conditions and when required , can be differentiated into all types of cells, such as retina pigment epithelium (RPE) cells [99]. Using hES cell-derived RPE, Lu and colleagues have demonstrated photoreceptor rescue in the Royal College of Surgeons (RCS) rats [100]. The first use of hES cell-derived RPE cells in human patients was described by Schwartz group, in one patient with Stargardt's macular dystrophy and another with dry AMD. Initial results show no significant improvement in visual function (Because of the loss of photoreceptor cells is at an advanced stage, the likelihood of recovery of vision in this population is low), but do suggest a good safety profile [101]. A number of clinical trials investigating the safety of ESC-RPE are now underway or planned. The use of hES cell-

derived cells transplantation not only entails ethical obstacles, but also carries a risk of immune rejection.

The difficulties associated with hES cells can be overcome with the use of hiPS cells. Patient specific iPS cells can be differentiated into any type of cells, which are genetically identical to the patient and will not be immunogenic (Figure 4) [90].

Hanna, Jaenisch and colleagues repaired the genetic defects in iPS cells derived from a humanized mouse model of sickle cell anaemia. Directed differentiation of the repaired iPS cells into haematopoietic progenitors followed by transplantation the cells to the mice, led to the rescue of the disease phenotype. The iPS cell derived haematopoietic progenitors could stable engraft and correct the disease phenotype [102].

In another landmark study about transplantation of iPS cells from Jaenisch's group, they derived dopaminergic neurons from iPS cells and implant them into the rat brain. The cells can functionally integrate and improve the condition of a rat model of Parkinson's disease. This work is the evidence of therapeutic value of pluripotent stem cells for cell-replacement therapy [103].

The study of transplantation of hiPS-derived RPE sheet in human with exudative age-related macular degeneration is underway in Japan. The first patient receiving transplantation was in September 2014. This is the first human clinical trial to use iPS-derived cells. The outcomes of this trial are anxiously awaited.

These promising applications of hES cells and hiPS cells have opened exciting avenues for regenerative medicine, disease modelling and drug screening. To harshness these potentials, we need to further understand the fundamental mechanisms of hES/hiPS cells self-renewal, pluripotency and reprogramming in order to manipulate the process and improve the quality, efficiency, accuracy and consistency of generating target cells.

1.1.4 Regulation of Pluripotency in Human Pluripotent Cells

Human pluripotent stem cells (hES cells and hiPS cells) maintain pluripotency through regulating the extracellular signal pathways and intracellular transcription factors (Figures 5-7) [24].
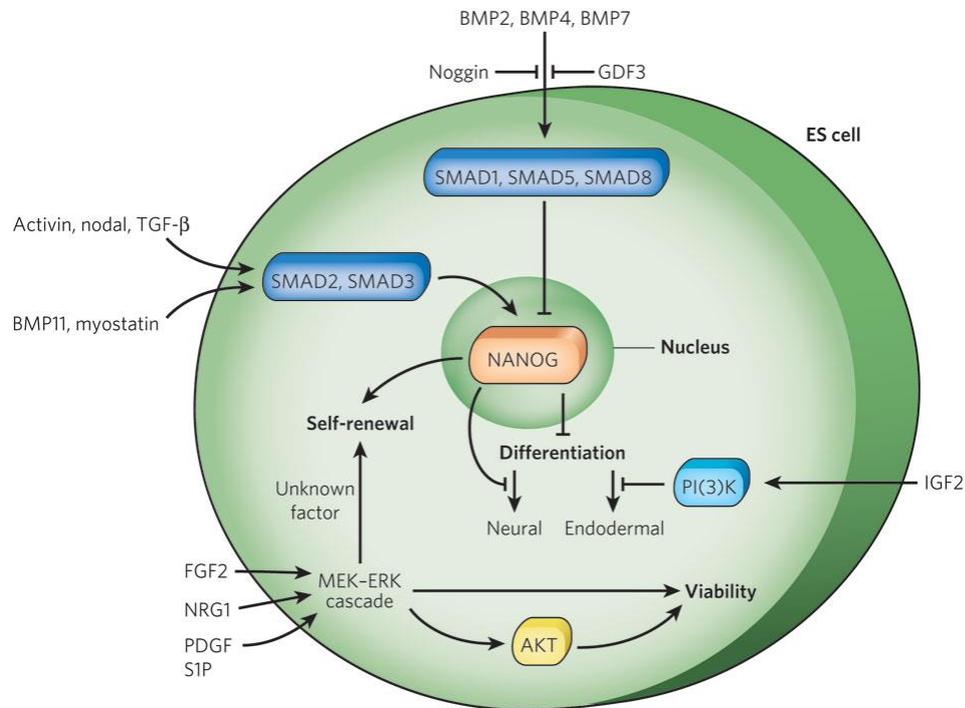
Figure 5. Extrinsic signals that affect self-renewal, differentiation and viability of hES cells.

Signalling mediated by TGF-β family, such as TGF-β, activin and nodal, growth differentiation factors (GDFs, including myostatin) and BMPs converges mainly on NANOG, which maintains ES cells in an undifferentiated state with the ability to self-renew, FGF2, PDGF, IGF2 and ERBB2 are also involved in maintaining hES cell maintenance (From Martin F. Pera & Patrick P. L. Tam, 2010) [24].

Extracellular signal pathway

The main extracellular signal pathways involved in regulating hES cells self-renewal include transforming growth factor-β (TGF-β), receptor tyrosine kinases (RTKs) mediated by growth factors [24].

TGF- β family

The TGF-β family includes the TGF-β proteins, activin, nodal, growth differentiation factors (GDFs) and BMPs, all of which are involved in maintaining the stem-cell state [24].

TGF/Activin/Nodal signal via type I receptors ALK-4,-5 and -7 to activate downstream SMADs, whereas BMP/GDF signalling activates SMADs via ALK-1,-2,-3 and -6.

The nodal- and activin- mediated signalling pathway activates the transcription factors SMAD2 and SMAD3, which can translocate into nuclear and regulate various targets, like NANOG [21,104]. SMAD2 and SMAD3 can bind to the promoter region of NANOG and activate its expression, while SMAD1, 5, 8, which are activated by BMPs, inhibit NANOG expression [105]. Activin and nodal have been shown to suppress the differentiation of hES cells. Blockade the activity of this pathway induces repaid hES cells differentiation [106]. Consistent with this finding, hES cells express receptors for nodal and a co-receptor for nodal (TDGF1). Interestingly, hES cells also express the nodal antagonists LEFTY1 and LEFTY2, as well nodal itself [107-109]. In culture, LEFTY1 or LEFTY2 might modulate the level of Nodal-mediated signalling in hES cells, indicating that this pathway is precisely regulated by internal and external factors.

The BMPs- mediated pathway activates the SMAD1, SMAD5 and SMAD8. When the cells are treated with BMP pathway activator, they will differentiate to various cell types. Antagonizing the BMP pathway will enhance hES cell self-renewal or drive ES cell to neural cell fate [110-112]. Activation of Activin-/ Nodal- SMAD2, 3 signalling or FGF2-mediate signalling suppresses BMP4 expression in hES cells, preventing spontaneous differentiation [105].

Another TGFβ member, the GDFs, could maintain hES cells self-renewal through supporting the pluripotency marker expression and blocking BMP-mediated induction of differentiation [113].

In summary, the balance between Activin-/Nodal- SMAD2, 3 pathways and BMPs-SMAD1, 5, 8 pathways is important for maintenance the hES cells self-renewal [21,114]. Various studies have shown that TGF β signalling could synergize with several other extracellular signalling proteins, for example FGF2 or WNTs to promote stem cell maintenance. Similarly, TGF β can interact with other pathways (e.g. PI3K) to induce differentiation (e.g. endoderm) [115,116].

RTK signalling mediated by growth factors

RTK signalling mediated by fibroblast growth factor 2 (bFGF), sphinigosine-1-phsphate (S1P), and platelet derived growth factor (PDGF) is also important for hES cell self-renewal.

FGF2 was the first factor found to be crucial for the maintenance of hES cells. Many chemically defined media incorporate this factor to enhance hES cell growth. hES cells express receptors for FGFs and produce FGF2 [117], which activates signalling through the RTKs ERK1 and ERK2 in these cells, inhibition of this pathway results in cell differentiation [118,119]. How bFGF-mediated signalling interacts with the network of pluripotency factors still remains unclear. For cell culture, activating Activin-/Nodal-signalling together with FGF2 could maintain hES cells long term self-renewal [4,19-21].

S1P (sphinigosine-1-phsphate), a bioactive lysophospholipid, has been implicated in a diverse range of biological processes, including cell growth, differentiation, migration and apoptosis in many different cell types [120]. PDGF has also been implicated in the prevention of apoptosis [121]. PDGF can activate sphingosine kinase, an enzyme responsible for the conversion of sphingosine to S1P by phosphorylation. When cultured in the presence of S1P and PDGF together, hES cells have shown the ability to retain their pluripotency and undifferentiated state in the absence of co-culture or serum [122], indicating a role for lysophospholipid signalling in the maintenance of stem cells.

WNT signalling

WNT signalling has an extensive role in controlling animal development, including embryonic induction, the generation of cell polarity and cell fate processes [123-125]. Canonical WNT signalling involves the binding of WNT ligands to the Frizzled receptors. This activates Dishevelled, which displaces GSK-3β from the Axin/adenomatous polyposis coli (APC) complex, preventing ubiquitin-mediated degradation of β-catenin. β-catenin accumulates and translocates into the nucleus where it associates with T cell factor/lymphoid enhancer (TCF/LEF) proteins to activate transcription of WNT targets [2].

However the role of WNT signalling in pluripotent cells *in vitro*, has been difficult to decipher because of conflicting reports. Some studies suggest roles for WNT signalling and inhibition of GSK3β in hES cells maintenance [126]. WNT signalling activation by 6-bromoindirubin-3'-oxime (BIO), a specific pharmacological inhibitor of GSK-3, maintains the undifferentiated phenotype of hES cells and sustains expression of the pluripotent state-specific transcription factors OCT4, REX-1 and NANOG [126]. Whereas others found WNT signalling could stimulate hES cells proliferation, but also differentiation. They found the β-catenin-mediated transcriptional activation in the canonical WNT pathway was minimal in undifferentiated hES cells, but greatly

upregulated during differentiation [127]. Therefore, the function of WNT signalling in regulating hES cells pluripotency is inconclusive.

PI3K signalling

The phosphoinositide-3-kinase (PI3K) family are lipid kinases that form three classes (I, II, and III). The activated PI3K acts as intracellular second messengers recruiting pleckstrin-homology (PH) domain containing proteins, such as AKT [128]. PI3K signalling can switch TGFβ/SMAD activity between pro-self-renewal and pro-differentiation through regulating ERK and GSK/ β-catenin signalling [129].

Singh et al. 2012 found that blockage of PI3K signalling induced the expression of mesendoderm marker genes such as *Eomes*, *Goosecoid* and *MIXL1*. While simultaneous blockage of TGFβ/SMAD signalling abolished the induction of these mesoendoderm genes. As TGFβ/SMAD signalling is required for hES cell maintenance, these results suggeste that robust PI3K activity collaborates with TGFβ/SMAD to maintain hES cell self-renewal, while weak PI3K activity switches the function of TGFβ/SMAD to promote differentiation [129] (Figure 6).

The authors proposed a model for maintenance of hES cell self-renewal. In this model, activated PI3K signalling could suppress MEK/ERK activity, leading to high GSK3β activity and low β-catenin activity; the low β-catenin activity does not allow the moderate level of TGFβ/SMAD activity to initiate mesendoderm gene expression and thereby maintains hES cells in their self-renewal state [129].

hESC Self-Renewal
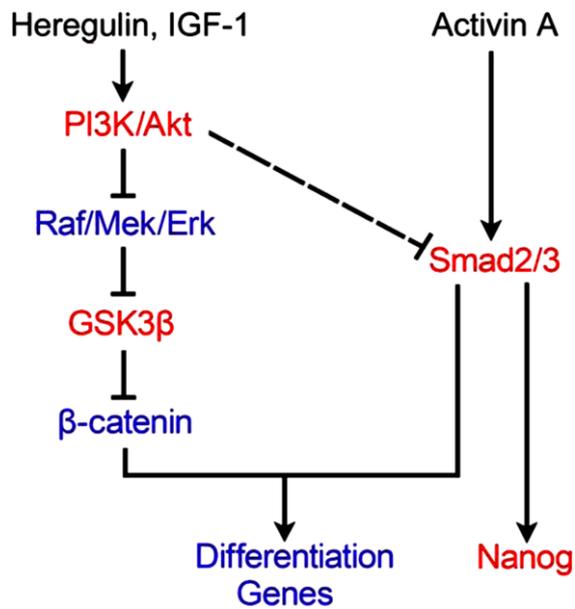
Figure 6. Heregulin and IGF-1 via PI3K/Akt and Activin via Smad2/3 Cooperate to Maintain Self-Renewal of hES cells.

Red indicates the activated state of signaling molecules, whereas blue indicates the repressive state. The dashed line indicates the regulation with unclear mechanisms. (From Yeguang Chen et al. 2012) [129]

Intracellular transcription factor

hES cells have a subset of transcription factors specifying "stemness", among which *OCT4*, *NANOG*, *SOX2* are considered to be the key factors that constitute the core pluripotency circuitry.

OCT4, also known as OCT3, a class V POU domain-containing transcription factor, was identified as essential for both early embryo development and pluripotency maintenance in ES cells [130,131]. OCT4 is highly expressed hES cells and its expression diminishes when these cells differentiate and lose pluripotency [132]. The precise level of OCT4 is important for ES cell fate determination. Loss of OCT4 causes inappropriate differentiation of ES cells into trophectoderm, whereas overexpression of OCT4 results in differentiation into primitive endoderm and mesoderm [133-136]. OCT4 regulates a broad range of target genes including FGF4, REX1, SOX2 and CDX2, through binding to enhancers carrying the octamer-sox motif (OCT-SOX enhancer), for synergistic activation with SOX2 [137-139].

SOX2 is an HMG-box transcription factor that is detected in pluripotent stem lineages and the nervous system[139]. Inactivate Sox2 in vivo results in early embryo lethality due to the failure of ICM maintenance [140]. SOX2 can form a complex with OCT4 protein to occupy OCT-SOX enhancer to regulate target gene expression. OCT-SOX enhancer could be found in the regulator region of most of the genes that are specifically expressed in pluripotent stem cells, such as OCT4, SOX2, NANOG, FGF4 and FBX15 [141-143].

NANOG is a NK2-family homeobox-containing transcription factor that is specifically expressed in pluripotent ES cells [144,145]. In hES cells, Activin/ TGF-β signalling stimulated expression of NANOG, which in turn prevent FGF-induced neuroectoderm differentiation [104]. Down-regulation of NANOG leads to a significant down-regulation of OCT4 and loss of ES cell-surface antigens and the differentiation[1]. Conversely, hES cells overexpressing NANOG can be maintained in the undifferentiated state over several passages in a feeder-free system, without the requirement for conditioned medium [146].

Many studies have demonstrated the importance of *OCT4*, *SOX2* and *NANOG* as the core regulators in regulation of hES cell pluripotency [104,147,148]. Besides regulating pluripotency, these genes also control specific cell fates in hES cells. Previous study

showed that *OCT4* regulates, and interacts with, the BMP4 pathway to specify developmental fates. High levels of *OCT4* enable self-renewal in the absence of BMP4 but specify mesendoderm in the presence of BMP4. Low levels of *OCT4* induce embryonic ectoderm differentiation in the absence of BMP4 but specify extraembryonic lineages in the presence of BMP4. *NANOG* represses embryonic ectoderm differentiation but has little effect on other lineages, whereas *SOX2* and *SOX3* are redundant and repress mesendoderm differentiation [149].

In addition, OCT4, SOX2 and NANOG physically interact with each other and coordinately regulate target genes in some cases, as their binding sites are often in close proximity to one another [8]. OCT4, SOX2 and NANOG together occupy a minimum of 353 of hES cell genes. Half of the promoter regions occupied by OCT4 and SOX2, and more than 90% of these sites were also occupied by NANOG. OCT4 , SOX2, NANOG are also bound to their own promoters, thus forming an interconnected autoregulation loop to maintain the ES cell identity [8]. OCT4 maintains NANOG expression by directly binding to the NANOG promoter when present at a sub-steady level, but represses it when OCT4 is above the normal level. And OCT4 represses its own promoter also when OCT4 level rises too high, thus exerting a negative feedback regulation loop to limit its own expression. This negative feedback loop keeps the expression of OCT4 at a steady level, thus maintaining the ES cell properties [150,151] (Figure 7).
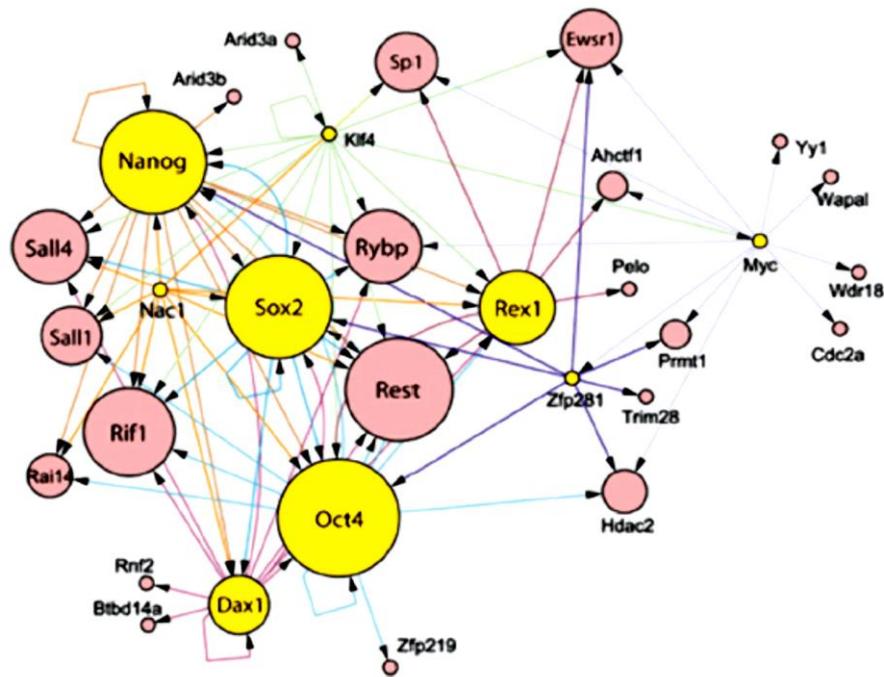
Figure 7. Expanded transcriptional regulatory network showing target hubs of multiple factors within the protein interaction network.

(From Kim et al. 2008) [146]

Besides the core transcription factors, *POLR3G* is a novel new identified pluripotency marker, which is expressed in undifferentiated hES cells, hiPS cells and early mouse blastocytes [9]. It plays an important role to maintain pluripotency of hES cells, as decreased levels of *POLR3G* results in loss of pluripotency and promotes differentiation of hES cells, while overexpression of *POLR3G* results in increased resistance to differentiation. *OCT4* and *NANOG* could regulate the level of *POLR3G* through binding at its promoter region [9]. The detail regulatory mechanism of *POLR3G* remains unknown. Further studies that focus on finding the downstream targets and upstream regulators of the *POLR3G* in hES cells and hiPS cells would be helpful for us to better to understand the regulatory network of self-renewal and pluripotency in hES cells and hiPS cells.

1.2 Cell Cycle

1.2.1 Introduction of Cell Cycle

The cell cycle is an important event that leads to cell division and duplication. The basic function of the cell cycle is to duplicate genetic information and equal segregation of copied DNA between two daughter cells [152]. The cell cycle includes four different phases: G1, S, G2 and M phase. G1, S and G2 phases are also called interphase (Figure 8). Interphase is an important part of cell cycle. During this stage the cells grow, prepare nutrients and duplicate its DNA for mitosis. M phase is the short acronym for mitosis phase. During M phase cell's division into two daughter cells is achieved [153].
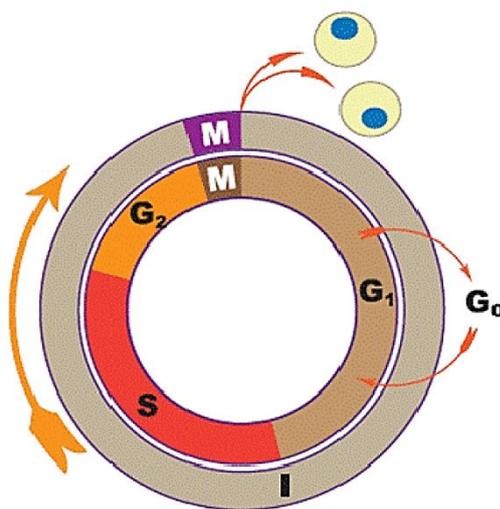
Figure 8. Schematic representation of the cell cycle.
(From Murtala B. Abubakar et al, 2012) [154].

G1 phase

The G1 phase of the cell cycle encompasses the time from the end of the previous mitosis until the next DNA replication. During this phase, the cells synthesize many of the proteins and enzymes which are required for DNA duplication in S phase [155]. Cells in G1 phase are very sensitive, during which the cell fate is often decided. The length of G1 is highly variable between different cell types. G1 checkpoint is located at late G1 phase is also for cells make decision for whether divide, delay division, or enter a resting stage [156].

S phase

The S phase is a period between G1 and G2 phase in the cell cycle. The major event occurring during this phase is DNA replication, resulting in doubling of DNA amount. Another important event in this phase is the detection and repair of DNA damage [157]. This is achieved through activation of special signalling pathways, involving DNA damage sensors (ATR) and effectors (Chk1) which detect the damage and cause a stop in DNA replication and stabilize the DNA polymerase complex to fix the DNA damage [158,159].

G2 Phase

The G2 phase is the last interphase before the mitosis. In this phase, cells synthesise proteins which are necessary for mitosis. Microtubules, which are required for mitosis, are also synthesized in G2 phase. But in some cell types, such as *Xenopus* at the embryonic stage [160] and some cancers [161], G2 phase is not necessary: they can directly enter mitosis.

M phase

The M phase is the stage during which the cells separate into two daughter cells. The M phase can also be divided into several sequentially parts namely prophase, metaphase, anaphase, telophase and cytokinesis. During the M phase, pairs of chromosomes condense and attach to fibres that pull the sister chromatids to opposite sides of the cell [162]. Then the cell starts cytokinesis immediately by dividing itself into two equal cells which share the cell components. The mitosis is also a very important part of the cell cycle as mistakes during this stage are likely to lead to cell apoptosis or initiation of cancer [163].

1.2.2 Cell Cycle Regulation

Cell cycle regulation is very important for deciding cell fate and as such it needs to be precisely regulated. Two main regulators of cell cycle are cyclins and cyclin-dependent kinases (Cdks) along with other cell cycle positive and negative regulators act to control the cell cycle process [152].

Cyclins

The first cyclin was discovered by R. Timothy Hunt in 1982 [164]. They were initially named cyclins because their expression changes in a repeatable and specific pattern (cycled) during the cell cycle. The basic function of cyclins is to regulate the cell cycle by activating cyclin-dependent kinases (Cdks) through protein-protein interactions.

Based on their expression profiles, the cyclins can be divided into four classes, G1/S cyclins, S cyclins, G2 cyclins and M cyclins. Different type of cyclins may bind with different Cdks during the cell cycle, for example, cyclin D/Cdk 4/6, cyclin E/Cdk 2 and cyclin A/Cdk 2 (Figure 9).
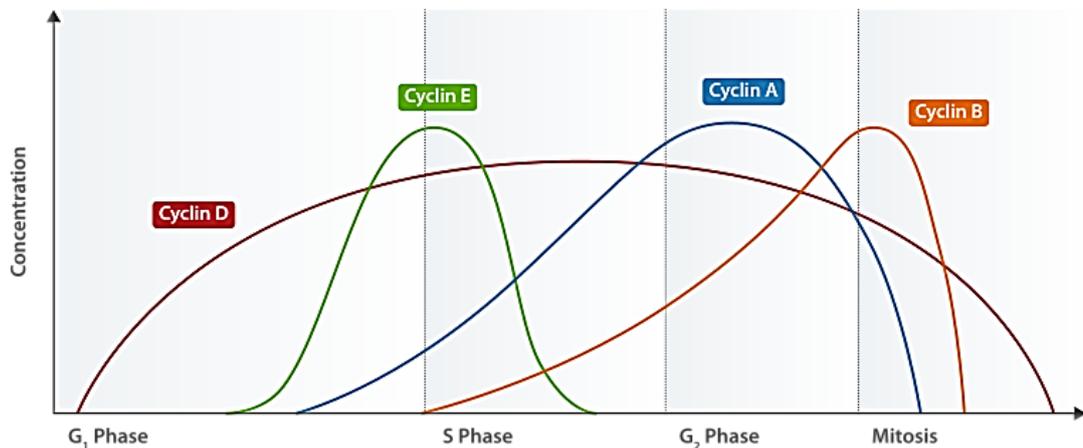
Figure 9. Expression of human cyclins through the cell cycle.

The concentrations of cyclin proteins change throughout the cell cycle (From https://en.wikipedia.org/wiki/Cyclin-dependent_kinase_complex).

Cdks

Cdks is the acronym for cyclin-dependent kinases. Cdks promote the cell cycle through binding with cyclins[152]. However, they can play additional roles in transcriptional regulation, mRNA processing, DNA damage and cell cycle checkpoint activation as well as cell differentiation (Table 3) [165].

The Cdks have negligible kinase activity without the cyclins [121]. When a Cdk associate with a cyclin to form the cyclin-Cdk complex, its kinase activity can then are activated.

However, only cyclin binding is not sufficient to fully activate Cdks. The inhibitory phosphate groups are also need to be removed by Cdc25 phosphatases [166]. In addition, the active sites of Cdks need to be phosphorylated by cyclin activating kinase (CAK) to enable full kinase activity.

CDK	Cyclin partner	Function	Knockout Phenotype in Mice	Function in hES cells
Cdk1	Cyclin B	M phase	None. ~E2.5.	G2/M arrest
Cdk2	Cyclin E	G1/S transition	Reduced size, imparted neural progenitor cell proliferation. Viable, but both males & females sterile.	G1 phase arrest; differentiation to extraembryonic
Cdk2	Cyclin A	S phase; G2 phase		
Cdk3	Cyclin C	G0 phase	No defects. Viable, fertile.	
Cdk4	Cyclin D1,2,3	G1 phase	Reduced size, insulin deficient diabetes. Viable, but both male & female infertile.	Induce differentiation; reduce proliferation
Cdk5	p35	Transcription	Severe neurological defects. Died immediately after birth.	
Cdk6	Cyclin D1,2,3	G1 phase	Slight anaemia and defective proliferation of some haematopoietic cells	Induce differentiation; reduce proliferation
Cdk7	Cyclin H	CDK-activating kinase; transcription		
Cdk8	Cyclin C	Transcription		

Table 3. Cyclins and Cdks function in human and consequences of deletion in mice. (Adapted from Gopinathan L et al 2011) [121].

Cyclin and Cdks interaction

The interaction between cyclins and Cdks is to form a heterodimer in which the cyclins provide the regulatory subunits, whilst Cdks provide the catalytic subunits. Without cyclins, the Cdks only have negligible kinase activity as the active site of Cdk is blocked by a flexible loop. Binding of Cdks to cyclins causes a structural change which promotes the ATP binding to some amino acid site, Cdks can be activated by CAK [167]. The active cyclin-Cdk complex is able to phosphorylate their specific target proteins to lead the cell's entry into next cell cycle phase. This is corroborated by studies performed in human fibroblast cells by Ohtsubo showing that overexpression of cyclin D or cyclin E in early G1 phase cause premature S phase entry [168], suggesting that these cyclins at least partially regulate the G1/S phase entry.

Cdks are constitutively expressed during the cell cycle; however cyclins are expressed in specific time of the cell cycle. This cyclic expression pattern is regulated by various signalling pathways. Different types of cyclin-Cdk complex have different functions in each cell phase [152]. For example, cyclin E can bind to Cdk2, to form the cyclin E / Cdk2 complex, which will promote the G1/S transition (Table 4) [169]. Cyclin B can bind to Cdk1 and this active complex is able to initiate the G2/M transition [170].

G1 component	Downregulate phenotype in mouse ES cells
Cdk2	lengthening G1 phase, increased differentiation, decreased proliferation
Cdk2/cyclin E	lengthening G1 phase, increased differentiation, decreased proliferation
Cyclin D1	lengthening G1 phase, increased differentiation, decreased proliferation
Cyclin D2	lengthening G1 phase, increased differentiation, decreased proliferation
Cyclin D3	decreased proliferation
Cdk4/cyclin D1	lengthening G1 phase, increased differentiation, decreased proliferation
Cdk4/6	decreased proliferation

Table 4. Phenotype in mouse ES cells with downregulating G1 phase component. (Adapted from Momciilovic et al. 2011) [152].

Cell cycle inhibitors

Cell cycle inhibitors also play an important role in cell cycle regulation. These are classified in two families: cip/kip family (CDK interacting protein/Kinase inhibitory

protein) and the INK4 (Inhibitor of Kinase 4). Members of these two families are also known as tumour suppressors, as they play a role in prevention of tumour formation [171].

The cip/kip family includes p21, p27 and p57. These genes can arrest the cell cycle by inactivating relevant cyclin/Cdk complex. Cyclin D/Cdk4-6, cyclin E/Cdk2 and cyclin B/Cdk1 are all regulated by cip/kip family. The INK4 proteins include p16INK4a, p15INK4b, p18INK4c and p19INK4d. These proteins only bind with Cdk4 and Cdk6 to inhibit their activity[171].

1.2.3 G1 to S Transition

G1/S transition is regulating expression and phosphorylation of G1/S specific Cdk, cyclins and Rb gene family. The activity of Cdks is largely depending on binding with Cyclins, which are regulating by many internal and external signals. Phosphorylation of Rb by Cdks is a key point of progress of G1 to S transition [171].

Significance of the G1/S transition

Many studies show that the G1 phase of the cell cycle is a key factor for cell's decision to differentiate, proliferate, apoptosis, become quiescent or enter into senescence [171].

The length of G1 phase is very different between somatic cells and murine embryonic stem cells [172]. Cell cycle has been proved to be much shorter in embryonic stem cells (8~10 h) compared to somatic cells (murine fibroblasts, 22~25h) [169,173]. Many studies have shown that lengthening of G1 can cause the differentiation of embryonic, neural and hematopoietic stem cells [174-176]. These models are based on "the concept that time, i.e., G1 length, may be a limiting factor for cell fate change to occur because differentiation factors require time in order to trigger a physiological response" [172]. Previous study also showed G1 phase cells in naïve ES cells appeared to be more susceptible to differentiation [177]. Recent study also uncovered mechanisms by how G1 phase control cell fate choice. Endoderm induction is only possible in early G1 phase when the cyclin D expression level is low, allowing Smad2/3 to bind and to activate endoderm genes, and late G1 cells only receptive for neuroectoderm initiation [178].In view of the above findings, it is very important to understand mechanisms of G1 to S transition in detail in embryonic stem cells and how this impacts the maintenance of pluripotency.

1.2.4 Regulation of the G1/S Transition in Somatic Cells

There are several specific cyclin/Cdk complexes involved in G1 to S transition, and these are cyclin D/Cdk4, cyclin D/Cdk6, cyclin E/Cdk2 and cyclin A/Cdk2 [171].

In differentiated mammalian cells, G1 to S transition is regulated by three main pathways, retinoblastoma (Rb) pathway, c-Myc pathway and p53 pathway (Figure 10) [152,171].
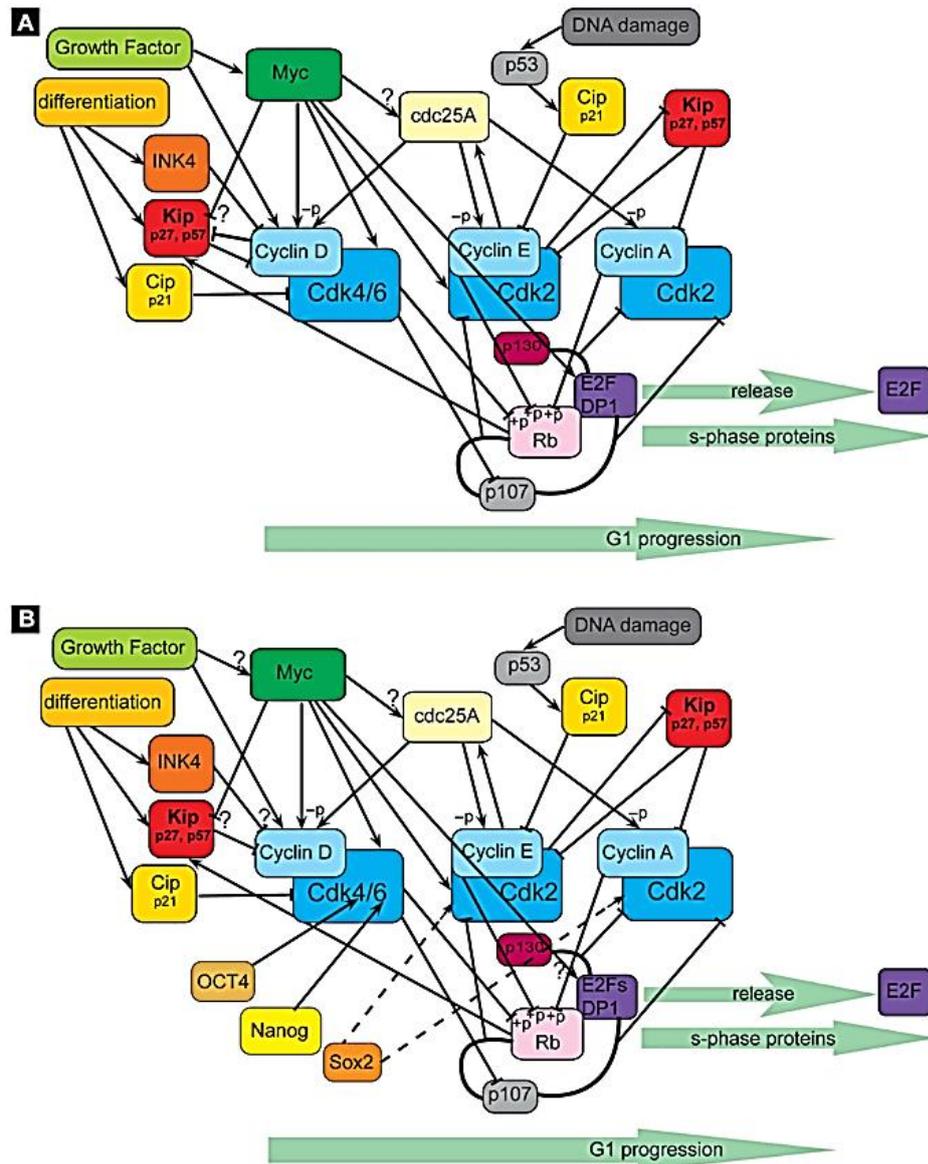
Figure 10. Simplified schematic representations of the key molecular pathways controlling G1 to S phase transition in somatic cells (A) and in hES cells (B).

In proliferating cells, Rb phosphorylation by cyclin/Cdk complexes releases E2F, which then induces genes that mediate S phase entry. Arrows indicate stimulatory modifications, blocked lines show inhibitory modifications. –p and +p indicate removal and addition of phosphorylation respectively (From Neganova et al, 2008) [171].

Retinoblastoma (Rb) is a negative regulator of the cell cycle and a positive regulator of cellular differentiation. G1 to S progression is regulated by hypophosphorylated Rb genes (Rb1/p105, Rb2/p107, Rb3/p130), which inhibit the expression of genes required for entry into S phase by sequestering E2F [179]. In somatic cells, at the mid-late G1 phase, cyclin D/Cdk4-Cdk6 complex phosphorylates Rb protein leading to partial release of the E2F gene, which in turn activates the transcription of cyclin E and Cdc25A. The cyclin E binds to Cdk2 and further phosphorylates Rb completely, allowing the cell to pass through the restriction point entry the S phase [180].

The c-Myc pathway, which stimulates directly the expression of cyclin E and the Cdc25a gene, maintain cyclinE/Cdk2 activity by sequestering p21 and p27 protein [181]. Overexpression of c-Myc in growing cells leads to reduced growth factor requirements and a shortened G1 phase, while reduced c-Myc expression causes lengthening of the cell cycle [182].

Tumor suppressor protein, p53 is inactivated by its negative regulator mdm2 in normal cell. Many types of cellular stresses cause activation of p53, disassociation from mdm2 and translocation to the nucleus [183]. p53 can induce cell cycle arrest through regulating many target genes, including p21 and Bax, to enable either arrest of cell stop cycle and activation of DNA repair pathways or in cases where damage is too extensive activation of apoptosis to eliminate the damaged cells from the population [184].

1.2.5 G1/S transition in Mouse ES Cells

Mouse ES cells have a very short cell cycle (11-16 h) and G1 is much shorter (2 h) compared to somatic cells [169]. This cell cycle strategy is one of the key factors enabling the rapid proliferation of mouse ES cells and minimizing the differentiation events during G1 phase. To enable such short G1 phase, Rb proteins are hyperphosphorylated and inactive throughout the cell cycle of murine ES cell. Without Rb, E2F is constitutively activated resulting in E2F target genes constitutively active throughout the cell cycle [185].

In mouse ES cells, cyclin D expression is very low and Cdk4 kinase activity is almost undetectable [169,186]. Cyclin E/Cdk2 shows cell cycle independent activity and cyclin A/Cdk2 is constitutively active. Only Cdk1 and Cyclin B1 are regulated in a cell-cycle

dependent manner [185]. Initiation of ES cell differentiation results in acquisition of cell cycle features that are common in somatic cells (Figure 11).
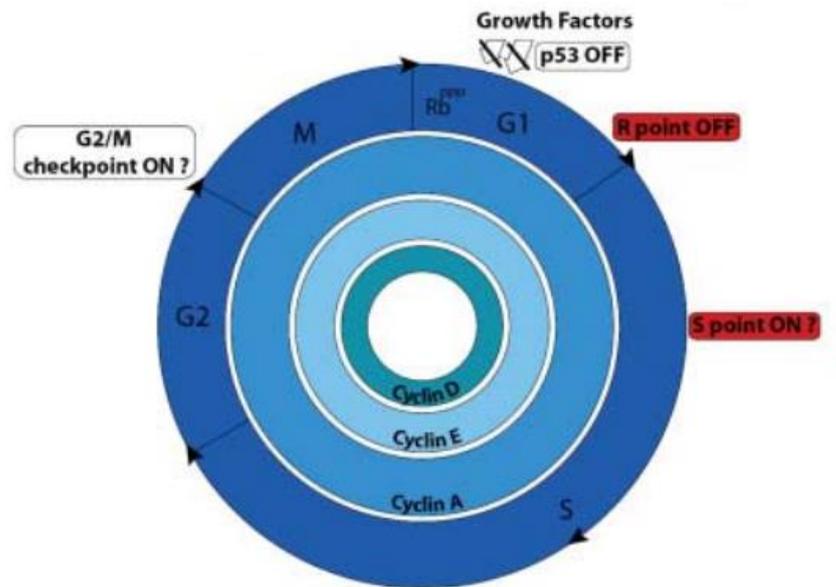
Figure 11. A simplified presentation of the fluctuation of expression of cyclins and Cdks involved in G1 to S progression in mouse ES cells.

Expression of cyclin D, cyclin E and cyclin A is not dependent on the cell cycle progression in murine ES cells. Hyperphosphorylated Rb is present at all cell cycle stages and the only cyclin that demonstrates cell cycle periodicity in mouse ES cells is cyclin B1 at G2 stage of the cell cycle (not shown). Although it is clear that R point does not operate in murine ES cells, the existence of a functional S point and G2/M is not clear. Recent investigations suggest that although the mitotic-spindle checkpoint, which helps to maintain chromosomal integrity during all cell divisions, functions in human and mouse ES cells, it does not initiate apoptosis as it does in somatic cells. (Adapted From Neganova and Lako 2008)[171]

1.2.6 G1/S Transition in hES Cells and hiPS Cells

hES cells and hiPS cells display also a very short G1 phase similarly to murine ES cells [187]. In hES cells and hiPS cells, cell cycle duration is 15-16 h and G1 phase accounts for about 20% of the cell cycle [173]. However, unlike mouse ES cells, Cyclins and CDKs show cell cycle dependent manner expression (Figure 12). The expression of Cdk4 is higher than Cdk6 in hES cells and human iPSCs compared with mouse ES cells.

Furthermore, the expression of cell cycle inhibitors, INK and Cip/Kip family is almost undetectable [171].

	Mouse ES cells	Human ES cells
Cyclin D1	Almost undetectable	High in G_1
Cyclin D2	Very low	High in G_1
Cyclin D3	High	G_1
Cdk4	Almost undetectable	High activity in G_1
Cdk6	High	G_1
Cyclin E	Constitutively expressed	G_1–S
Cyclin A	Constitutively expressed	S–G
Cdk2	Constitutively active	Active in S
Cyclin B/Cdk1	Cell cycle dependent – G_2	Cell cycle dependent – G_2
p21	Undetectable	Very low

Figure 12. Comparison of expression and activity of cell cycle controllers in mouse and hES cells.

(From Momciilovic et al. 2011) [152].

1.2.7 G1/S Checkpoint

Cell cycle checkpoints are an important part of cell's life cycle as they act as key monitors and regulators of cell cycle [188,189]. The main role of checkpoint is to assess DNA damage and ensue the necessary response (this being cell cycle arrest or apoptosis) to enable either DNA repair or elimination of "faulty" cells from the cell population [190]. The cells cannot entry next phase until checkpoint requirements have been completed.

The G1/S checkpoint is the first point located at the end of G1 phase. The main function of this checkpoint is to assess genome stability prior to DNA duplication in S phase. Two key regulators of G1/S checkpoint are and two PIKK (Phosphatidylinositol 3-kinase-related kinase) family members, ATM (ataxia-telangiectasia mutated) and ATR (ATM and Rad 3-related) [190]. DNA damage caused by ionizing radiation leads to activation of ATM, which in turn causes phosphorylation and activation of Chk2 (Figure 13). Activated Chk2 phosphorylates p53 at Ser 20 [191]. The phosphorylation of Ser20 blocks the interaction between p53 and mdm2, thus releasing p53 from mdm2, and increasing the p53 protein level (Figure 13) [192].

ATM or ATR can also phosphorylate the Ser15 residue of p53 following UV irradiation and stalling of DNA replication forks [191]. The phosphorylation of Ser15 will enhance

subsequent phosphorylation of p53 at Ser18 [193]. The phosphorylation at these two sites activates p53 and reduces its interaction of p53 with mdm2 (Figure 13) [194].

ATM is also able to phosphorylate the mdm2 directly at Ser395. The phosphorylation of mdm2 at Ser395 affects its shuttling activity [195]. As consequence, the p53/mdm2 complex cannot be normally exported out of the nucleus for proteosomal degradation in the cytoplasm, resulting in p53 stabilization [196].

Activated p53 leads to upregulation of its target genes. One of the key targets is p21, whose activation results in inhibition of the cyclin E/Cdk2 activity and stalling of G1 to S phase progression [197].

Several studies showed mouse ES cells lack of a functional DNA damage induced G1/S cell cycle arrest [198-200] and defect on expression of checkpoint proteins [200,201]. Unlike mouse ES cells, hES cells have been shown to be capable of executing G1/S checkpoint activation in response to DNA damage [202,203]. Previous study in our group showed downregulation of CDK2 triggers the G1 checkpoint through the activation of the ATM-CHK2-p53-p21 pathway (Figure 13) [203].
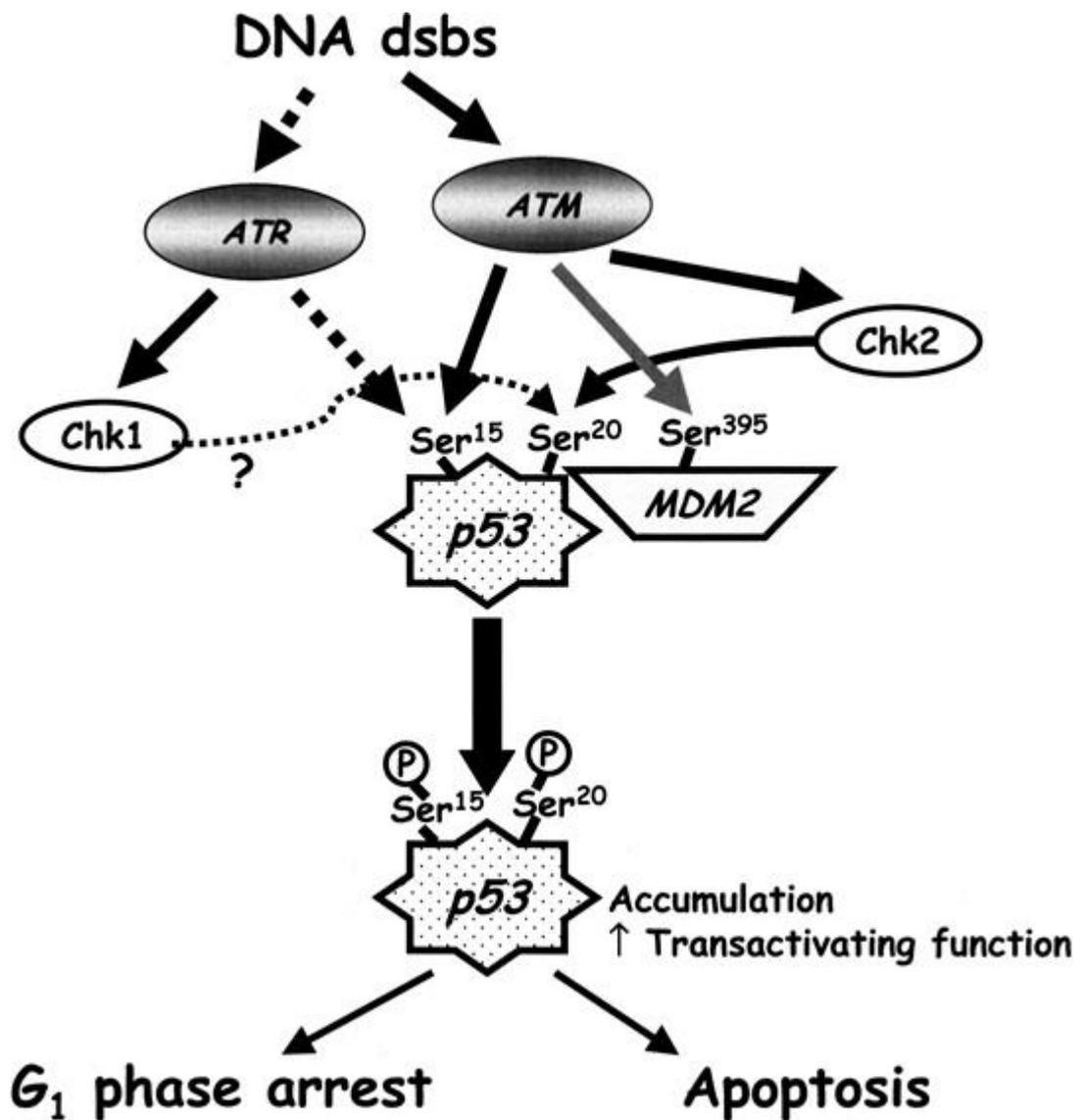
Figure 13. ATM/ATR-dependent signalling through the G1checkpoint.

Cells that have incurred DNA double-strand breaks (dsbs) during G1 phase activate p53 primarily via an ATM-dependent pathway. In cells that express both ATM and ATR, the activation of p53 is reinforced and maintained by ATR (pathway indicated by dotted lines). ATM regulates p53 accumulation by indirect pathways involving the Chk2-mediated phosphorylation of Ser 20 on p53, by promoting casein kinase-I-dependent phosphorylation of Ser 18 (not shown), and by directly phosphorylating MDM2 on Ser 395. ATR may influence Ser 20 phosphorylation through activation of Chk1. (From Robert T. Abraham) [190].

1.2.8 The Cell Cycle and the Regulation of Pluripotency

Rapid cell cycling is the feature of hES cells and hiPS cells. A short G1 phase has been considered as means of pluripotency maintenance that limits the window of opportunity during which a cell can be responsive to differentiation[178,204]. During differentiation, the G1 phase is prolonged. Interestingly, lengthening G1 phase by manipulating cell cycle

regulators is sufficient to induce differentiation, implying that G1 lengthening is a cause rather than a consequence of differentiation and that a short G1 phase is crucial for ES cell self-renewal and pluripotency. Recent studies have revealed that specific cell cycle components could regulate the pluripotency [205]. Use of the CDK inhibitor rescovitine in hES cell culture prompted G1/S arrest, accumulation of hypophosphorylated Rb, smaller hES cell colonies and the down-regulation of the pluripotency marker *OCT4* [206]. Specific knockdown of CDK2 using siRNA induced cell arrest in G1 and differentiation of hES cells to extra-embryonic lineages [25].

Furthermore, a study revealed a role of $p27^{KIP1,}$ the negative regulator of CDK2, in self-renewal of hES cells differentiation [207]. Cell cycle components could also regulate the differentiation capacity through controlling the differentiation signals. One recent study addressed the variation of differentiation capacity during the progression of hES cell cycle. They found that the hES cells in early G1 could only initiate endoderm/mesoderm differentiation, whereas the hES cells in later G1 could only initiate the neuroectoderm. On the other hand, cells in G2/M phases of the cell cycle responded poorly to differentiation signals[178]. The results confirm that induction of differentiation on hES cells occurs during the G1 phase and also the hES cells in early and late G1 might have a different capacity of differentiation. Knockdown of Cyclin Ds in hES cells systematically dimish pluripotency and neuroectoderm marker expression. Whereas hES cells with overexpressing Cyclin Ds maintained self-renewal and pluripotency, but showed an increase in neuroectoderm marker expression and have a limited capacity to differentiate into meso/endoderm[178]. These mechanisms are governed by the Cyclin Ds which can regulate the differentiation signalling such as the TGFβ/SMAD pathway[178].

Recent studies have shown that transcription factors such OCT4, SOX2 and NANOG regulate pluripotency by transcriptional regulation of cell cycle genes. OCT4, SOX2 and NANOG have been found to bind to promoters of several cell cycle regulatory genes, including *CDC25A*, *CDK1*, *CDK6* [8]. NANOG was shown to directly regulate *CDK6* and *CDK25A* at the transcriptional level and by this mechamism to regulate G1 progression and S phase entry in hES cells [208]. Vice versa, cell cycle regulatory proteins can regulate expression of core pluripotency regulators or of their target genes. For instance, Geminin, a negative regulator of prereplication complex assembly, antagonizes the chromatin remodelling protein Brg1 to maintain expression of Oct4,

Sox2 and Nanog. In the absence of Geminin, Brg1 represses expression of Oct4, Sox2 and Nanog, and ES cells differentiate [209].

In addition, core pluripotency factors indirectly regulate cell cycle through miRNAs. Pluripotency factors Oct4, Sox2 and Nanog can bind the promoter region of the miR-302 cluster in hES cells, however only Oct4 and Sox2 are required for expression of the miR-302 cluster [210,211]. Further study showed miR-302 regulates cyclin D1 in hES cells, which indicate the link between pluripotent factors with cell cycle [210]. The miR-17-92 family is regulated by Myc, this family target cell cycle regulators include E2F, cyclins and Rb family [212].

Another intrinsic link between pluripotency and cell cycle has been proposed to be MYC. MYC has many roles in normal proliferative control and cell fate determination in ES cells. c-MYC upregulates expression of several pro-self-renewal miRNAs, miR-141, miR-200 and miR-429 [213,214], represses lineage determinants, such as the endoderm master regulator gene GATA6 in hES cells [208], and supports cell cycle and rapid G1 progression by directly upregulating cyclins and CDKs and indirectly downregulating negative cell cycle regulators [208].

1.2.9 The Cell Cycle during Reprogramming

hiPS cells exhibit the unique cell cycle program of pluripotent cells, similar with hES cells. While partially reprogrammed cells exhibit a cell cycle profile that is intermediate between fibroblasts and pluripotent cells [2]. The formation of iPS cells further support the essential role of specific cell cycle regulation in pluripotency and reprogramming [2].

It is generally observed that older or more slowly dividing cells are more difficult to reprogramme [204,215]. In addition, the fibroblasts which were permeabilized and incubated in meiotic Xenopus egg extract (high CDK1 activity), but not interphase egg extract (low CDK1 activity) were much easier to be reprogrammed by the four factors [216].

In 2011, Ruiz et al. found that induction of cell proliferation through ectopic expression of cyclin D1, cyclin D2 and cyclin E2 promotes formation of hiPS cells; while cell cycle arrest through ectopic expression of p15, p16, or p21 inhibits cell reprogramming [204]. The *Ink4/Arf* tumour suppressor locus encodes three potent inhibitors of

proliferation, namely p16, p15, and ARF. This locus is epigenetically silenced in hES cells, hiPS cells and upon reprogramming. *Ink4/Arf* deficient MEFs reprogramme with a 15-fold higher efficiency than wild-type MEFs[217]. Such conclusions are consistent with the previous study demonstrating the p53 tumour suppressor pathway is also a barrier to reprogramming [218]. By using short hairpin RNA against the p53 or p53 target gene *p21^cip1* both allowed increased reprogramming efficiency [218].

Also ES cell miRNAs, including miR-302b and miR-372, have been found to enhance the efficiency of reprogramming[219]. By targeting multiple inhibitors of CDK2 activity, miRNAs mediate rapid progression through G1 phase and promote the unique cell cycle program of pluripotent cells in reprogrammed cells[219].

These studies highlighted the role of the cell cycle in the somatic cell reprogramming process, the higher proliferation rate is required for cell reprogramming.

1.3 MicroRNA

1.3.1 MicroRNA Biogenesis

MicroRNAs (miRNAs) are 20-25 nucleotides, endogenous non-coding RNAs. The first miRNA was discovered in 1993 by Rosalind Lee, Rhonda Feinbaum, and Victor Ambros while studying the function of the gene *lin-14* during the development of *Caenorhabditis elegans*. They discovered that "the lin-14 protein expression was regulated by a short RNA product encoded by the *lin-4* gene" [220]. Since then, more than 700 miRNAs have been identified, while 1000 miRNAs are predicted to play role in gene regulation in human cells [221].

More than half of mammalian miRNAs are located in introns of host gene as well as in long non-coding transcripts [222]. However, some miRNAs can also be found in the exons. Most of the miRNAs located in intron region are expressed in the same tissues as their host gene [223]. For example, in human and zebrafish, miR-126 is located in an intron of the *EGFL7* gene. The expressions of miR-126 and *EGFL7* are observed in endothelial cells of the heart and blood vessels [224].

The generation of mature miRNAs usually needs a series of cleavage processing. First, the pri-miRNA, which has a cap structure (7MGpppG) and a polyadenylation tail (AAAAA), is transcribed in nucleus by RNA polymerase II [225]. Then the pri-miRNA is cleaved in the nucleus by the *RNaseIII* enzyme Drosha and its RNA binding partner Dgcr8 [226-228]. This cleavage generates a 60-75 nucleotides pre-miRNA with a short hairpin. The pre-miRNA is transported to the cytoplasm by Exportin 5 through a Ran-GTP dependent manner [229-231]. In the cytoplasm, the pre-miRNA is cleaved by another *RnaseIII* enzyme Dicer and its partner TRBP to generate the mature miRNA duplex [232]. This duplex is loaded with Ago2 into a protein complex called RNA induced silencing complex (RISC). In this complex, the miRNA can regulate its target mRNAs through mediating the mRNA target cleavage, translational repression or mRNA deadenylation. The interaction between miRNAs and their targets is largely dependent on the seed sequence, which located at 2-8 position at the five prime untranslated regions (5'UTR) of miRNA and three prime untranslated regions (3'UTR) of target mRNA [233]. Recently, many studies show that miRNA can also regulate target miRNA expression through binding to the coding region or the 5'UTR of the mRNA (Figure 14).
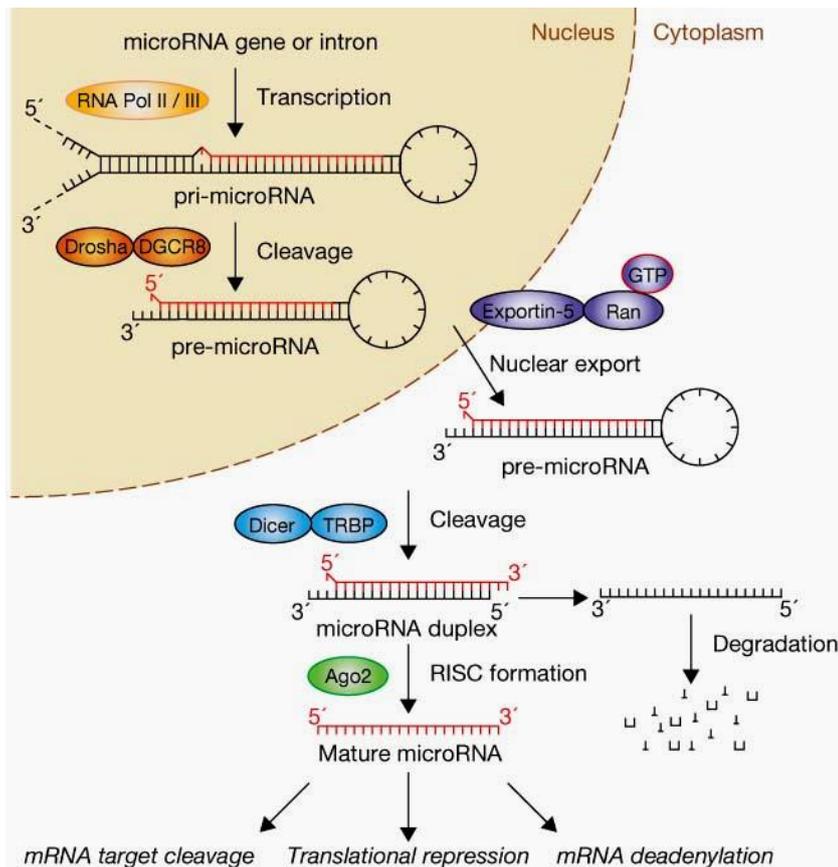
Figure 14. The 'linear' canonical pathway of miRNA processing.

The miRNA generation includes the primary miRNA transcript (pri-miRNA) by RNA polymerase II or III and cleavage of the pri-miRNA by the microprocessor complex Drosha–DGCR8 (Pasha) in the nucleus. The pre-miRNA, is exported from the nucleus by Exportin-5–Ran-GTP. In the cytoplasm, the RNase Dicer in complex with the double-stranded RNA-binding protein TRBP cleaves the pre-miRNA hairpin to its mature length. The mature miRNA is loaded together with Argonaute (Ago2) proteins into the RNA-induced silencing complex (RISC) to silence target mRNAs through mRNA cleavage, translational repression or deadenylation (Adapted from Winter et al. 2009) [234].

1.3.2 miRNA Function

The function of miRNAs has been studied for many years. It was first found that the binding of miRNA to its target mRNA can repress the translation process. For example, the *let-7* miRNA of *C. elegans* can repress *lin-41* mRNA translation, and *lin-4* can repress lin-14 protein synthesis. Initial studies suggest that these repressions do not affect mRNA degradation [220].

In contrast, recent studies have shown that miRNAs can also regulate mRNA degradation, mainly through deadenylation [235,236]. Two genome-wide studies involving overexpression or knockdowns of various miRNAs in HeLa cells and mouse neutrophils

revealed that both target protein level and mRNA level were downregulated [233,237]. These results suggest that the mRNA degradation is likely to be a critical mechanism used for reducing protein expression levels by miRNAs in mammalian cells. Recent studies have also revealed that miRNAs may bind to promoter regions [238] and have the potential to activate gene expression [239]. In human genome, more than 1000 miRNAs had been found [240], however the number of mRNAs is typically estimated at about 30000. Thus, one miRNA may regulate hundreds of target mRNAs [241]. Through regulating target genes' mRNA level and protein translation, miRNAs are involved in almost every biological process, including a variety of developmental, physiological processes and play key functions in the cell differentiation (Table 5). In addition to these important biological process, miRNAs also involved in different cellular activities, such as insulin secretion [242], neurotransmitter synthesis [243], immune response [244], circadian rhythm [245], and viral replication [246]. Recent genome-wide analyses have also identified miRNAs can regulate oncogenic or tumor suppressor pathways [247,248].

Species	miRNA	Target(s)	Function(s)
C. elegans	lin-4	*lin-14, lin-28*	Early developmental timing
	let-7	*lin-41, hbl-1 , daf-12 pha-4 , Ras*	Late developmental timing
	miR-273	*Die-1*	Left/right neuronal asymmetry
Drosophia	miR-7	Notch targets	Notch signalling
	miR-14	*Drice*	Programmed cell death and fat metabolism
Mus Muscles	miR-196	*Hoxb8*	Developmental patterning
	miR-181		Hematopoietic lineage differentiation
	miR-1	*Hand2*	Cardiomyocyte differentiation and proliferation
	miR-375	*Mtpn*	Insulin secretion
Human and other vertebrate	miR-16	Several	AU-rich element-mediated mRNA instability
	miR-32	*Retrovirus PFV -1*	Anitviral defense
	miR-143	*Erk5*	Adipocyte differentiation
	miR-15/16/195 / 424/497	*CCNE1,CCND1,CCND3, CCND2,CDC25A,CCNE1, WEE1, E2F3, CCND1, CCND3,CCND2, CDC25A*	cell cycle; G1-to-S
	miR-15/16/195 / 424/497	*FZD10, DVL1, CCND1, PAFAH1B1,PPP2R5C, FZD6,CCND3,DVL3, MAPK9, PRKCI ,CCND2, WNT7A, FOSL1,WNT2B*	Wnt pathway
	miR-135	*SMAD5,ROCK2,SMURF2 THBS2, ROCK1, SMAD2, FKBP1A,NODAL,PPP2R 1B,INHBA,TGFBR1,ACV R1B,BMPR1A,SP1,RPS6 KB1,BMPR2,RUNX2, RBX1, SKI*	TGF beta signalling
	miR-17-5p/20/93. miR-106/519d	*CCNE1,CCND1,CDC25A, SMAD3,CCNG2RBL1,RP A2,WEE1,E2F1,CCND2, CDKN1A,MCM3,CDC25A ,RB1,E2F3,CCND1, CCNE2*	cell cycle; G1-to-S
	let-7/98	*E2F6,TP53,PRIM2, CDKN1A,CDC25A,RB1, CCND2,CCND1,CCND2, CCND2*	G1-to-S

Table 5. Biological functions of miRNAs in animals, disease and cancer [249-251].

1.3.3 The Role of miRNAs in Regulating Self-renewal

miRNA expression has been examined in mouse ES cells and human ES cells by comparing undifferentiated ES cells to their differentiated counterparts. Those experiments revealed that ES cells seem to be characterized by a unique miRNAs signature [252].

The fact that many miRNAs have the same seed sequence and that a single miRNA can target multiple mRNAs make difficult to study their function individually. Remove of all miRNAs can be achieved by deleting the genes encoding the enzymes involved in the processing of miRNAs. Deletion of proteins in the miRNA biogenesis, such as Dgcr8 and Dicer, in mouse ES cells results in the loss of miRNA in cells. These global miRNA- knockout cells provide a valuable tool for studying the function of miRNAs. Individual miRNAs can then be reintroduced as mimics to assess their functions. Mouse ES cells with Dgcr8 or Dicer proliferate slower, with a slight cell accumulation at G1, couldn't silence the self-renewal when induced to differentiation, indicating the important roles of miRNA in controlling the self-renewal and differentiation [253,254]. Knockdown of Dicer or Drosha in hES cells also dramatically attenuates cell division and results in the formation of stem cells with high levels of stem cell factors, correlating with delayed differentiation [255].

By screening the miRNAs which could enhance proliferation in Dgcr8 knockout mouse ES cells, miR-290/371 cluster was determined as ES cell specific cell cycle regulating miRNAs, which can increase proliferation in the mutant ES cells and reduce cells accumulated in G1 phase [256]. The miR-290-295 cluster is regulated by Oct4 in mouse ES cells, and also binds to the promoter region of *Oct4*, *Sox2*, *Nanog* and *Tcf3* [257], suggesting a regulatory loop between pluripotency factors and miR-290-295 cluster.. Overexpression of miR-290 promotes G1/S transition in mouse ES cells by regulating p21, Rbl2, and Lats2, and prevents early differentiation by directly targeting two cell cycle regulating genes, Wee1 and Fbx15 [258].

hES cell enriched miRNAs can be categorized in four major groups: miRNA from the miR-302 cluster, miRNAs from the miR-17 family, miRNAs from the miR-371-373 cluster, and miRNAs from chromosome 19 miRNA cluster. More additional families have been found enriched in hES cells by recent studies, such as miR-130 and miR-200 [252]. The promoter region of most of those miRNAs can be regulated by OCT4, SOX2, and NANOG [257]. These groups of miRNAs are important for maintenance of hES cell in

and undifferentiated state. Such as the miR-302 family, which include miR-302a/a*/b/b*/c/c*/d and miR-367, is highly expressed in hES cells and hiPS cells [259]. The transcription factors *OCT4, NANOG* and *SOX2* are required for the transcription regulation of miR-302 through binding to its promoter [210]. Conversely, miR-302–367 is required for the expression of these pluripotency factors forming an autoregulatory positive loop in pluripotent cells. The miR-302 also promotes G1/S transition by inhibiting cyclin D1 and inhibition of miR-302 induce pluripotent hES cells accumulate in G1 phase [210].

1.3.4 The Role of miRNAs in Reprogramming

The iPS cells were first generated from mouse fibroblasts by overexpression of four Yamanaka factors, *OCT4, SOX2, KLF4* and *c-MYC* [42,43]. Except Yamanaka factors, other methods have also been investigated to generating iPS cells, including using miRNAs. Previous study showed overexpression miR-291-3P, miR-294 and miR-295 with *OCT4, SOX2 and KLF4* can generate iPS cells [260]. The same group also demonstrated that miR-302 and miR-372 family transfected with Yamanaka factors can enhance reprogramming efficiency [219]. Overexpression of miR-302/367 can reprogramme mouse and human cells without other factors [55]. Transfected a combination of miR-200c, miR-302 family and miR-369 family can reprogram mouse somatic cells and human somatic cells to pluripotency [261].

Downregulation of some miRNAs also contribute to increase reprogramming efficiency. Knockdown miR-21 and miR-29A in MEFs enhances reprogramming efficiency by reducing expression of P53 [262]. miR-34 is a target of p53 during reprogramming. Knockdown of miR-34 in MEF promoted iPSC generation without affecting self-renewal or differentiation [263]. These results indicate the important roles of miRNAs in regulating reprogramming of somatic cells into iPS cells.

Recent studies have also demonstrated the potential role of miRNAs as regulators of trans-differentiation. miR-124 combined with *MYT1L* and *BRN2*, was sufficient to directly reprogram adult human primary dermal fibroblasts (mesoderm) to functional neurons (ectoderm) in the absence of other cell types [264]. miRNA have been used to improve the direct reprogramming efficiency of fibroblasts into cardiomyocytes. Recent study indicated that transient transfection of miR-1, miR-133a, miR-208a, and miR-499 could induce mouse fibroblasts reprogramming into cardiomyocytes, both *in vitro* and *in vivo* [265].

1.3.5 The Role of miRNAs in Regulating ES Cell Differentiation

Recent studies have shown that some miRNAs promote the transition from self-renewal to differentiation by either directly suppressing self-renewal state or stabilizing the differentiated state [266].

In mouse ES cells miR-134, miR-296, and miR-470 induce differentiation by directly targeting the pluripotency genes, Oct4, Nanog, and Sox2 [267,268]. miR-200c, miR-203, and miR-183 were found to repress Sox2 and Klf4 [269].

In hES cells, miR-145 is significantly upregulated during differentiation and directly suppresses self-renewal by targeting *OCT4, SOX2* and *KLF4* [270]. miR-145 itself is repressed by *OCT4* in hES cells by a negative feedback loop [270]. Let-7 is repressed in ES cells but rapidly upregulated during differentiation. The introduction of let-7 into Dgcr8-knockout ES cells successfully silences their self-renewal and pluripotency [213]. It also been reported that knockdown of the *let-7* family can promotes reprogramming efficiency [271].

As shown in Figure 15, miRNAs also have functions in regulate lineage-specific differentiation.
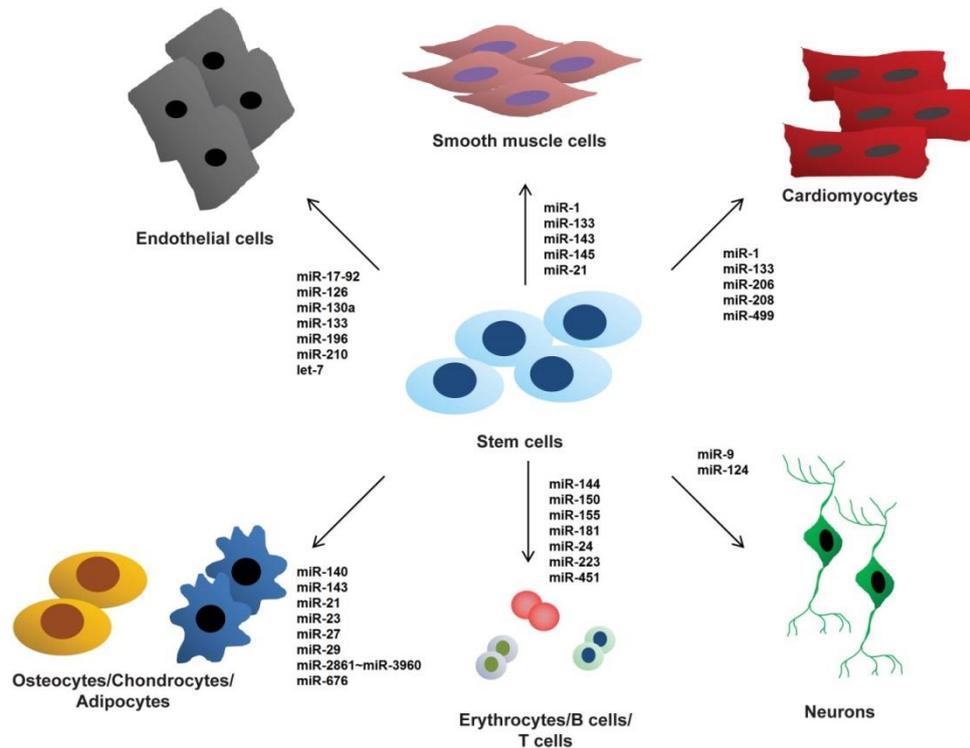
Figure 15. miRNAs are capable of regulating proliferation and differentiation in various somatic stem cells.

Selected miRNAs can regulate lineage-specific cells differentiation (Adapted from Ong et al 2015) [266].

1.3.6 miRNAs Regulate the G1/S Transition in Mouse ES cells

Mouse ES cells have a high self-renewal capacity. The cycling time of mouse ES cells is ~10 h, while in differentiated cells is more than 18h. ES cells have a very short G1 phase (~2 h) and more than 50% of the cells are in S phase of the cell cycle [249]. This has been attributed to high activity of constitutively active cyclin E/Cdk2 complex throughout the cell cycle [185]. The high activity of Cdk2 leads to rapid proliferation and avoids the differentiation of mouse ES cells during G1 phase. Studies in Dicer or Dgcr8 knockout models indicate an important role for miRNAs in regulation of cell cycle. Knockdown of Dicer or Dgcr8 in murine ES cells results in negation of miRNA generation ability [254]. Furthermore, murine ES cells show reduced proliferation, impaired differentiation [254,272] and cell accumulation in G1 phase of the cell cycle, thus suggesting that miRNAs may play an important role in G1/S transition in murine ES

cells. To understand miRNAs function in ES cells, the miRNA mimics, were individually transfected into the Dgcr8 knockout cells [256]. Several of those miRNAs rescued the Dgcr8 knockout phenotype. These miRNAs include miR-290 cluster, miR-302 cluster and a group of miRNAs with similar seed sequence "AAAGUGC" including miR-20, miR-93, and miR-106 [273].

In wild type ES cells, the expression level of the miR-290 cluster is the highest [257]. The miR-290 cluster includes miR-291a-3p, miR-291b-3p, miR-294 and miR-295 [256,274]. Transfection of these miRNAs individually can fully rescue the G1 phase arrest and promote cell proliferation thus demonstrating that these miRNAs play a role in regulating G1/S transition [275].

The group of miRNAs, which are enriched in ES cells and can regulate cell cycle, are named as ESCC miRNAs for Embryonic Stem cell specific Cell Cycle regulating miRNAs [256]. It has been found that the ESCC miRNAs can regulate cyclin E/Cdk2 by suppressing cell cycle inhibitors such as p21, Rbl1, Rbl2 and Lats2 [256,274].

1.3.7 miRNAs Regulate Cell Cycle in hES Cells

hES cells proliferate quickly, and similarly to mouse ES cell are characterized by a short G1 phase. Similarly, miRNAs also play roles in regulating hES cells cell cycle. For example, the miR-302 cluster can promote G1/S transition in hES cells [210]. miR-302 cluster is abundant in hES cells and decreases dramatically during the ES cell differentiation. Inhibition of the miR-302 cluster increases percentage of cells in G1 phase of cell cycle, down regulates pluripotency maker SSEA-3 and decreases the number of Oct4 positive clones. The miR-302 cluster promotes hES cells entry S phase by repressing CyclinD1/Cdk4 [276].

Knockdown of DICER or DROSHA in hES cells results in reduced generation of miRNAs, cell accumulation not only in G1 phase but also G2/M [187]. The G1 related phenotype is rescued by overexpression of miR-372 which is thought to regulate the cyclin E/Cdk2 pathway in G1/S transition by inhibiting the cell cycle inhibitor CDKN1A (p21) [277]. In addition, miR-92b regulate the Cdk2/Cyclin D complex in G1/S transition by inhibiting the cell cycle inhibitor CDKN2B (p57) [278]. The G2/M phenotype can be rescued by overexpression of miR-195 which regulates WEE1 kinase, a known inhibitor of cyclin B/Cdk1 proven to be necessary for G2/M transition (Figure 16) [275]. This miR-195/WEE1 pathway may be specific for hES cells because there is no

significant G2/M arrest in mouse Dicer or Dgcr8 knockout ES cells model and furthermore miR-195 is not highly expressed in mouse ES cells [275].

The miRNAs involved in regulate cell cycle in mouse ES cells and hES cells is summarized in Figure 16.
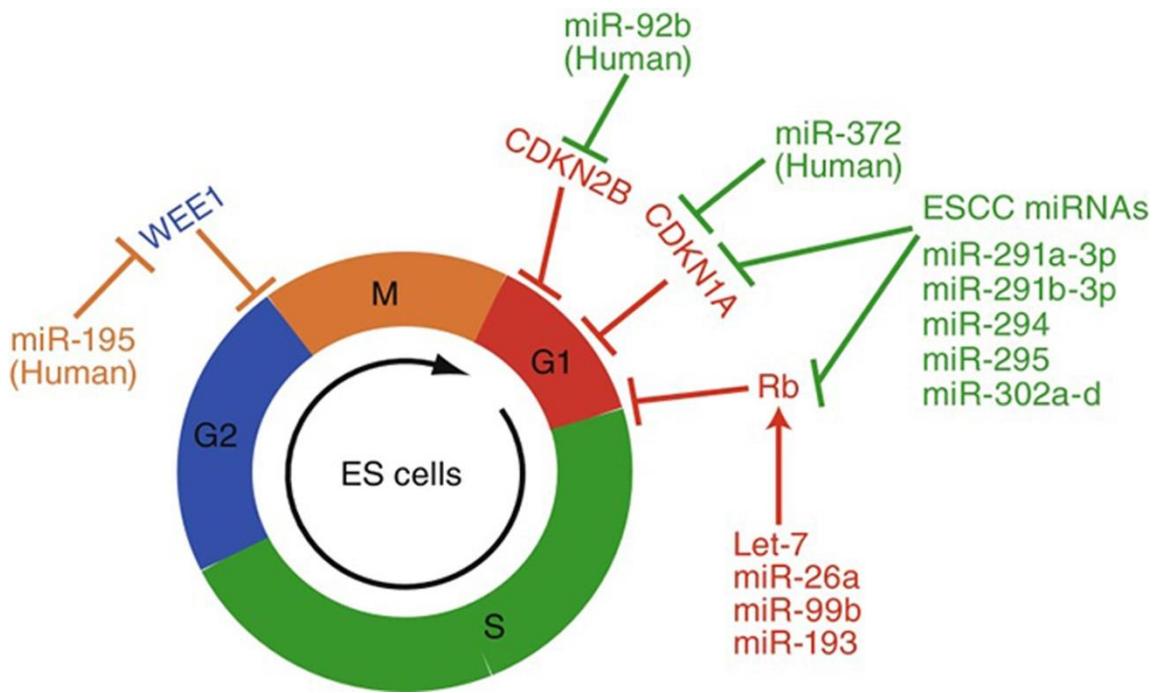
Figure 16 . miRNAs that regulate cell cycle of mouse ES cells and hES cells.

(From WenTing Guo et al 2014) [27].

Recent studies suggest that several miRNAs can regulate cell cycle through the p53 pathway [279-281]. miR-125b and miR-504 can induce cell cycle arrest through directly down-regulating p53 expression level [282]. And miR-34a/b/c can upregulate p53 via repressing the level of SIRT1, which is a negative regulator of p53 [283]. miR-122 upregulates p53 by inhibiting Cyclin G1, which can form a complex with PP2A [284,285]. This complex can phosphorylate and increase the activity of MDM2 to repress p53. The miR-192 family regulate p53 by targeting the IGF pathway and MDM2, which reduce p53 activity [286,287]. More details of regulation of p53 by miRNAs are summarized in Figure 17.
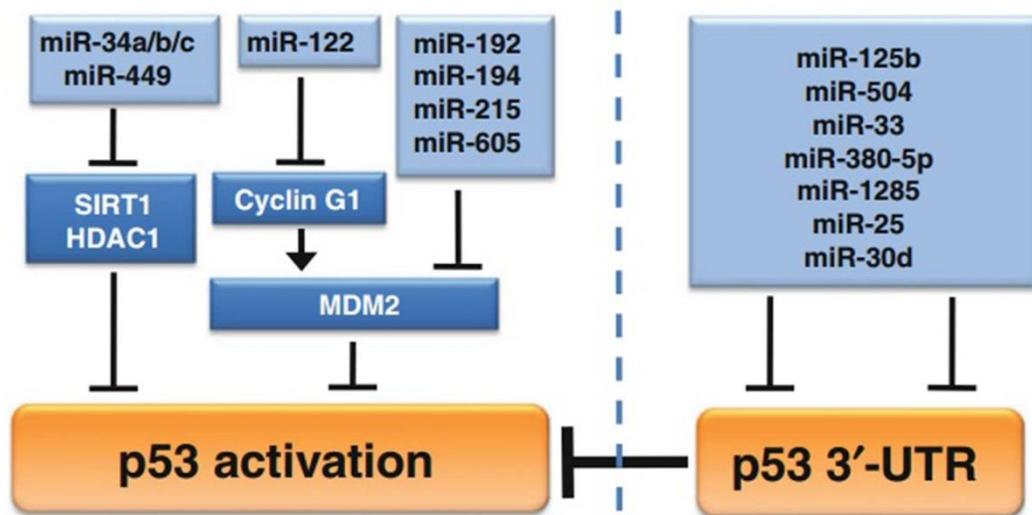
Figure 17. Multiple miRNAs regulate the activity and function of p53.
Model summarizing the regulation of the 3'-UTR of p53, and the down-regulation of p53-modifying enzymes by miRNAs. (Adapted from Sabine Hüntenet et al. 2013) [288].

In summary, miRNAs play a role in regulating G1/S transition in hES cells [275]. As hES cells maintain rapidly self-renewal and pluripotency is partly due to their unique cell cycle structure characterized by a short G1 phase [187], it is very important to understand the mechanisms that govern the G1 to S phase progression in detail in embryonic stem cells and how this impacts the maintenance of pluripotency by miRNA.

CHAPTER 2 METHODS

Chapter 2. Methods

2.1 MEF Generation

Swiss MF1 pregnant females (12.5-13.5 dpc) were sacrificed by experienced, qualified animal handlers. All embryos were removed from the uterus using sterile surgical instruments and placed in a dish containing Phosphate Buffered Saline (PBS) supplemented with 10% Fetal Bovine Serum (FBS) and antibiotic (penicillin/streptomycin; 1%) to reduce potential infections. All visible organs (head, tail, limb, heart and liver) were removed under a dissection microscope and the remaining embryo was washed in fresh PBS. Scissors were used to mince the remaining bodies before further incubation in 1% Trypsin-EDTA (Sigma) for 5 minutes at 37°C. Cell suspension was pipetted repeatedly till single cell disassociation was achieved. The trypsin was inactivated by adding fresh MEF culture media containing 10% FBS. The cell suspension was centrifuged at 1000 rpm for 3 minutes. After removal of supernatant, the cell pellet was resuspended in fresh media and transferred to T75 (Iwaki) flasks (one embryo per flask). Flasks were incubated at 37°C in a humidified atmosphere (>95%) and with 5% CO_2.

2.2 MEF Culture and Passage

Primary MEF cultures were inspected every day to check for cell density and morphology. MEF media (Table 6) was changed every 2 days and MEFs were sub-cultured when 80%-90% confluence was observed. Sub-culturing was carrying out by washing MEFs with PBS and incubating with 0.05% trypsin-EDTA at 37°C for 5 minutes. Trypsin was inactivated by adding fresh MEF media. The cells suspension was centrifuged at 800 rpm for 3 minutes. The supernatant was removed and cells were passaged in a ratio of 1:3 by resuspending in fresh MEF media. Flasks were incubated at 37°C in a humidified atmosphere (>95%) and with 5% CO_2.

Reagent	Proportion	Supplier
Dulbecco's Modified Eagle's Medium	87%	Gibco
Fetal Bovine Serum (FBS)	10%	Gibco
Non-Essential Amino Acids (NEAA)	1%	Gibco
L-Glutamine	1%	Gibco
Penicillin-Streptomycin	1%	Gibco

Table 6. MEF media composition

2.3 Mitotic Inactivation of MEFs

Normally MEFs were inactivated at passage 5. The media was removed and the MEFs were washed with PBS. The cells were cultured in the media supplemented with 10 µg/ml Mytomycin C for 3-4 hours. Then the media was removed, the cells were washed 5-7 times with PBS and digested with 0.05% trypsin-EDTA, and centrifuged at 800 rpm for 3 minutes. The cells were resuspended in fresh MEF media and plated in pre-gelatinized 6 well plates at the concentration of 1.5×10^4 cells/cm^2 or 5.6×10^4 cells/cm^2 (as the quality of MEFs are variable among batches).

2.4 Cryopreservation of MEFs

Confluent flasks of MEFs were washed by PBS and digested with 0.05% trypsin-EDTA at 37°C for 5 minutes. The cell suspensions were centrifuged at 800 rpm for 3 minutes, the supernatant was removed and the cells were resuspended in MEF freezing media (Table 7). The cell suspensions were transferred to the cryovials (Nunc) and stored at -80°C in the "Mr Frosty" box. 1 day later, the vials were removed for long term storage in liquid nitrogen.

Reagent	Proportion	Supplier
MEF media	90%	-
DMSO	10%	Sigma

Table 7. MEF freezing media

2.5 hES Cells and hiPS Cells Culture on MEF Feeder Layer

hES cells and hiPS cells were cultured on MEF feeder layers in the 37°C incubator with a humidified atmosphere (>95%) and with 5% CO_2. The media (Table 8) was changed every 24 hours. The cell morphology was observed under inverted phase contrast microscope every day. All visible differentiated cells were manually removed before further   passaging.

Reagent	Proportion	Supplier
Knock Out-Dulbecco's Modified Eagle's Medium (KO-DMEM)	77%	Gibco
Knock Out-Serum Replacement (KO-SR)	20%	Gibco
Non-Essential Amino Acids (NEAA)	1%	Gibco
L-Glutamine	1%	Gibco
Penicillin-Streptomycin	1%	Gibco
Basic Fibroblast Growth Factor (bFGF)	8 ng/ml	Sigma

Table 8. hES cells and hiPS cells media

2.6 hES Cells and hiPS Cells sub-culture on MEF Feeder Layer

hES cells and hiPS cells were passaged every 4-5 days by mechanical procedure or collagenase IV. The cell morphology was observed under the microscope and the differentiated parts of the colonies were scraped away before sub-culturing.

For the mechanical procedure, the colonies were cut into smaller pieces (3 or 4 smaller pieces) with needles or tips, then they were transferred into a new 6 well plate with feeder layer by using a P200 (200μl) pipette, and cultured in the 37°C incubator with a humidified atmosphere (>95%) and with 5% CO_2.

For the collagenase method, the culture media was aspirated first, and then 1 ml collagenase IV (5 mg/ml) was added to each well. The plate was incubated at 37° C for 5 minutes. Then the collagenase was removed, 2 ml of fresh media was added in each well and pipetted up and down gently for several times. The cell suspensions were collected in a new tube and centrifuged at 900 rpm 3 minutes. The supernatant was removed and the cells were resuspended in the fresh media by gentle mixing. The cell suspensions were distributed to a new 6 well plate covered with feeder layers (split ratio

1:3 or 1:4), and cultured in the 37°C incubator with a humidified atmosphere (>95%) and with 5% CO_2.

2.7 hES Cells and hiPS Cells Feeder free Culture with Condition Media

Sub-culturing of hES cells was carried out as outlined in 2.6 and the cells were transferred to the matrigel coated plates with MEF conditional medium (Table 9) at 37°C incubator with a humidified atmosphere (>95%) and with 5% CO_2.

Reagent	Proportion	Supplier
hES cell media		See Table 5
Extra Basic Fibroblast Growth Factor (bFGF)	16ng/ml	Sigma
Insulin-Transferrin-Selenium Supplement (100X)	1%	Gibco

Table 9. MEF conditioned medium.
Inactivated MEFs were incubated with hES cell media. The media could be collected everyday (<10 days) and filtered through a 0.2 μm filter to remove any remaining cells.

2.8 hES Cells and hiPS Cells Culture in mTeSR1 Media

All hES cells and hiPS cells lines were transferred from feeder culture to the matrigel (growth-factor-reduced; BD Biosciences) coated plates with mTeSR1 media (Stem Cell Technologies) according to Wicell Inc. protocols. Cells were passaged every 4-5 days at ~80% confluence by using 0.02% EDTA (Versene). All visible differentiated cells were manually removed before further passaging.

2.9 Embryoid Body (EB) Culture

The hES cells were cultured on Matrigel coated plate with mTeSR1 media. The differentiation parts were removed. When 80%-90% confluence was observed, the cells were digested by collagenase IV and resuspended in human EB media (Table 10). Three wells of hES cell colonies were transferred to one well of the ultra-low attachment 6 well plates (Corning) for EB formation. The EBs were incubated at 37°C incubator with a humidified atmosphere (>95%) and with 5% CO_2. Media was changed every 3-4 days.

Reagent	Proportion	Supplier
Knock Out-Dulbecco's Modified Eagle's Medium (KO-DMEM)	77%	Gibco
Fetal Bovine Serum (FBS)	20%	Gibco
Non-Essential Amino Acids (NEAA)	1%	Gibco
L-Glutamine	1%	Gibco
Penicillin-Streptomycin	1%	Gibco

Table 10. EB media

2.10 Cell Cycle Synchronization

hES cell were cultured under feeder free culture condition. To achieve cell synchronization in G2/M phase, the media was removed and the cells were re-covered with the fresh media with 200 ng/ml nocodazole (Sigma-Aldrich Ltd, Dorset, UK) as described by Becker et al [187]. After 16 hours, the media was removed and the cells were washed with warm media for 5 times. This treatment results in cell accumulation in G2/M phase [171]. To achieve cell synchronization in G1 phase, the cells were first synchronized into G2/M phase, and then the cells were further cultured in the media with 10 mg/ml of aphidicolin (Sigma) for 10 hours. To achieve cell accumulation in S phase, the cells were first synchronized into G2/M phase and replaced with the fresh media, then further cultured for 10 hours [171].

2.11 miRNA Isolation by TaqMan® MicroRNA Cells-to-C ™ Kit

TaqMan® MicroRNA Cells-to-C ™ Kit (Cat. 4391848) was used for miRNA isolation. Medium was removed and cells were washed with PBS once. Then 1 ml Accutase was added in to 1 well of the 6 well plate to detach the cells. The plate was incubated at 37°C for 3 minutes. 2 ml of cold media was added in to the well to inactivate the Accutase. The media was pipetted up and down gently. The cell suspensions were collected in a new tube, and centrifuged at 800 rpm for 3 minutes.

Approximately 1×10^5 cells were required for each sample according to the instruction of the kit. The samples were washed with cold PBS, and centrifuged at 800 rpm for 3 minutes. PBS was removed and cells were resuspended in 5 µl cold PBS and 50µl lysis solution with DNase I (1:100). The lysis were gently mixed by pipetting up and down for 5 times, and then incubated at room temperature (19-25°C) for 8 minutes. 5 µl stop

solution was added to the tube and mixed by gently pipetting 5 times and incubating at room temperature for 5 minutes to inactivate the lysis solution. These lysates are subsequently stored at -20°C.

2.12 miRNA Reverse Transcription (RT)

TaqMan® MicroRNA Reverse Transcription Kit was used for miRNA reverse transcription. 1 to 10 ng of total RNA sample were used per 15 µl RT reaction. TaqMan® MicroRNA probe was used as the Reverse Transcription (RT) primer. Each reaction included 7 µl master mix (Table 11), 3 µl 5 X RT primers and 5 µl of RNA sample (1-10 ng).

Components	Master mix volume per 15-µL reaction
100 mM dNTPs (with dTTP)	0.15 µL
MultiScribe™ Reverse Transcriptase, 50 U/µL	1.00 µL
10✕ Reverse Transcription Buffer	1.50 µL
RNase Inhibitor, 20 U/µL	0.19 µL
Nuclease-free water	4.16 µL
Total volume	7.00 µL

Table 11. TaqMan® MicroRNA Reverse Transcription master mix components

The samples were incubated at 16°C for 30 min, followed by 42°C for 30 min, and then 85°C for 5 min to inactivate the RT enzyme (Table 12).

Step	Time	Temperature
Hold	30 minutes	16°C
Hold	30 minutes	42°C
Hold	5 minutes	85°C
Hold	--	4°C

Table 12. Reverse Transcription program

2.13 miRNA Real-time quantitative PCR by Taqman System

TaqMan® Small RNA Assays kit was used for Real-time quantitative PCR (qPCR). Details of reaction composition are shown in Table 13.

Components	Volume per 20-µL Reaction
TaqMan® Small RNA Assay (20x)	1.00 µL
Products from RT reaction	1.33 µL
TaqMan® Universal PCR Master Mix II (2X), no UNG	10.00 µL
Nuclease-free water	7.67 µL
Total volume	20.00 µL

Table 13. Real-time quantitative PCR reaction components

Thermal Cycling Conditions are as follows: enzyme activation (95°C, 10mins), 40 cycles of Denaturion (95°C, 15 seconds) and Anneal/extend (60°C, 60seconds) (Table 14). The program was performed on an ABI 7900 machine. Data was analysed by using the ABI Sequence Detection System 2.3 (SDS 2.3) software. Further data analysis and normalization was applied using the qBase v1.3.5 software.

Steps	Enzyme Activation	PCR Amplification	
	HOLD	CYCLE (40 cycles)	
		Denature	Anneal/extend
Temperature	95°C	95°C	60°C
Time	10 minutes	15 seconds	60 seconds

Table 14. Real-time quantitative PCR program

2.14 Cell Cycle Analysis by Flow Cytometry

BD Cycletest™ Plus DNA Reagent Kit was used to analyze cell cycle progression. First, the cells were washed by PBS. Then the PBS was removed and Accutase were added into the well to digest the cells at 37°C for 3 minutes. Cold hES cell media was added to inactivate the Accutase. The media was pipetted gently up and down until single cell suspension was achieved. The cell suspension was centrifuged at 800 rpm for 3 minutes. The culture media was aspirated, the cells were resuspended in 3 ml buffer solution and centrifuged at 800 rpm for 3 minutes. The buffer solution was discarded and the cell pellet was incubated at room temperature for 10 minutes with 200 µl solution A (trypsin in spermine tetrahydrochloride detergent buffer), then added 200 µl solution B (RNase A and trypsin inhibitor in spermine buffer) for further 10 minutes incubation, and final 10 minutes incubation by adding 100-150 µl solution C (Propidium Iodide (PI) in spermine buffer) at 4°C.

2.15 Plasmid Transformation

One Shot® of TOP10 Chemically Competent E. *coli* was used for plasmid transformation. 50-100 ng of plasmid DNA was added to the competent cells gently. The cells were incubated on ice for 30 minutes and then subjected to a heat shock for 30 seconds in 42°C water bath followed by incubation on ice for 2minutes. 250 µl Luria-Bertani (LB) broth (Table 15) was added to the cells and placed in a 37°C shaking incubator for 0.5-1 hour. Then 10-50 µl cells were spread on a pre-warmed agar plate (Table 16). The plates were incubated at 37°C overnight.

Reagent	Proportion
Tryptone	1%
Sodium Chloride	1%
Yeast Extract	0.5%
Ampicillin	100 µg/ml

Table 15. LB Broth with Ampicillin

Reagent	Proportion
Tryptone	1%
Sodium Chloride	1%
Yeast Extract	0.5%
Agar	1.5%
Ampicillin	100 µg/ml

Table 16. Agar Plates with Ampicillin

2.16 Mini Bacterial Culture

Small single colonies were picked up from the bacterial plates using a 100 µl pipette tip and placed in a 15 ml tube with 2-5 ml LB broth (with 100 µg/ml ampicillin). The tube was then cultured in a 37°C shaking incubator for 16-20 hours.

2.17 Plasmid DNA isolation by QIAGEN® Plasmid Maxi Kit

2-5 ml bacterial from bacterial mini cultures were transferred in to a conical flask with 200 ml LB and 100 µg/ml ampicillin and incubated at 37°C shaking incubator (250 rpm) for 16-20 hours. The bacterial cells were harvested by centrifugation at 4000 rpm for 30 minutes at 4°C. All the bacterial media was removed and 10 ml buffer P1 containing RNase was added to the tube. The cells were suspended sufficiently by gently pipetting up and down for several times. Then 10 ml of buffer P2 was added into the tube and the suspension was mixed gently by inverting 10 times. After 5 minutes incubation at room temperature, 10 ml of chilled buffer P3 was added into the tube, the mixture were mixed gently and immediately. The tube was incubated on ice for 5 minutes. After centrifugation at 4000 rpm for 30 minutes, the supernatant fluid was transferred into a new 50 ml tube with 2.5 ml buffer ER. The mixture was mixed gently by inverting the tube and incubating on ice for 30 minutes. During the waiting time, a QIAGEN-tip 500 was equilibrated by adding 10 ml buffer QBT. The column was emptied by gravity flow. After the tip was empty, the lysates were added into the QIAGEN-tip and allowed to enter the resin by gravity flow. The tip was washed by 30 ml buffer QC twice. 15 ml buffer QN was added in the tip to elute the DNA. The eluted liquid flowing from the tip was collected into a new tube and plasmid DNA was precipitated by adding 10.5 ml isopropanol. After centrifugation at 4000 rpm for 1 hour at 4°C, the supernatant was

decanted and the DNA pellet was air dried at room temperature for 5 minutes. The DNA pellet was further washed in 5 ml endotoxin-free 70% ethanol and centrifuged at 4000 rpm for 1 hour at 4°C. The ethanol supernatant was carefully decanted and the DNA precipitate was dried in air for 5 minutes, and then dissolved in TE buffer or endotoxin-free water.

2.18 Plasmid Restriction Enzyme Digestion

Restriction enzyme digestion was used to test the correctness of plasmids. The reaction was performed in the system as shown in Table 17, and incubated at the enzyme's optimum temperature for 1-4 hours.

Components	Volume
Sterile, deionized water	15.8 µl
Restriction Enzymet 10X Buffer	2 µl
Acetylated BSA, 10 µg/µl	0.2 µl
DNA, 1 µg/µl	1.0 µl
Mix by pipeting, then add:	
Restriction Enzyme, 10 u/µl	1 µl
Final volume	20 µl

Table 17. Digestion reaction

2.19 Plasmid Linearization and Purification

The correct plasmid need to be linearized and purified before the transfection. The components of linearization are shown in Table 17. After the linearization, an equal volume of phenol/chloroform/isoamyl alcohol (24:25:1, Invitrogen) was added into the plasmid linearization mixture and mixed gently. The aqueous phase which contains plasmid DNA can be separated by centrifuged at 10000 rpm for 1 minute. The aqueous phase were removed carefully to a new tube with 1/10X volume 3M sodium acetate (pH 5.2) and 2.2X volume absolute cold ethanol. The reaction was incubated at -20°C overnight or -80°C for 30minutes. The plasmid DNA was collected by centrifugation at 12000 rpm for 5 minutes at 4°C. The ethanol was removed carefully and DNA pellet was further washed with 70% ethanol to remove excess salt from the pellet. The tube was centrifuged at 12000 rpm for 2 minutes. The ethanol was removed, and the plasmid

was air dried for 5 min. The DNA pellet was resuspended in TE buffer (pH 8.0) and stored at -20°C.

2.20 Plasmid Electroporation

Amaxa® Cell Line Nucleofector® Kit L (Lonza) was used for Electroporation. The hES cells were cultured on matrigel coated dishes. Upon reaching 80%-90% confluent, cells were harvested using collagenase IV and pipetted into single cell. The single cell suspension was resuspended into 90 μl mix (81.8 μl Cell Line Nucleofector® Solution and 18.2 μl Supplement) with 5-10 μg plasmids. The mix of cells and DNA was transferred into a cuvette and the Nucleofector® Program A-023 was applied for electroporation. 500 μl of hES media supplemented with 10 μM ROCK-inhibitor was added to the cuvette and the cells were gently transfer to a pre-prepared 12 well feeder dish and incubated at 37°C in a humidified atmosphere (>95%) and with 5% CO2.

2.21 Lipofection

Lipofectamine® RNAi Max reagent (13778-075, Life Technologies) was used for miRNA mimic/inhibitor transfection and Lipofectamine® 3000 regent was used for plasmid transfection. In brief, hES cells were dissociated by incubating with EDTA (0.02 %) for 5 minutes. The disassociated cells were collected and centrifuge at 500g for 5 minutes. Then the supernatant was aspirated and the cell pellet was resuspended into 1 ml of media. Cell counting was performed prior to replating of cells at the density $3X10^5$ cells into one well of a 12 well plate one day before lipofection.

For miRNA mimic/inhibitor lipofection, 6μl Lipofectamine® RNAiMax reagent was diluted into 100 μl Opti-MEM® media. In parallel, 6 μl (60 pmol) miRNA mimic/inhibitor was diluted into 100 μl Opti-MEM® media. The diluted Lipofectamine reagent and miRNA mimic/inhibitor were mixed together in a 1:1 ratio, incubated for 5 minutes and then added to one well of a 12 well plate which was seeded with hES cell as indicated above.

For plasmid lipofection, 3 μg plasmids (each well of 12 well plate) were used to transfect hES cells following manufacturer's recommendations.

2.22 RNA and miRNA Isolation by ReliaPrep™ RNA Cell Miniprep System

ReliaPrep™ RNA Cell Miniprep System (Promega) was used for RNA and miRNA isolation. Details of reaction compositions are shown in Table 18. In brief, media was removed from cells and one cold PBS wash was carried out. Then 250 µl BL+TG lysis buffer was added to the cells and the lysate was transferred to a sterile centrifuge tube, followed by adding of 85µl of 100% isopropanol. The mixed lysate was transferred to a ReliaPrep™ minicolumn then centrifuged at 12,000 x g for 30 seconds in room temperature. The column was washed with 500µl RNA wash solution prior to a further centrifugation step at 12,000 x g for 30 seconds at room temperature. 30µl DNase I enzyme and Yellow core buffer mixture was added into each tube and further incubated for 15 minutes at room temperature. After incubation, a further wash with 200µl Column wash solution followed by a centrifugation step at 12,000 x g for 15 seconds. Two more washes with RNA wash solution were carried out (the first with 500µl and the second with 300µl RNA wash solution) followed by a final centrifugation step at 12,000 x g for 2 minutes. 20-30 µl nuclease-free water was added to the membrane and RNA solution was collected in a new collection tube after centrifugation at 12,000 x g for 1 minute. The purified RNA was stored at -80 °C.

Reagents	Composition
BL+TG buffer	4 M Guanidine thiocyanate 0.01 M Tris (pH7.5) 2 % 1-Thioglycerol
Yellow Core buffer	0.0225 M Tris (pH7.5) 1.125 M NaCl 0.0025 % yellow dye (w/v)
RNA wash solution	16.82 mM potassium acetate 27.1 mM Tris-HCl (pH 7.5)

Table 18. Composition of RNA isolation buffers and solutions

2.23 Reverse Transcription

GoScript™ Reverse Transcription system was used for reverse transcription. Details of reaction compositions are shown in Table 19 and 20. First the RNA and Oligo (dT) $_{15}$ were incubated at 70°C for 5 minutes. The tube was chilled on ice for 5 minutes. 15 µl reverse transcription mix was combined with 5µl of RNA and Oligo (dT) $_{15}$ mix. The

tube was further incubated at 25°C for 5minutes. This step was followed by further 42°C incubation for 1 hour.

Components	Volume
RNA	X µl (up to 0.5 µg/reaction)
Oligo (dT) $_{15}$	1 µl
Nuclease-free water	4-X µl
Final volume	5 µl

Table 19. GoScript™ Reverse Transcription components part 1

Components	Volume
GoScript™ 5X reaction buffer	4.0 µl
$MgCl_2$	1.5 µl
PCR Nucleotide Mix	1 µl
Recombinant Rnasin® Ribonuclease inhibitor	0.5 µl
GoScript™ Reverse Transcriptase	1 µl
Nuclease-free water	7 µl
Final volume	15 µl

Table 20. Reverse Transcription components part 2

2.24 Real-Time quantitative PCR by SYBR Green System

GoTaq® qPCR master mix reagent was used for quantitative PCR. Details of reaction composition are shown in Table 21. Thermal Cycling Conditions are as follows: hot-start activation (95°C，2 minutes), 40 cycles of Denaturation (95°C, 15 seconds) and Anneal/extend (60°C, 60seconds; shown in Table 14). The program was performed on an ABI 7900 machine. The data was analyzed by using the ABI Sequence Detection System 2.4 (SDS 2.4) software. Further data analysis and normalization was applied by qBase v1.3.5 software.

Components	Volume per-10 µl Reaction
GoTaq® qPCR master mix 2X	5 µl
CXR Reference Dye	0.1 µl
Products from RT reaction	0.4 µl
PCR primers	0.4 µl (0.04 µM)
Nuclease-free water	4.1 µl

Table 21. GoTaq® qPCR master mix reagent components

2.25 Western Blot

Cells were washed with ice-cold PBS and lysed in RIPA buffer (50 mmTris-HCl pH 8.0, 150 mm NaCl, 1% IGEPAL CA 630, 0.5% Na-DOC and 0.1% SDS) with PMSF(1mM) and protease inhibitors (Thermo). The total protein concentration was determined by Bradford Kit (Bio-Rad Laboratories Ltd, Hemel Hempstead, UK) using the manufacturer's instructions. Lysates (30 µg total protein) were electrophoresed on a 10–12% SDS–PAGE gel and electrophoretically transferred to a polyvinylidene difluoride membrane (Hybond-P (hydrophobic polyvinylidene difluoride membrane, cat no. RPN303F); Amersham Biosciences, Piscataway, NJ, USA). Membranes were blocked in Tris-buffered saline with 5% milk and 0.1% Tween. The blots were probed with anti-ZIC2 (1:1000, Abcam), LIN28A (1:1000, Santa Cruz Biotechnology, Inc.), GAPDH (1:750, Abcam), POLR3G (1:500, Santa Cruz Biotechnology, Inc) overnight and revealed with horseradish peroxidase-conjugated secondary anti-rabbit or anti-mouse antibodies (DAKO). Antibody–antigen complexes were detected using ECL Plus reagent (Pierce). Antibodies to GAPDH were used after membrane stripping to confirm uniform protein loading.

2.26 Luciferase Reporter Assays

The 3'-UTR of human POLR3G was cloned into a commercial psiCHECK™-2 vector, which contains two luciferase, Renilla and firefly. The predicted binding regions were mutated by PCR with individual mutant primers by using Quick Change II XL site-Directed mutagenesis kit (Agilent Technologies, Inc.). Thermal Cycling Conditions are showed in Table 22. The H9 cells were co-transfected by Lipofectamine 3000 (Invitrogen). Luciferase reporter assays were performed 48h post-lipofection using Dual-Luciferase® Reporter Assay (Promega) according to manufacturer's recommendations.

Segment	Cycles	Temperature	Time
1	1	95°C	1 minute
2	18	95°C	50 seconds
		60°C	50 seconds
		68°C	1 minute/kb of plasmid length
3	1	68°C	7 minutes

Table 22. Quick Change II XL site-Directed mutagenesis kit PCR program

2.27 RNA Interference

POLR3G was knocked down by using Silencer® Select siRNA (Invitrogen). 5.0 p mol of *POLR3G* siRNA was transfected into cells by Lipofectamine® RNAi Max reagent according to manufacturer's recommendations.

2.28 Statistical Analysis

Quantitative data are expressed as means ± SD. Statistical significance was determined by the Student's t-test. P-value < 0.05 was considered as statistically significant (*P < 0.05, **P <0.001).

CHAPTER 3 RESULTS I

Chapter 3. (Results I): Microarray-based Expression Profiling

3.1 Microarray-based Expression Profiling at different Stages of the hES Cell Cycle and Differentiation Process

Pluripotent stem cells, including hES cells and hiPS cells, can maintain unlimited self-renewal and have the potential to generate every differentiated cell type. These remarkable properties make them valuable resources for modelling early human development and regenerative medicines [44,289]. Much effort has been spent in recent years to understand the molecular mechanisms underlying hES cell pluripotency and differentiation, although a lot of work still remains in this respect. Regulation of cell cycle is closely related with the pluripotency and differentiation properties of hES cells and hiPS cells [215]. Specific knockdown of *CDK2* induces cell arrest in G1 and causes hES cells to differentiate into extra-embryonic lineages [25]. *NANOG* controls entry into S-phase in hES cells by promoting the expression of *CDC25C* and *CDK6* [208]. Recent studies have also demonstrated that miRNAs play important roles in modulating hES cell self-renewal and differentiation and somatic cell reprogramming [55,256,261,270,290-292]. For example, the miR-302 cluster, which is regulated by *OCT4*/*SOX2*, is highly expressed in hES cells[210], overexpression of this miRNA cluster can maintain stemness of hES cells and promote somatic cell reprogramming [55] and in parallel it can also regulate the cell cycle and apoptosis pathways by targeting Cyclin D1 [210], and BNIP3L/Nix respectively [293].

We hypothesised that miRNAs are hES cell specific (i.e. that they are expressed in hES cells and are downregulated during the differentiation process), that their expression levels significantly change during cell-cycle transition, and that they are likely to affect the regulation of both pluripotency and the cell cycle. To identify miRNAs which are potentially important in the regulation of both the cell cycle and hES cell pluripotency, Dr. Joseph Collin and Dr. Irina Neganova in our group collected the hES and human fibroblast cells samples (pluripotent vs. differentiated control), as well as hES cell samples that were specifically synchronized in G1, S, and G2/M phase. These samples were used for miRNA screening analysis using an Agilent human miRNA (V3) 8X15K microarray (Agilent, G4470) which contains 866 human and 89 human viral miRNAs probes.

The data was analysised by our collaborator Dr. David Montaner (Centro de Investigation Principe Felipe, Valencia, Spain). First the expression data generated from

the array was normalized using quintile normalization [294] and differential miRNA expression was subsequently estimated using the limma package [295] from Bioconductor. Statistical probability of significance (adjusted p values, set at $p < 0.05$) and a fold-change of more than two were used to select the miRNAs that were differentially expressed between hES cells, human fibroblast cells, or synchronised hES cells from different stages of the cell cycle. The number of miRNAs identified is summarized in Table 23.

Different stages of hES cells	Number ofmiRNAs identified (Fold change > 2, P<0.05)
G1 phase compared to S phase	55
S phase compared to G2 phase	142
G2 phase compared to G1 phase	212
hES cells compared to differentiated cells	375

Table 23. Summary of the miRNAs that were significantly changed between hES cells versus human fibroblast cells, and synchronised hES cells in different stages of the cell cycle.

These miRNAs were selected using a statistical probability of significance set at $p < 0.05$ and by accepting only miRNAs with a fold-change > 2.0.

A Venn diagram analysis of the miRNAs listed in Table 23 was carried out by Prof. Lako to identify the candidate miRNAs which were differently expressed between both hES cells versus human placental fibroblast cells, and hES cells from different stages of the cell cycle (Figure 18).
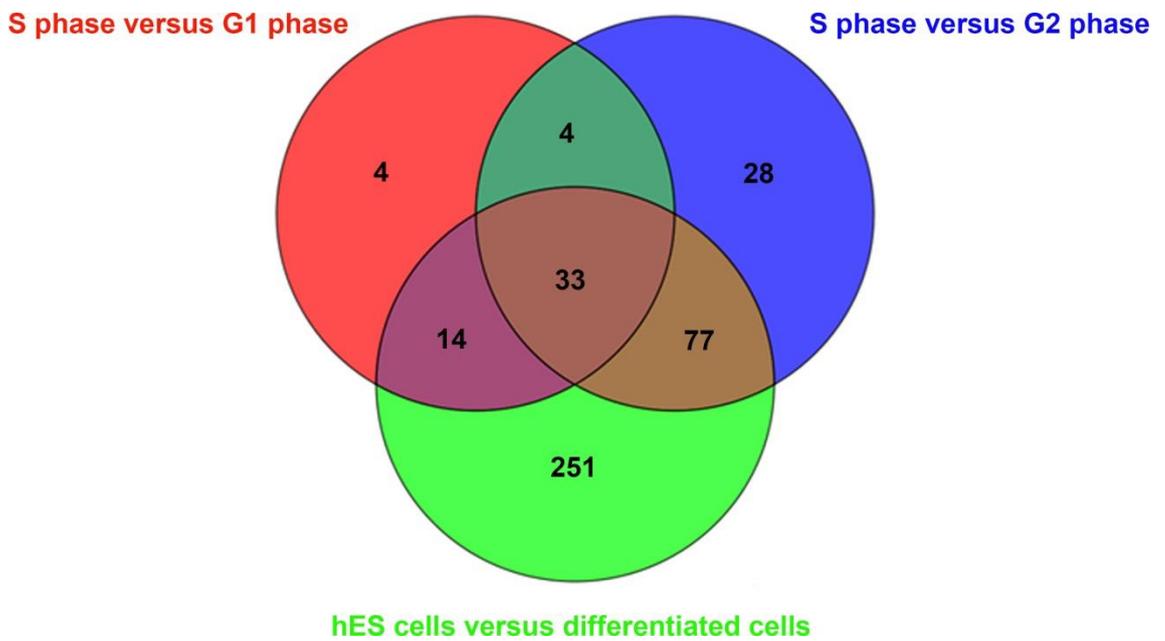
Figure 18. Venn diagram analysis of the miRNAs listed in Table 23.

The shared area in the middle indicates that 33 miRNAs were differently expressed between hES cells versus human placental fibroblast cells, S phase versus G1 phase, and S phase versus G2 phase.

This analysis identified 33 miRNAs in the central shared area (Figure 18), meaning that these miRNAs are differently expressed between hES cells versus fibroblasts, S phase versus G1 phase hES cells, and S phase versus G2 phase hES cells. The 33 miRNAs in the middle changed during hES cells differentiation and cell cycle process. The fold change in expression of these 33 miRNAs is summarized in Table 24.

The validity of our array data was further confirmed by checking the changes in expression of several other well-known miRNAs matched those reported in the literature. For example, in our array, miR-372, which is enriched in hES cells and promotes the G1/S transition, was also highly expressed in hES cells in S phase relative to the G1 and G2 phases.

miRNA	Fold change (S phase versus G1 phase)	Fold change (S phase versus G2 phase)	Fold change (hES cells versus differentiated cells)
hsa-miR-1305	6.1	15.2	25.9
hsa-miR-372	5.7	14.0	7.0
hsa-miR-892b	4.9	7.7	8.9
hsa-miR-1288	4.6	10.3	13.1
hsa-miR-181d	4.0	7.9	6.1
hsa-miR-371-3p	4.0	8.0	-5.1
hsa-miR-28-5p	3.5	4.4	-2.5
ebv-miR-BART12	3.4	7.1	16.6
hsa-miR-501-5p	3.3	6.2	5.8
hsa-miR-500	3.3	6.2	4.9
hsa-miR-503	3.1	3.2	-7.3
hsa-miR-874	-3.0	-2.8	10.2
hsa-miR-663	-3.1	-5.5	25.1
hsa-miR-30a*	-3.1	-9.9	-10.4
hsa-miR-9*	-3.2	-3.0	4.0
hsa-miR-1225-3p	-3.4	-3.5	3.6
hsa-miR-1228	-3.5	-2.7	7.7
hsa-miR-1238	-3.7	-3.6	3.2
hsa-miR-1234	-3.8	-5.5	19.5
hsa-miR-1181	-4.3	-7.0	20.2
hsa-miR-1207-5p	-4.4	-5.9	72.8
hsa-miR-125a-3p	-4.5	-3.0	11.8
hsa-miR-134	-4.6	-8.6	38.8
hsa-miR-150*	-4.8	-4.2	18.9
hsa-miR-885-5p	-4.8	-2.8	6.0
hsa-miR-1224-5p	-4.9	-6.0	19.0
hsa-miR-135a*	-5.2	-7.8	5.8
hsa-miR-629*	-5.6	-6.5	22.8
hsa-miR-1249	-5.6	-5.6	12.8
hsa-miR-1915	-5.8	-9.2	59.0
hsa-miR-601	-6.1	-4.4	11.2
hsa-miR-1226*	-7.6	-5.9	16.3
hsa-miR-1208	-8.0	-6.7	6.4

Table 24. List of miRNAs (33) that were differently expressed between hES cells versus human placental fibroblast cells, S phase versus G1 phase hES cells, and S phase versus G2 phase hES cells.

To narrow these target miRNAs down for further investigation, I checked the literature in the NCBI (National Center for Biotechnology Information) database which referred to the 33 miRNAs listed in Table 25, and listed their functions and targets, paying special attention to studies relating them to cell-cycle and/or pluripotency regulation.

miRNA	Target(s)	Funcion(s)
hsa-miR-1305	PTK2;RUNX2	Upregulated in periodontal ligament-derived stem cells from smokers
hsa-miR-372	CDK2/BCL2/TP53/CCNA1	Involved in cell cycle arrest at the S phase
hsa-miRNA-892b		
hsa-miR-1288		Highly expressed in embryonic tissues in ectopic pregnancies
hsa-miRNA-1181	SOX2/STAT3	Inhibits stem cell-like phenotypes and suppresses SOX2 and STAT3 in human pancreatic cancer.
hsa-miR-371-3p		Involved in neural differentiation
hsa-miR-28-5p	NRF2; MAD2	Regulates Nrf2 expression in breast epithelial cells; Involved in chromosomal instability in VHL-associated cancers and in cell proliferation
ebv-miRNA-BART12		Epstein-Barr virus
hsa-miRNA-501-5p		
hsa-miR-500	CYLD/OTUD7B/TAX1BP1	Involved in gastric cancer cell proliferation, survival, and tumorigenicity
hsa-miR-503	L1CAM; IGF-1R	Tumor Suppressor in Osteosarcoma; Tumor suppressor in glioblastoma
hsa-miR-874	AQP3; caspase-8; CDK9; STAT3/VEGF-A pathway	Inhibits cell proliferation, migration and invasion in gastric cancer; Myocardial necrosis; Cell proliferation and induces apoptosis in human breast cancer; Tumor suppressor in gastric cancer.
hsa-miR-663	Bcl-2; TGF-β1	Induces apoptosis of lung cancer cells; Inhibits radiation-induced bystander effects
hsa-miR-30a-3p	HIF2A	Involved in cellular proliferation, angiogenesis, and xenograft tumor growth in VHL-deficient H1H2 tumors

miRNA	Target(s)	Funcion(s)
hsa-miR-9-3p		Cell proliferation, colony formation, migration, invasion and promotes apoptosis
hsa-miRNA-1225-3p		
hsa-miRNA-1228	MOAP1	Promotes the proliferation and metastasis of hepatoma cells through a p53 forward feedback loop; Prevents cellular apoptosis by targeting of MOAP1 protein.
hsa-miR-1234	STAT3	Promotes tumorigenesis of activeated B cell type DLBCL
hsa-miRNA-1181	SOX2/STAT3	Inhibits stem cell-like phenotypes and suppresses SOX2 and STAT3 in human pancreatic cancer.
hsa-miR-1207-5p	HBEGF	CFHR5 Nephropathy
hsa-miR-125a-3p	P53 pathway	Induces the invasive and migratory capabilities of lung cancer cells in apoptosis.
hsa-miR-134	NANOG	Promotes glioblastoma cell invasion; Targeting integrin β1 in hepatocellular carcinoma; Biomarker for the diagnosis of acute pulmonary embolism; Cell proliferation, apoptosis, and migration involving lung septation.
hsa-miR-150-3p		Involved in chronic heart failure; HIV/AIDS disease progression and therapy
hsa-miR-885-5p	CDK2/MCM5	Activates p53 and inhibits proliferation and survival
hsa-miRNA-1224-5p		
hsa-miR-135a-3p	BCL-2; HOXA10	Involved in LPS-induced apoptosis; Tumor suppressor
hsa-miR-629-3p	NBS1	Increases the risk of lung cancer
hsa-miRNA-1249		
hsa-miR-1915	BCL-2	Involved in apoptotic response to DNA damage.
hsa-miR-601		Biomarker of colorectal cancer
hsa-miRNA-1226*		
hsa-miRNA-1208		

Table 25. Summary of the biological functions and downstream targets of the candidate miRNAs identified in previous experiments.

These miRNAs were expressed in hES cells but were downregulated during the differentiation process, and also changed during the G1 to S transition and S to G2-phase transition**.**

miR-1305 was particularly interesting, which is the top candidate in our array data when expression of miRNAs during G1/S transition is investigated. It fulfils the selection criteria highlighted above (i) it is specific to hES cells, and its expression is higher in hES cells compared to differentiated cells (it is upregulated 25.9-fold in hES cells compared to differentiated cells [p = 2.76^{-71}] and (ii) it is significantly modulated during the G1 to S transition (its expression is higher in S phase compared to G1 phase in our array data and it is upregulated 6.1 fold during the G1 to S transition; [p = 5.80^{-07}]).Using online software TargetScan the predicted targets for miR-1305 (http://www.targetscan.org/vert_61/) [296-298] include DICER1, *CDK6, CYCLIND2, LIN28A,* and *POLR3G*, indicating a potential function for miR-1305 in regulating hES cell pluripotency and cell cycle.

3.2 The miRNA Expression Kinetics of Candidate miRNAs during the hES Cell Cycle Regulation and Differentiation Process

First we confirmed the expression kinetics of miR-1305 in hES cells during the cell cycle and differentiation process by qRT-PCR, using miR-367, a well-known miRNA that controls self-renewal and pluripotency in hES and hiPS cells, as a positive control [276,299,300].

To analyse the expression levels of this candidate miRNA in hES cells at different cell cycle stages, the cells were synchronised (see methods) and then analysed by Flow cytometry and qRT-PCR.

hES cells treated with nocodazole-aphidicolin were effectively blocked at G1 phase (G1: 80.5%; Figure 19b), while most cells treated with nocodazole alone were blocked at G2 phase (G2: 85.02%; Figure 19d). After 10 hours a subset of the cells were released from the G2 phase, and most were in S phase at the time of analysis (S: 71.06%; Figure 19c). This is consistent with previous work in our group which achieved similar results [25,208].
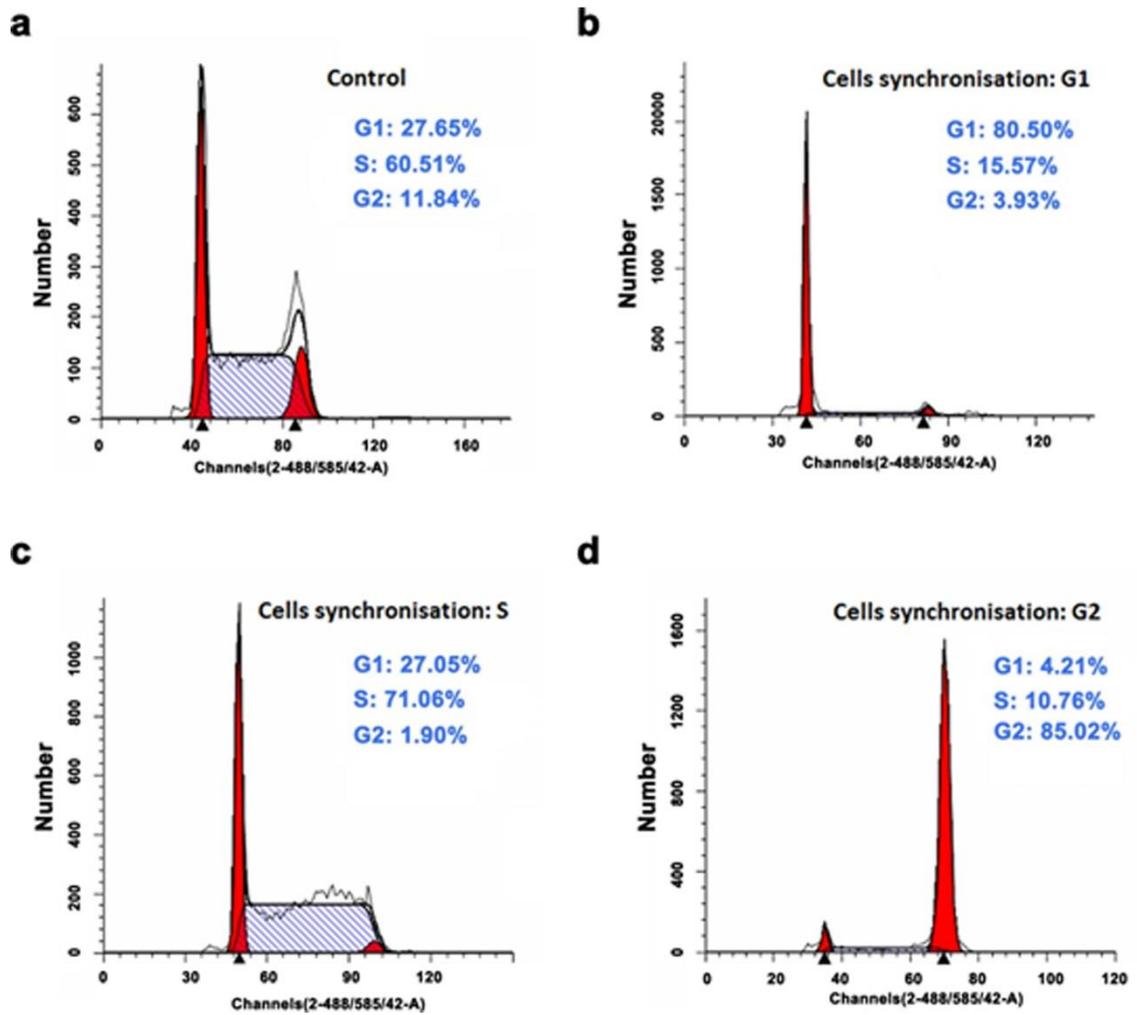
Figure 19. The cell cycle profile of H9 cells after cell-cycle synchronization.

(**a**) Normal hES cell-cycle profile. (**b**) 80.50% of cells in G1 phase after cell-cycle synchronization with nocodazole-aphidicolin. (**c**) 71.06% of cells in S phase after cell-cycle synchronization with nocodazole. (**d**) 85.02% of cells in G2 phase after cell-cycle synchronization with nocodazole and release after 10 hours. This is a representative example of 3 independent experiments.

The miR-1305 expression levels were then checked in these synchronized cells by qRT-PCR; consistent with array data, miR-1305 was highly expressed in S phase (Figure 20a), while miR-367 was highly expressed in G1 phase (Figure 20b) in agreement with previously published results [276].

The fold change of miR-1305 expression between G1 and S phase in qRT-PCR is about 2.5, while in the array analysis is 6.1. This is because array analysis (based on the probe-hybrdization) and qRT-PCR (based on the PCR-amplification) are two different technologies. All potential candidates we want to study in the future need be confirmed by qRT-PCR analysis. This difference will not affect the selection strategy, as the trend of miR-1305 during hES cells differentiation and cell cycle process are the same in both the array analysis and qRT-PCR.

a

b
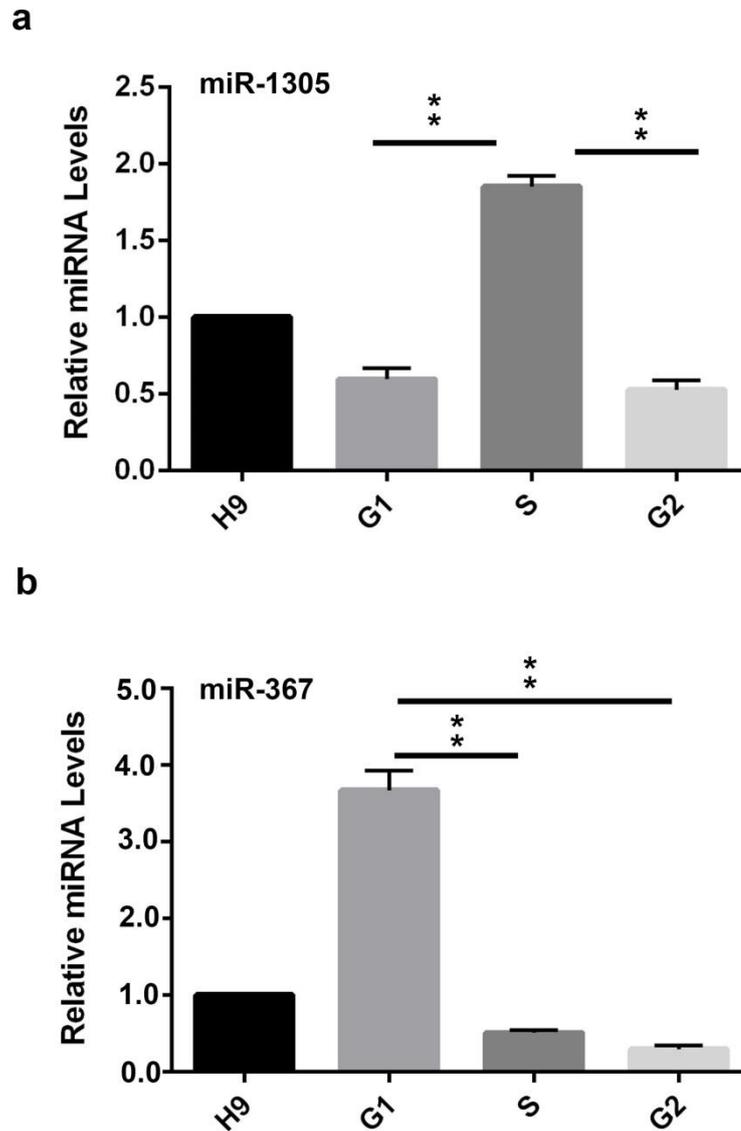
Figure 20. Quantitative RT-PCR analysis of the relative expression levels of the expression profile of mi0R-1305 during the hES cell cycle.

The expression profile of (a) miR-1305 and (b) miR-367 (control) during the hES cell cycle. Unsynchronized H9 hES cells were used as an unsynchronised cell-cycle control, and H9-G1, H9-S, and H9-G2 samples were collected after performing cell-cycle synchronization as described in Figure 19. Quantitative RT-PCR data are represented as the mean $\pm$ SD; n = 3. The statistical probability of significance was *p < 0.05, as measured using the Student-t test. The unsynchronised H9 control was set to 1.0.

hES cells remain undifferentiated when adhesion-cultured with mTESR 1 media, but grow as small aggregates (known as embryoid bodies or EBs), which undergo spontaneous differentiation to all three germ layers when cultured in suspension without bFGF and TGFβ [79]. This is a classic method for studying the hES cell differentiation. To study the expression profiles of these two miRNAs during the differentiation process, hES cells and EBs at different differentiation time points were tested by qRT–PCR. We collected undifferentiated H9 cells as a control and EBs at different time points (Day 1,

3, 5, 7, 14, 18, and 21), as well as adult AD3 fibroblast cells as another differentiated cell sample.

Consistent with previously published studies, the expression level of miR-367 is much higher in H9 cells than in differentiated cells (EBs and fibroblasts; Figure 21) [276,299]. The level of miR-367 decreased from the start of EB differentiation (day-1; D1) and was almost undetectable in D14 EBs and fibroblasts.

Consistent with the array data, miR-1305 expression was much higher in hES cells compared with adult fibroblasts (AD3) cells. But interestingly, unlike miR-367, miR-1305 expression was significantly increased (~1.5 fold) in D1 EBs at the beginning of differentiation. It then decreased from D3, but was still detectable in D21 EBs and fibroblasts (Figure 21), which indicates miR-1305 might play an important role in the initial stages of hES cell differentiation.
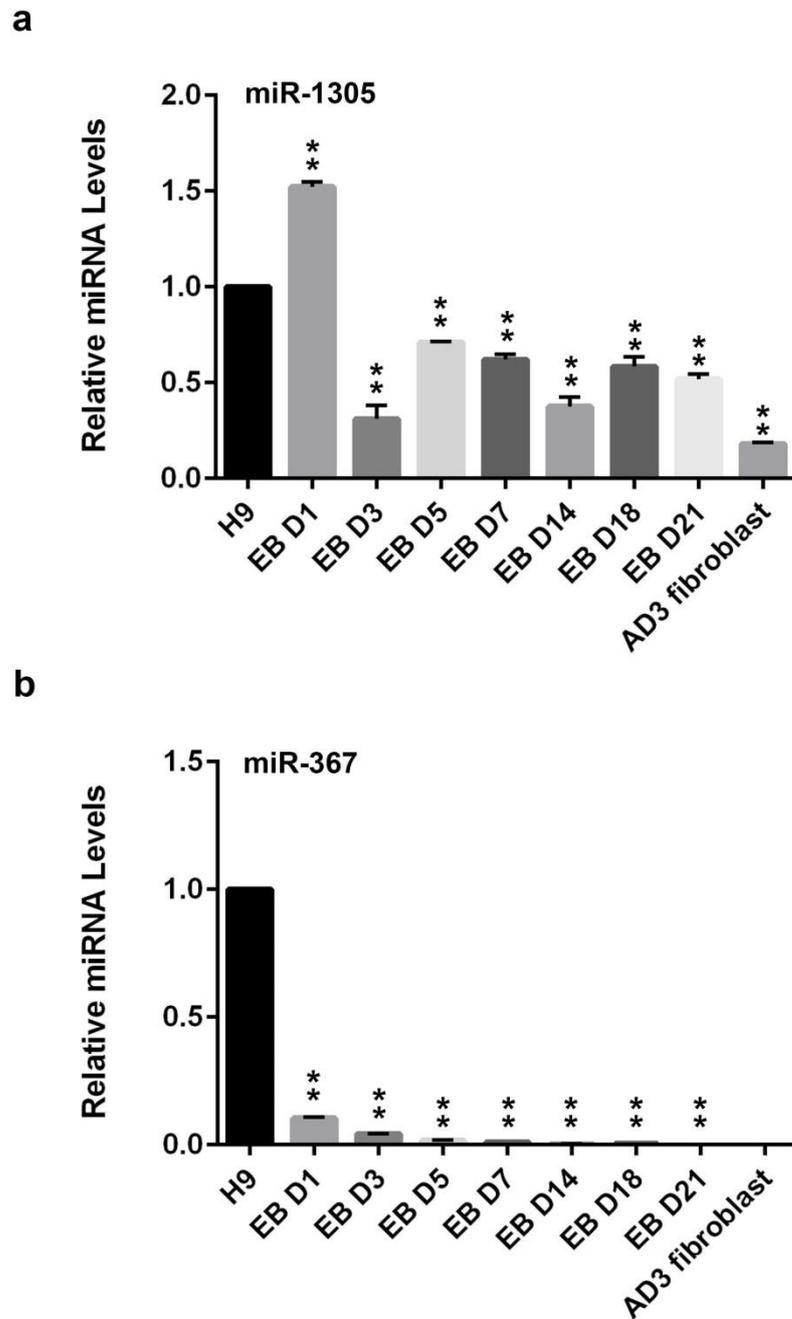
Figure 21. Quantitative RT-PCR analysis of the relative expression levels of the expression profile of (a) miR-1305 and (b) miR-367 in H9 hES cells, day (D) 1-21 embryoid bodies (EBs) and adult dermal skin fibroblasts (AD3 cell line).

Quantitative RT-PCR data are represented as the mean ± SD; n = 3. The statistical probability of significance was *p < 0.05 as measured using the Student-t test. The miRNA expression levels in H9 cells were set to 1.0.

In summary, based on these microarray-screening experiments, reviewing the literature, and target prediction, we selected the candidate miRNA, miR-1305. Further qRT-PCR results, which are consistent with our array data, showed that miR-1305 expression levels were higher in S phase compared to the G1 and G2 phases, and that it was higher

in H9 cells compared to differentiated cells (EBs and fibroblasts). However miR-1305 expression initially increased at the beginning of differentiation (EB-D1), thus suggesting it has a potential role in inducing differentiation.

CHAPTER 4 RESULTS II

Chapter 4. (Results II): Investigation of the function of miR-1305 in hES Cell Cycle Regulation and Pluripotency Maintenance

4.1 miRNA Inducible Overexpression System

To further investigate the role of miR-1305 in regulating the cell cycle and maintaining pluripotency, we first generated an inducible miRNA overexpression system in order to perform gain-of-function studies.

The inducible system was chosen because of its unique advantages. 1) We could generate a stable cell line before starting to overexpress miRNA; in our case this avoided survival potential problems because our miR-1305 may be able to induce cell differentiation and/or proliferation. 2) By using the inducible cell lines the miRNA overexpression could be induced and maintained at any time by adding 4-OHT into the culture medium. 3) More cells could be easily be propagated for further studies in contrast to transient mimic-miRNA transfection. 4) A stable cell line is easier to work with in follow up experiments, such as functional rescue or reporter assays, designed to elucidate downstream targets. The inducible system from Cellutron contains the pCreER-IRES-Puro plasmid (Figure 22a) and the inducible miRNA expression plasmid pEGFP/RFP–miR–BL (Figure 22c). pCreER-IRES-Puro expresses a 4-hydroxytamoxifen (4-OHT)-activated form of Cre and a puromycin resistance gene for drug selection. The inducible miRNA expression plasmid (pEGFP/RFP–miR–BL) incorporates the expression of the candidate miRNA under a suitable hES cell promoter (CAG) which is resistant to DNA silencing which occurs during the differentiation process. The plasmid contains an EGFP fluorescent reporter, with a 3x termination sequence (stop codon) flanked by two loxP sites, followed by a RFP expression sequence, and miRNA transgenes, and a blasticidin (BL) expression cassette for drug selection to create the stable cell lines.
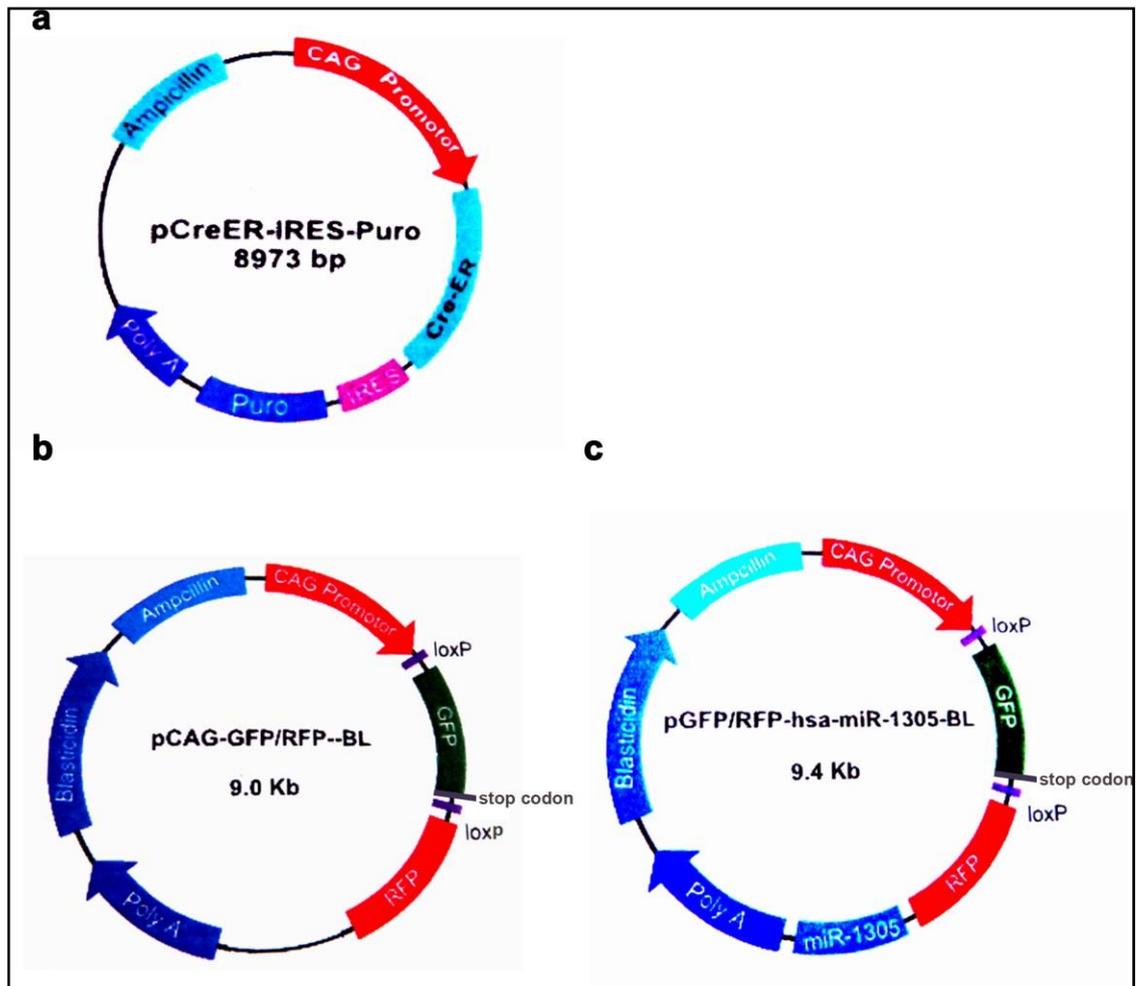
Figure 22. The construct information for the inducible miRNA expression system plasmids.

(**a**) The Cre expression vector: pCreER-IRES-Puro. (**b**) The control construct for the inducible miRNA expression vector, pEGFP/RFP–BL. (**c**) The inducible miRNA expression vector, pEGFP/RFP–miR1305–BL.

After the transfection and selection process (as described below), the stable cell lines containing both pCreER-IRES-Puro and pEGFP/RFP–miR–BL enabled us to conditionally express the miRNA transgenes. Without adding 4-OHT, the inactivate form of Cre is unable to cut the loxP sites hence the cells express EGFP but not the candidate miRNA. When 4-OHT is added to the culture medium Cre is activated leading the LoxP sites to be cut and the expression of RFP and the desired miRNA.

The sequence information of the plasmids is kept by the company (Cellutron) as confidential intellectual property. Even though the quality and correction of the products were guaranteed, we still tested the plasmids by restriction-enzyme digestion after we obtained the constructs. We used EcoRV/Xhol to cut pCreER-IRES-Puro (Figure 23a) and pEGFP/RFP–BL (Figure 23b), and BglII/EcoRV to cut pEGFP/RFP–miR1305–BL (Figure 23c).
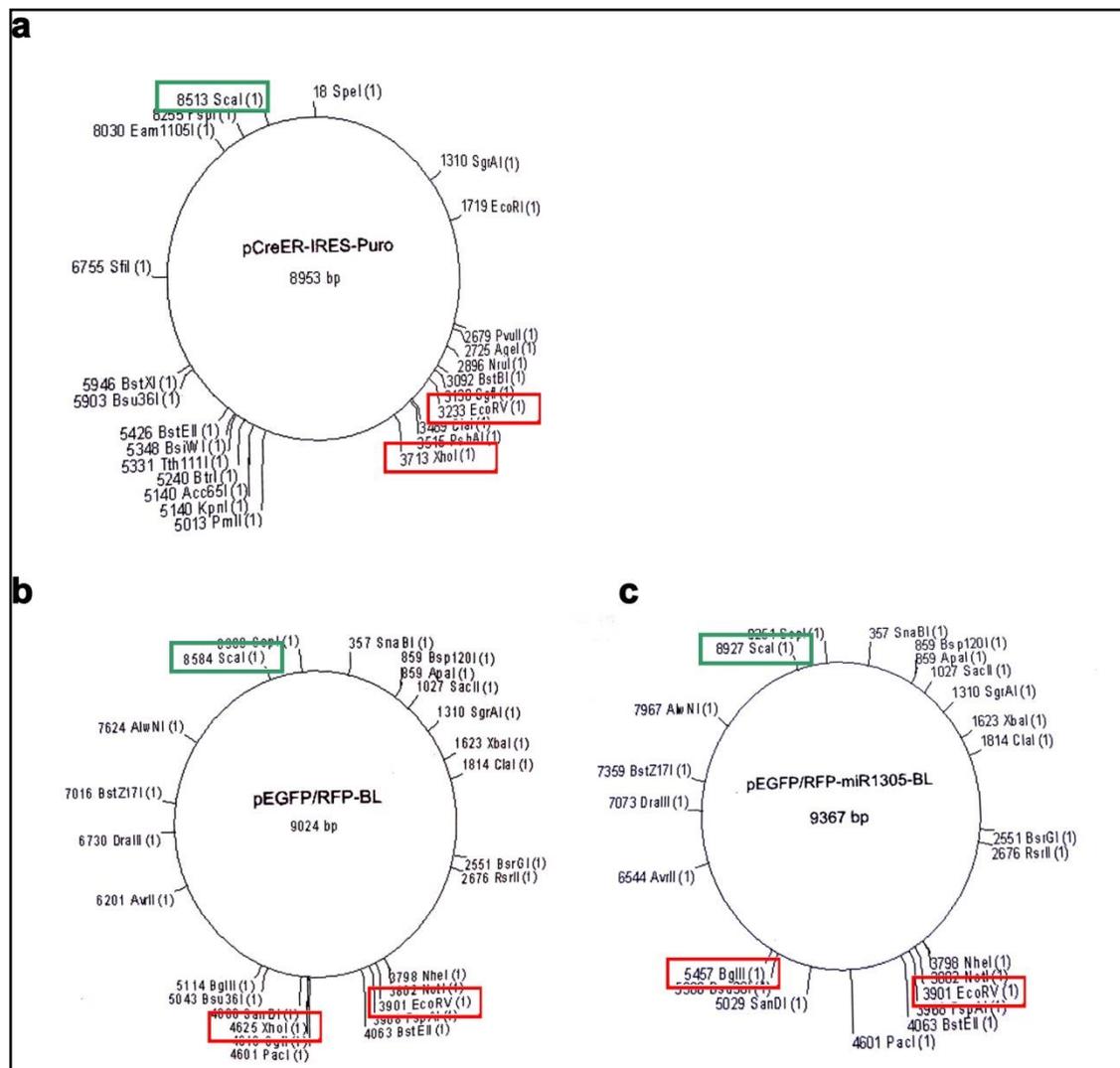
Figure 23. Restriction enzyme cut sites in the inducible miRNA expression system plasmids.

(**a**) The restriction sites in pCreER-IRES-Puro, (**b**) pEGFP/RFP–BL, and (**c**) pEGFP/RFP–miR1305–BL. The red boxes indicate the restriction sites used for this digestion-identification experiment. The green boxes indicate the restriction site use to linearize the plasmids.

The enzyme-digested construct samples were separated by agarose gel electrophoresis (Figure 24) and were consistent with the sizes predicted for each construct based on their restriction site maps (Figure 23), thus indicating that the plasmid constructs were correct.
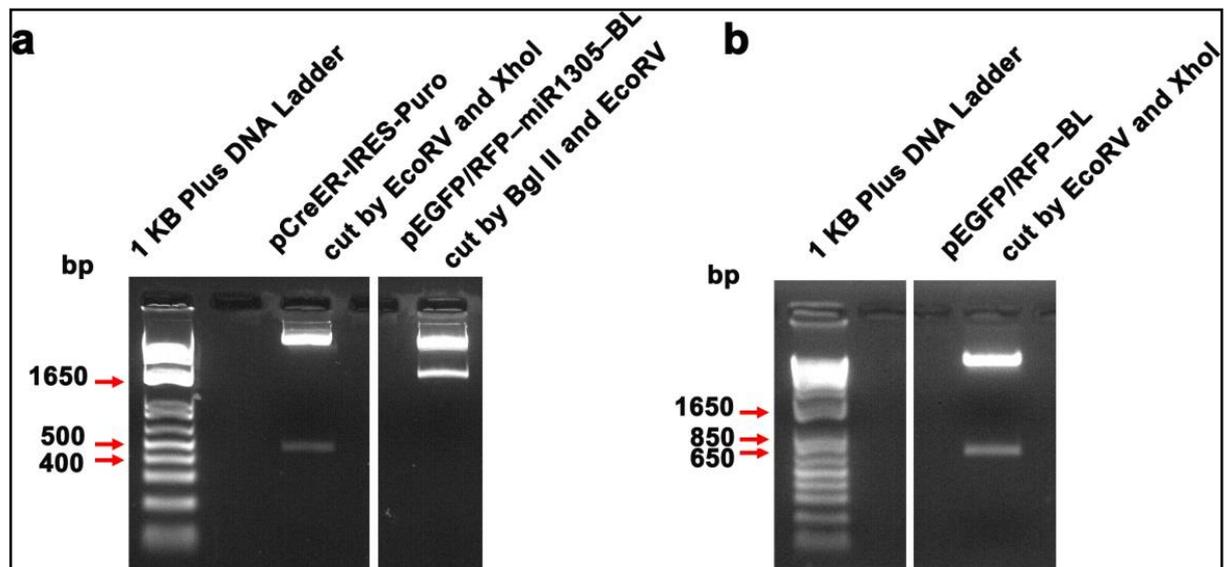
Figure 24. Identification of the plasmids in the inducible miRNA expression system by digestion with restriction enzymes and separation by agarose gel electrophoresis.

(**a**) pCreER-IRES-Puro was cut into two fragments, 480bp+8.5kb, using *EcoRV* and *Xhol,* pEGFP/RFP–miR1305–BL was cut into two fragments, 1556bp+7.8kb using *Bgl II* and *EcoRV*, and (**b**) pEGFP/RFP–BL was cut into two fragments, 724bp+8.3k using *EcoRV* and *Xhol*.

These plasmids were then linearized at the single enzyme cut site (as shown in the green boxes in Figure 23) and purified for further transfection by electroporation (Figure 25).
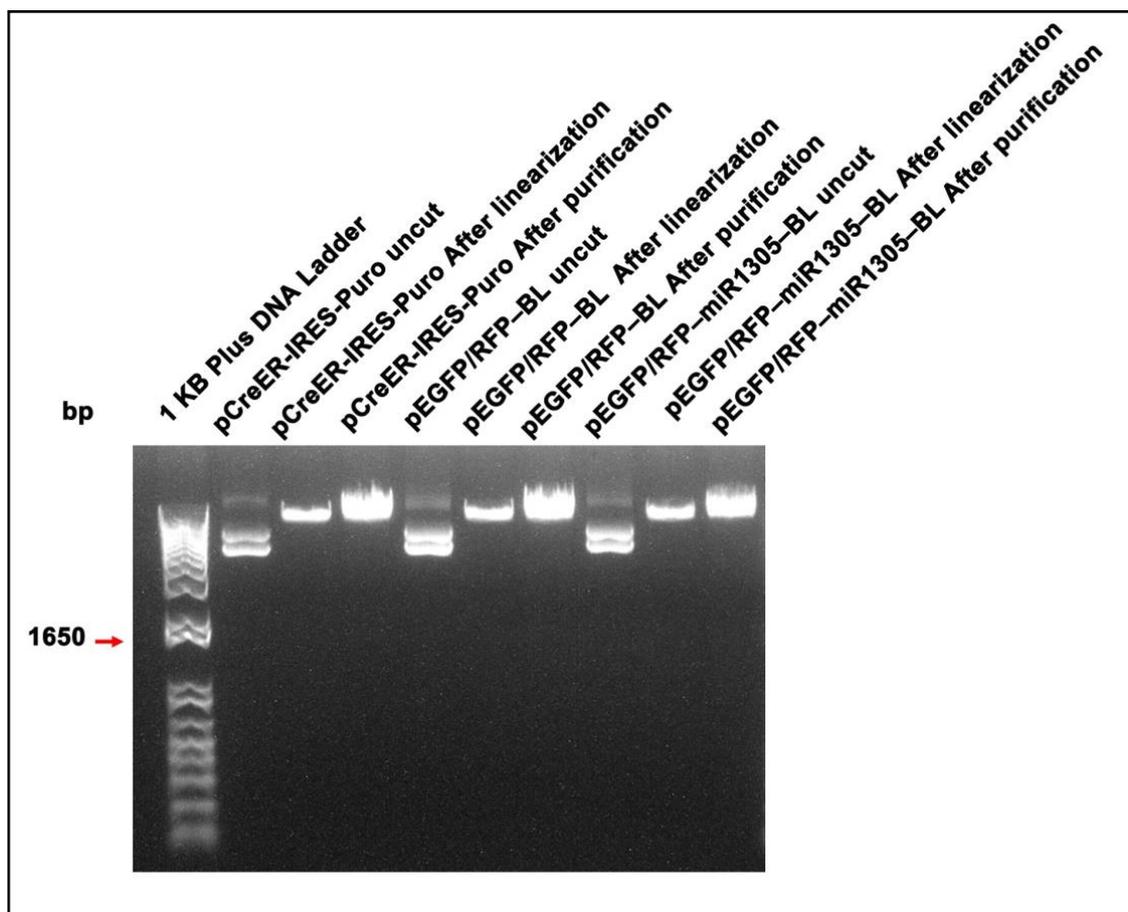
Figure 25. Agarose gel identification and separation of the inducible miRNA expression system plasmids after linearization using *ScaI* and subsequent purification.

All three cut and uncut plasmid products were the predicted sizes.

The concentrations of the purified products were measured using a Nano Drop 2000 spectrophotometer (Figure 26).

Sample ID	Nucleic Acid Conc.	Unit	A260	A280	260/280
pCreER-IRES-Puro	1167.5	ng/µl	23.349	12.478	1.87
pCAG-GFP/RFP-BL	678.1	ng/µl	13.562	7.164	1.89
pCAG-GFP/RFP-miR1305	1031.8	ng/µl	20.635	11.045	1.87

Figure 26. Concentrations of the inducible miRNA expression system plasmids after separation by agarose gel electrophoresis and purification, as measured using a NanoDrop spectrophotometer.

4.2 Generation of an Inducible miRNA Overexpression Cell Line

To generate a stable cell line which can consistently express Cre, the purified pCreER-IRES-Puro plasmid was transfected into H9 hES cells by electroporation. Ten days after puromycin (0.5 μg/ml) selection no cells survived in the control group (treated with the same transfection procedure but using a buffer instead of the construct). While several colonies with the typical undifferentiated hES cell morphology were detected in the pCreER-IRES-Puro group (Figure 27). The colonies were then picked out of the experimental dishes and expanded as described in the methods section.
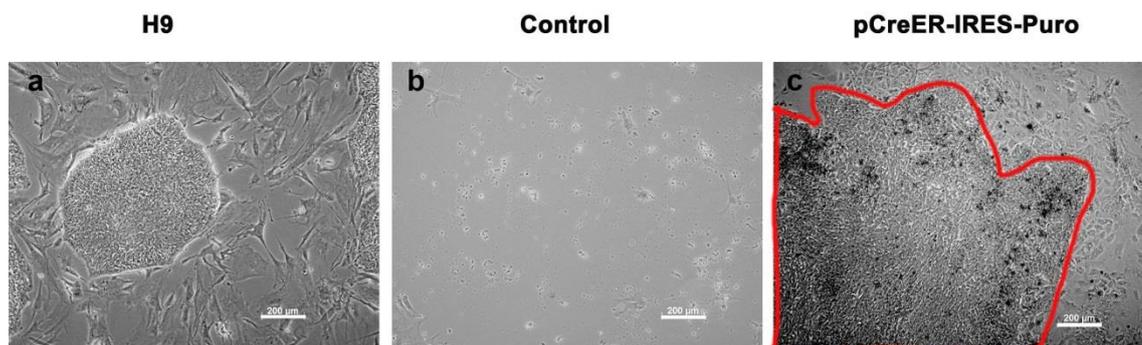
Figure 27. The cell morphology of normal (a) hES cells, (b) cells transfected with a control buffer, or (c) pCreER-IRES-Puro transfected cells after puromycin selection for 10 days.

(**a**) Normal morphology of an H9 hES cell colony. (**b**) No hES cells transfected with the control buffer survived the puromycin (0.5 μg/ml) selection. (**c**) Positive colonies were observed in the H9 hES cells transfected with pCreER-IRES-Puro after the puromycin (0.5 μg/ml) selection. The red line delineates the edge of the colony. Scale bar: 200 μm.

To further generated the inducible miRNA expression stable line, the pEGFP/RFP–BL or pEGFP/RFP-miR-1305-BL plasmid was transfected into pCreER-IRES-Puro cell line (as shown in Figure 27) and selected by blasticidin (10 μg/ml) for 10 days. 13 stable clones were generated from the pEGFP/RFP-miR-1305-BL group and 8 from the control pEGFP/RFP–BL group. Based on the expression level of GFP under the microscope, #4 and #10 from experimental group were selected because of the highest GFP expression (data not shown).

4.3 Determining the Optimal Concentration of 4-OHT

To select the optimum concentration of 4-OHT to induce the experimental plasmid, we performed a 4-OHT concentration gradient test by treating one of our stable lines, pEGFP/RFP-miR-1305-BL-1, with different concentrations of 4-OHT (0.25 µM, 0.5 µM, 1 µM, 2 µM, and 3 µM) for 3 days. The cells were then tested for RFP expression by flow cytometry (Figure 28).
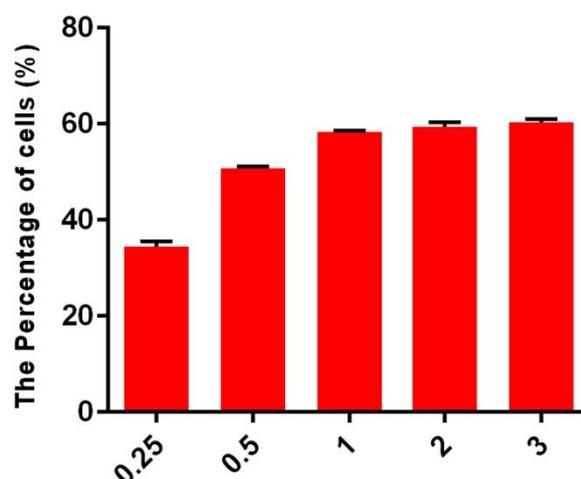
Figure 28. RFP expression in the pEGFP/RFP-miR-1305-BL-1 stable cell inducible cell line after treatment with different concentrations of 4-OHT (0.25 µM-3 µM).

To avoid any potential deleterious effects that 4-OHT might have on H9 cells, we also performed the same 4-OHT concentration gradient test on hES cell for 3 days. Their cell-cycle profile was assessed by flow cytometry (Figure 29). The result shows that 0.25µM 4-OHT was the optimal concentration because it caused minimum changes in the cell cycle profile when compared to untreated cells (Figure 29) and induce RFP expression in stable lines. Based on these results, 0.25 µM 4-OHT was chosen for further studies.
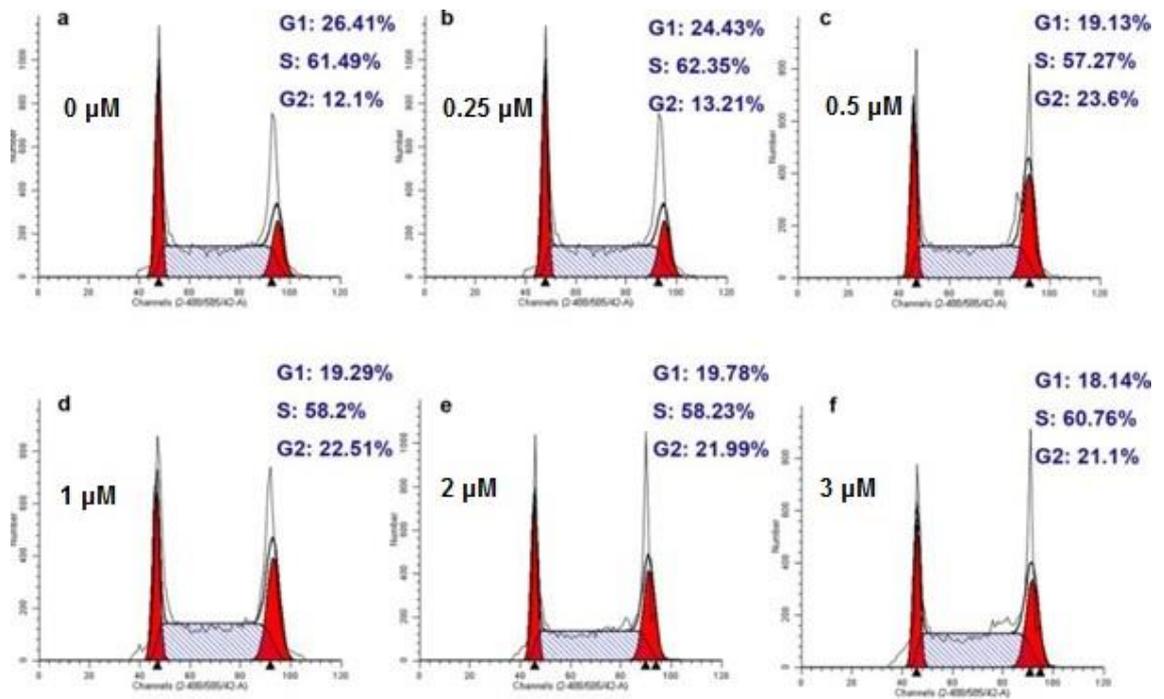
Figure 29. The cell cycle profile of H9 hES cells treated with different concentrations of 4-OHT.

 (a) 0 μM; **(b)** 0.25 μM; **(c)** 0.5 μM; **(d)** 1 μM; **(e)** 2 μM **(f)** 3 μM **for 3 days.** This is a representative example of at least three independent experiments.

4.4 Testing the miR-1305 Stable Cell Line

By treating both the pEGFP/RFP-miR-1305-BL (#4, #10) cell lines with 4-OHT (0.25 μM) most cells started to lose EGFP expression and acquired RFP expression (Figures 30 and 31). But a few cells in the colony still maintained EGFP expression after 3 days' induction. This might be because EGFP is very stable and may require more time to degrade. Another possibility is that there are multiple copies of the constructs within each cell, and LoxP site cutting may not have been 100 percent efficient after induction meaning that some cells might have continued to express EGFP, or EGFP and RFP at same time.
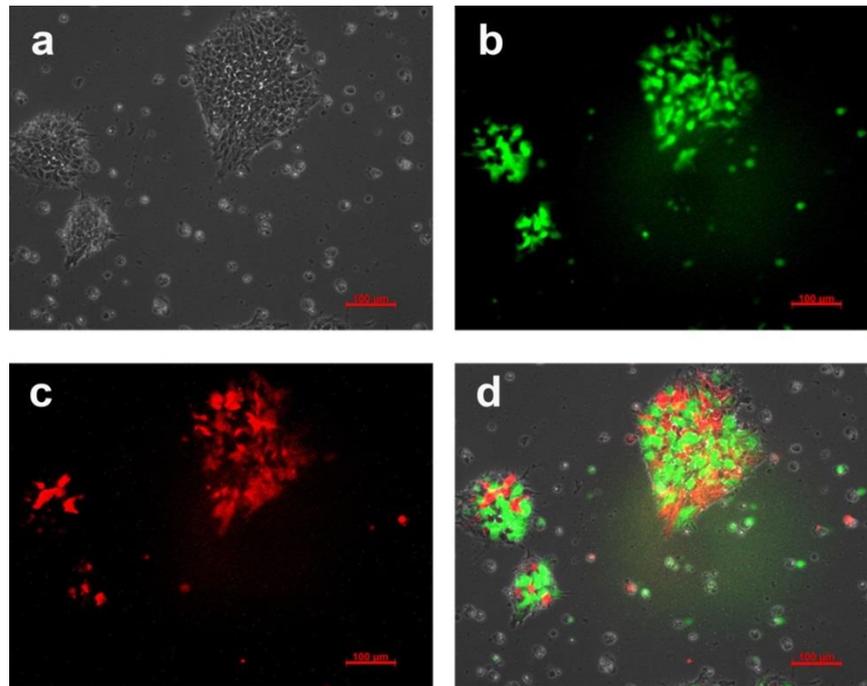
Figure 30. EGFP/RFP expression in the pEGFP/RFP-miR-1305-BL-4 stable cell line after treatment with 4-OHT for 3 days.

(**a**) Bright field; (**b**) EGFP; (**c**) RFP; (**d**) Merge. This is a representative example of at least three independent experiments.
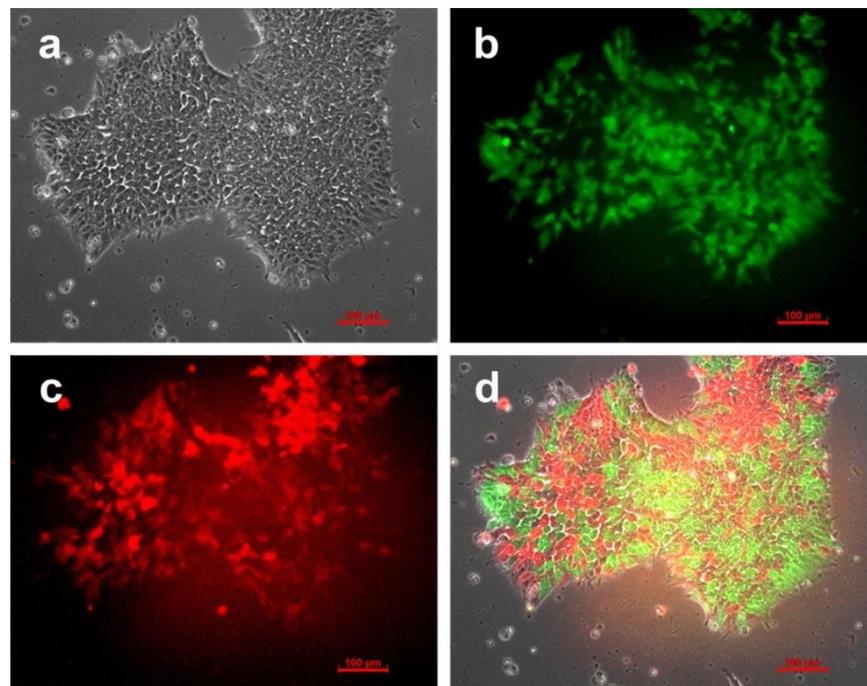
Figure 31. EGFP/RFP expression in the pEGFP/RFP-miR-1305-BL-10 stable cell line after treatment with 4-OHT for 3 days.

(**a**) Bright field; (**b**) EGFP; (**c**) RFP; (**d**) Merge. This is a representative example of at least three independent experiments.

Flow cytometry analysis showed that, about 10% of cells expressed only RFP in both the pEGFP/RFP-miR-1305-BL clones (#4, #10), about 50% of cells in clone #4 and 60% in clone #10 expressed both EGFP and RFP, and about 40% (#4) and 30% (#10) of cells continued to express EGFP after three days of 4-OHT treatment (Figure 32).
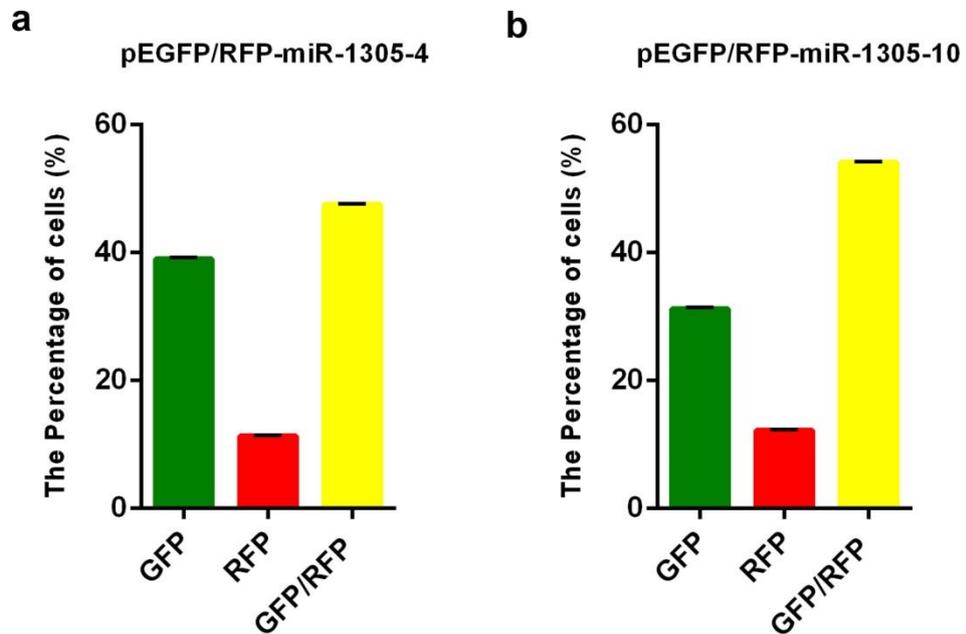
Figure 32. FACS results showed the percentage of cells that expressed EGFP/RFP in pEGFP/RFP-miR-1305-BL (#4, #10) cell lines after 3 days of 4-OHT treatment.

Data are represented as the mean ± SD; n = 3.

Further qRT-PCR analysis indicated that pEGFP/RFP-miR-1305-BL (clones #4 and #10) cell lines treated with 0.25 μM 4-OHT showed increased miR-1305 expression, but not at a high level (~1.5-fold compared with control; Figure 33).
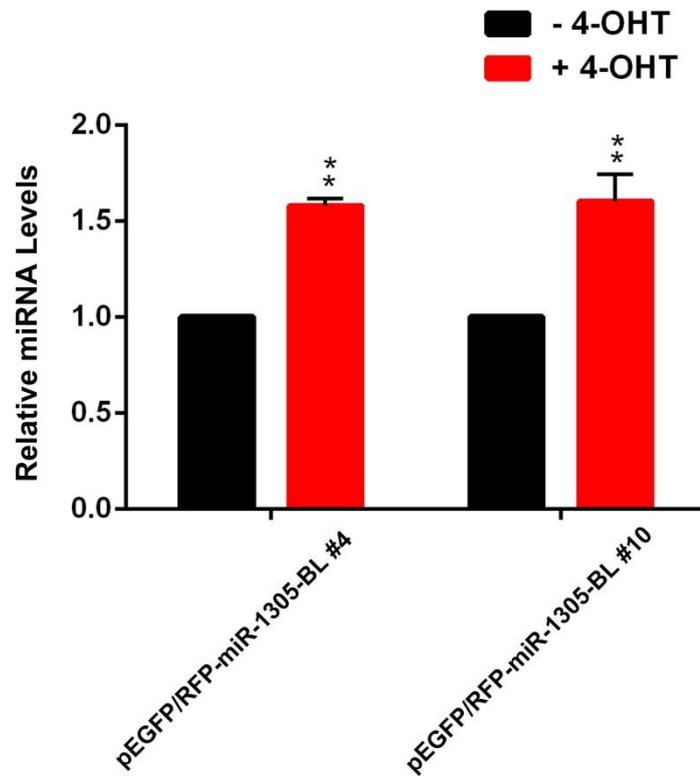
Figure 33. Quantitative RT-PCR analysis of the relative expression levels of miR-1305 in pEGFP/RFP-miR-1305-BL #4 and #10 cells treated with or without 4-OHT for 3 days.

Quantitative PCR data are represented as the mean ± SD; n = 3. *p < 0.05, calculated using the Student-t test. The control was set to 1.0.

Given that the miR-1305 overexpression level was similar in both two cell lines (clones #4 and #10), we decided to use clone #10 for further experiments because it had fewer EGFP positive cells after 4-OHT treatment than clone #4.

4.5 Selecting the pEGFP/RFP-BL Control Cell Line

To select stable pEGFP/RFP-BL control lines, the colonies generated were treated with 4-OHT and then the expression of GFP and RFP were checked. As expected, treating the control cell line with 4-OHT resulted in a decrease in EGFP expression in most of the cells, but surprisingly, there was no RFP expression. This induction was repeated in all 8 stable control cell lines and they all lost EGFP expression but did not express RFP, leading us to speculate that there may have been problems with the pEGFP/RFP-BL control plasmid sequence.

To overcome these problems, we obtained other two other batches of control plasmids from Cellutron and repeated the experiments. However, we continued to obtain results similar to those described above, suggesting that the commercially-available pEGFP/RFP-BL control plasmid could not be used to generate valid stable control cell line clones for this work.

We tested whether the pEGFP/RFP-BL plasmids could express RFP in 293 cells. All three different batches of control plasmids obtained from Cellutron were co-transfected with pCreER-IRES-Puro into the 293 cells. In parallel, pEGFP/RFP-miR-1305-BL and pCreER-IRES-Puro were also co-transfected as a positive control. 4-OHT was added to the culture media 24 hours after co-transfection. As expected, significant RFP expression was observed in the pEGFP/RFP-miR-1305-BL co-transfection group 48 hours after treatment with 4-OHT (Figure 34). But the RFP expression level in all three control plasmid groups was almost undetectable (Figure 34) indicating that there were technical issues with RFP expression when using these control plasmids.
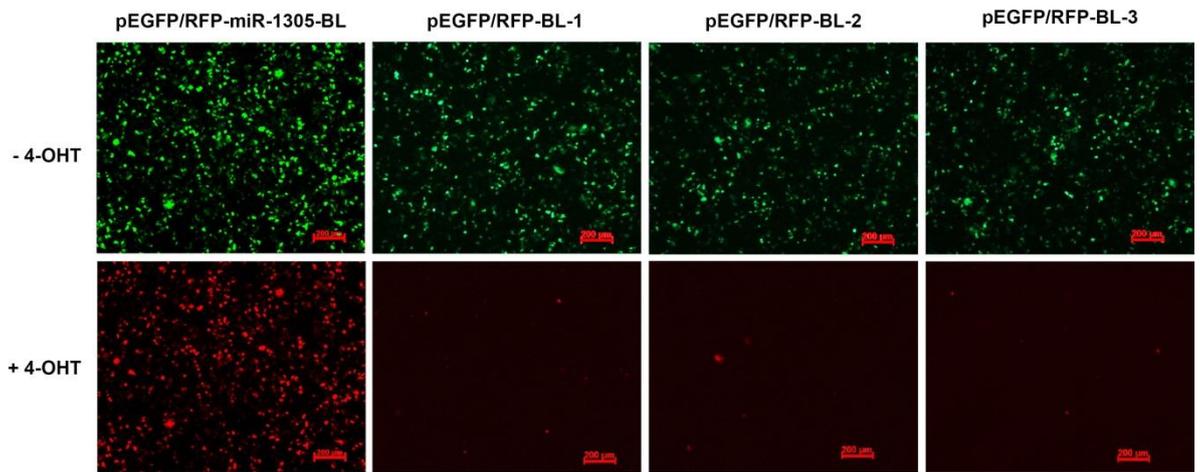
Figure 34. EGFP/RFP expression in 293 cells transfected with pCreER-IRES-Puro and pEGFP/RFP-miR-1305-BL, or pCreER-IRES-Puro and pEGFP/RFP-BL (clones #1, #2, and #3).

RFP expression was detected after the cells were treated with 4-OHT for 2 days. This is a representative example of at least three independent experiments.

While we were trying to establish a proper control cell line, we also investigated the impact of 4-OHT treatment on the established pEGFP/RFP-miR-1305-BL-10 clone. Although RFP was not expressed in the pEGFP/RFP-BL clone, we still choose one of the control clones (#6) to use in parallel with the miR-1305 overexpression clone.

To study the function of miR-1305 in hES cells, the control and miR-1305 overexpression lines were treated with 0.25 μM 4-OHT and were harvested 3 days after induction. When the control group treated with 0.25 μM 4-OHT, more apoptosis cells and less differentiation cells were observed (Figure 35).
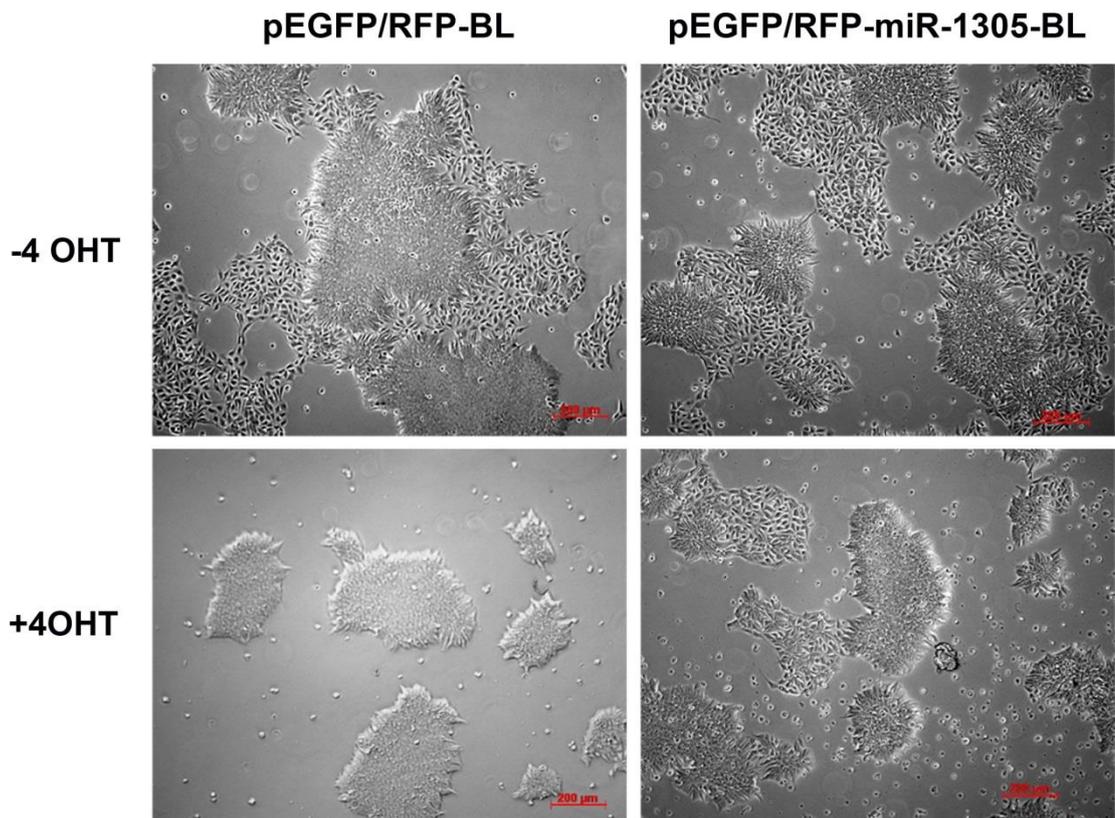
Figure 35. The cell morphology of pEGFP/RFP-BL and pEGFP/RFP-miR-1305-BL cells treated with or without 4-OHT (0.25 µM) for 3 days.

This is a representative example of at least three independent experiments.

Quantitative RT-PCR analysis was performed to test the relative expression of hES-cell pluripotency and specific germ-layer markers. The results showed that 4-OHT treatment decreased the levels of the *OCT4* and *NANOG* pluripotent markers, and the differentiation markers *CDX2*, *GATA4*, *PAX6*, and *T,* and increased *FGF5* and *FOXA2* expression in the control cells (Figure 36a). There was also change in the expression of *OCT4*, *PAX6*, *FOXA2,* and *GATA4* upon miR-1305 overexpression in the pEGFP/RFP-miR-1305-BL cell line upon the addition of 4-OHT (Figure 36b). However, because of the effect of 4-OHT on the control cell line we could not attribute these changes to miR-1305 overexpression or 4-OHT treatment.
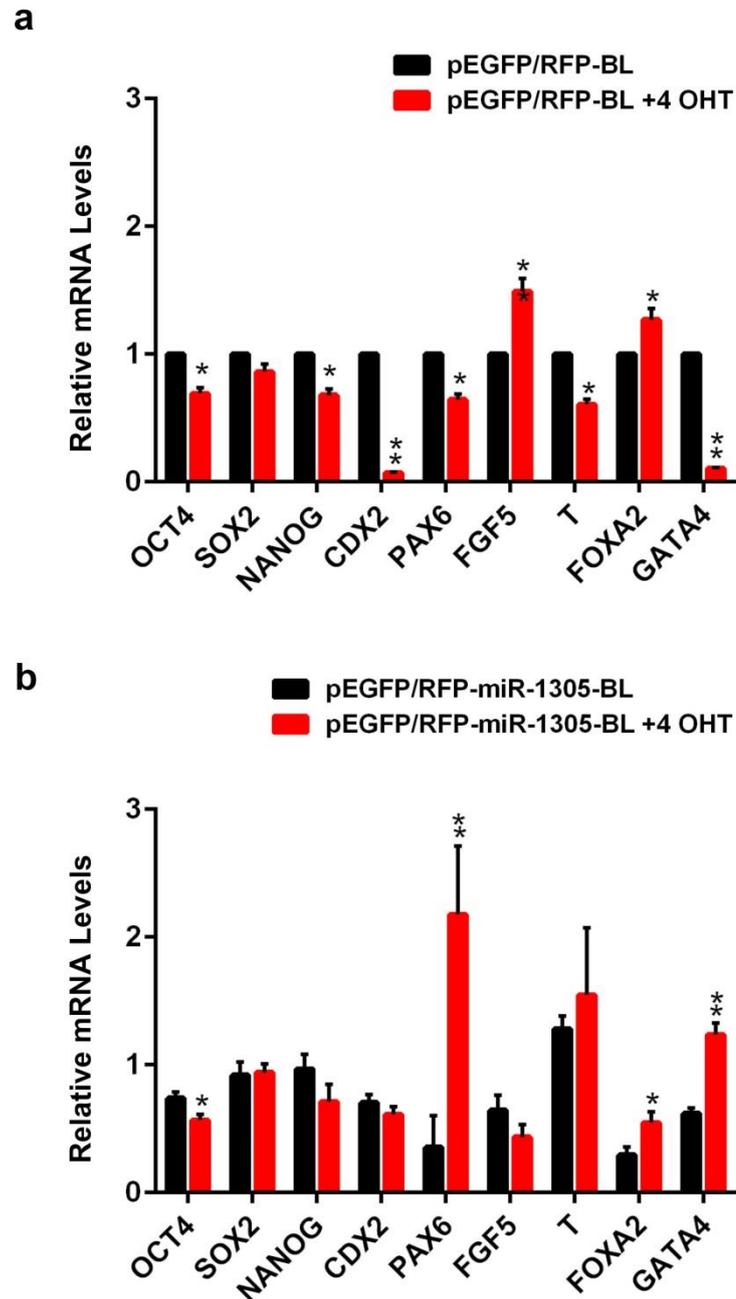
Figure 36. Quantitative RT-PCR analysis of the relative expression levels of pluripotent and differentiated markers in (a) pEGFP/RFP-BL and (b) pEGFP/RFP-miR-1305-BL cells treated with or without 4-OHT (0.25 μM) for 3 days.

qRT-PCR data are represented as mean ± SD; n = 3. *p < 0.05, **p<0.01 calculated using the Student-t test. The control was set to 1.0.

In summary, to study the function of miR-1305 we first tried to establish an inducible miR-1305 expression system in hES cells, but we encountered two main technical issues, 1) we were not able to create an appropriate control cell line which properly expressed RFP after induction; 2) The addition of even very low levels of 4-OHT (0.25

μM) affected pluripotency and differentiation markers. For these reasons, it was impossible to discern the impact miR-1305 overexpression in the inducible miRNA overexpression system tested.

After checking the recent literature relating to miRNA we decided to proceed with miRNA mimics/inhibitors from Invitrogen for further functional studies, as described in the following sections.

4.6 miRNA Gain-of-Function Study Using Mimics

4.6.1 Establishing a Technique for Effective miRNA Mimic/Inhibitor Transfection

The mirVana[TM] second generation mimics/inhibitors from Invitrogen have a high efficacy in both in vitro and in vivo studies, and have been widely used in the miRNA-research field [301,302]. miRNA mimics are small, chemically-modified double-stranded RNAs that mimic endogenous miRNAs and enable miRNA functional analysis by upregulating miRNA activity. The miRNA-mimic negative control and miR-1305 mimic (mirVana[TM] Mimics, Invitrogen) were used for these gain-of-function studies.

To test the transfection efficiency and the effect of miRNA mimic on hES cells, a well-studied miR-1 mimic was used as a positive control, as suggested by the manufacturer. After thoroughly checking the literature, we chose Lipofectamine® RNAiMAX to transfect the mimic into hES cells (see detailed protocol in the methods section). Forty-eight hours after transfection, cell inspection under a microscope showed that miR-1 overexpression significantly decreased the cell numbers compared with the control (Figure 37), which is consistent with previous studies [303-305]. An especial phenotype was observed in miR-1 group, empty holes formed between the clones, which may due to the increase of cell apoptosis in miR-1 group.
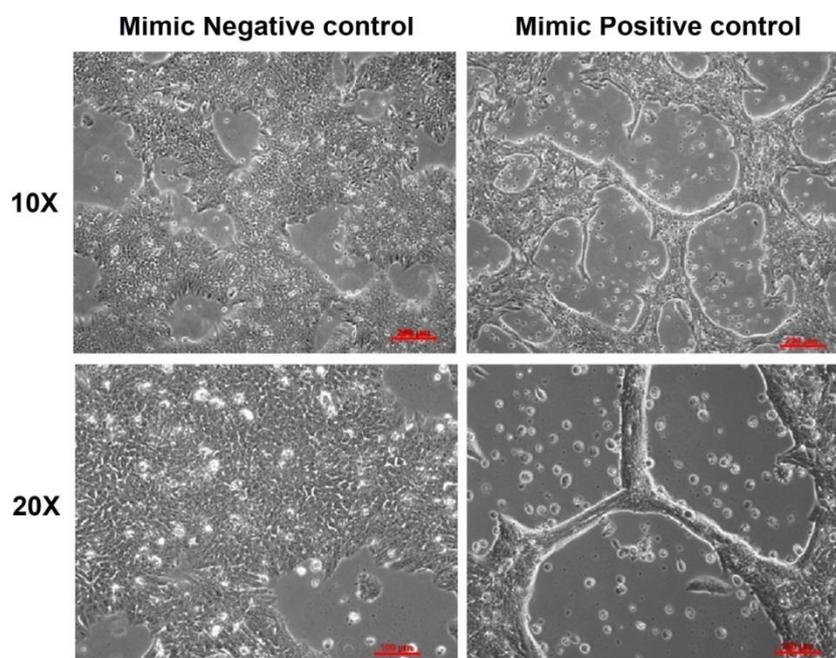
Figure 37. The morphology of H9 cells 2 days after transfection with the miRNA-mimic negative control or miR-1-mimic.

This is a representative example of at least three independent experiments.

The mRNA levels of some known miR-1 targets were tested by qRT-PCR and, as shown in Figure 38, miR-1 mimic efficiently decreased the mRNA levels of its target genes *KLF4* [306] and *TWF1* [307].
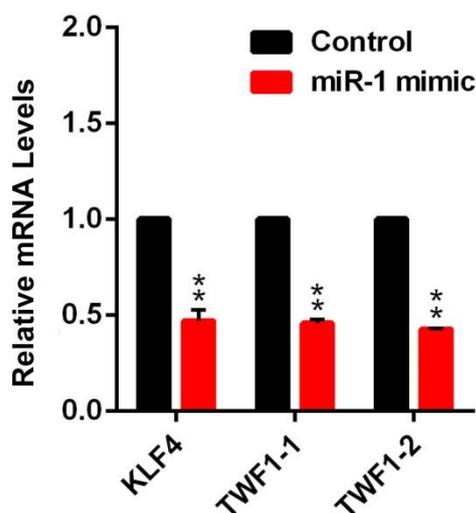
Figure 38. Quantitative RT-PCR analysis of the relative expression levels of miR-1 downstream targets *KLF4, TWF1-1,* and *TWF1-2* in H9 hES cells 2 days after transfection with miRNA-mimic (control) or miR-1-mimic.

Quantitative RT-PCR data are represented as the mean ± SD; n = 3. *p < 0.05, **p < 0.01 calculated using the Student-t test. The control was set to 1.0.

In summary, the above results indicate that the miRNA mimic and the transfection method (Lipofectamine® RNAiMAX) we used worked very well in hES cells.

4.6.2 Kinetics of miR-1305 Overexpression

We then transfected H9 hES cells with miR-1305 mimic using Lipofectamine® RNAiMAX and measured the expression levels of miR-1305 at different times after transfection (24h, 48h, 72h, and 96h). As shown in Figure 39, miR-1305 mimic significantly increased the miR-1305 levels at 24h post transfection. Peak overexpression miR-1305 overexpression was detected at 24h post transfection, and still remained high at 96h post transfection (Figure 39a). To show the specificity of the miR-

1305 mimic, we also tested the expression of miR-135a* after the transfection of miR-1305 mimic and did not observe any increase in its expression level (Figure 39b).
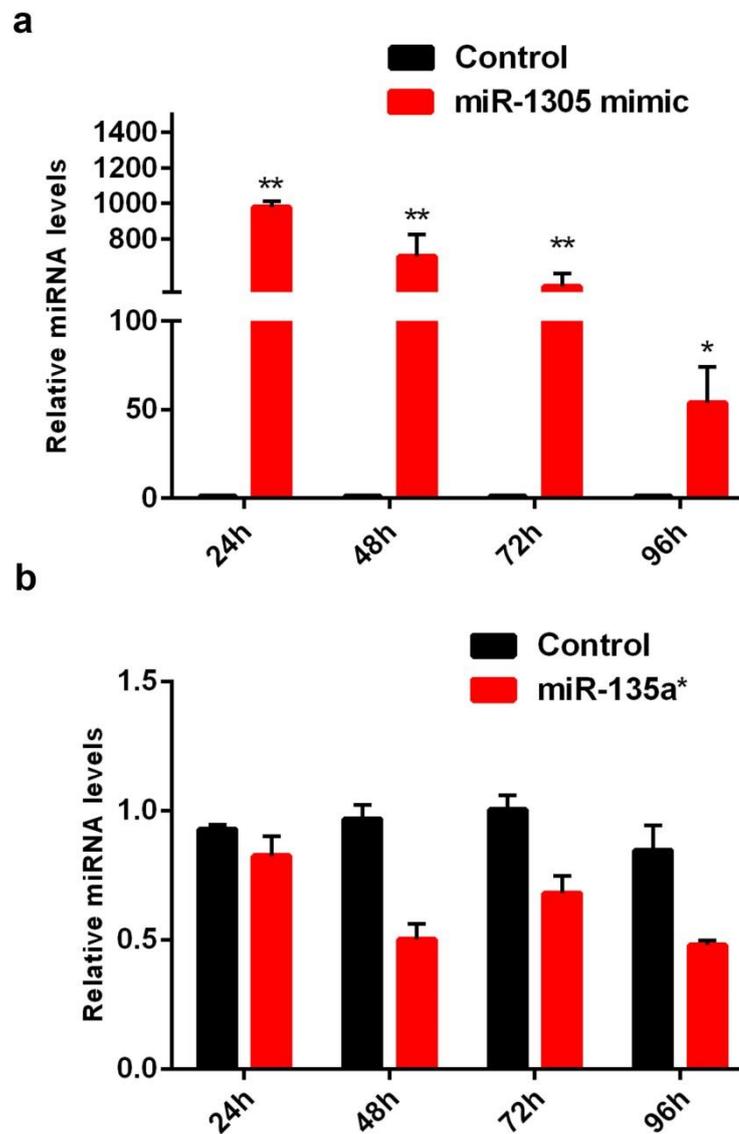
Figure 39. Quantitative RT-PCR analysis of the relative expression levels of (a) miR-1305 and (b) miR-135a* after miR-1305 transfection.

Quantitative RT-PCR data are represented as the mean ± SD; n = 3. $*p < 0.05$, $**p < 0.01$ calculated using the Student-t test. The control was set to 1.0.

4.6.3 Impact of miR-1305 Overexpression on hES Cell Pluripotency

We checked the cell morphology at different time points after miR-1305 mimic transfection. As shown in Figure 40, cells transfected with the miRNA-mimic control maintained a typical hES cell colony morphology. The colonies in the miR-1305-mimic-transfected group were smaller than control group and started to lose the undifferentiated hES colony morphology while and seeming to gain morphological features typical of differentiated cells. The colonies lost the typical compact morphology. The cells on the edge of the colony start differentiate.
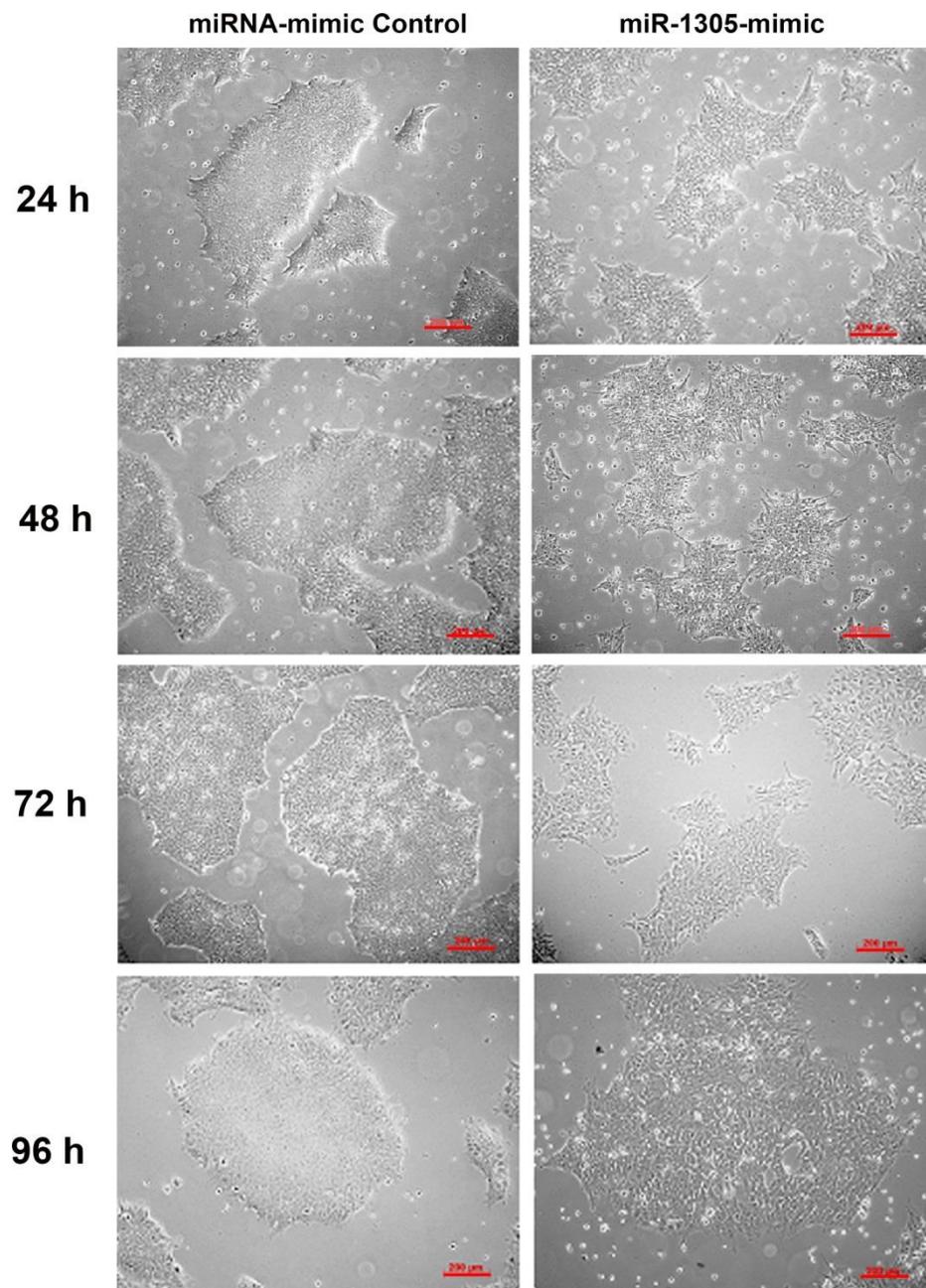
Figure 40. The morphology of H9 cells from 24 h to 96 h after transfected with a miRNA-mimic Control or miR-1305-mimic.

This is a representative example of at least three independent experiments.

The cells were also collected 48 hours after mimic transfection in order to check the expression of pluripotency and germ-layer markers by qRT-PCR. As shown in Figure 41, overexpression miR-1305 reduced the expression of the pluripotency markers *OCT4* and *NANOG* and increased the expression of ectoderm markers (*FGF5, PAX6*), mesoderm marker (*T*), endoderm markers (*GATA4* and *FOXA1*) and trophectoderm markers (*CDX2* and *HAND1*). It is interesting to note that unlike other germ-layer markers, the expression of *FOXA2*, a definitive endoderm marker, was downregulated upon miR-1305 overexpression on day 2 (Figure 42).
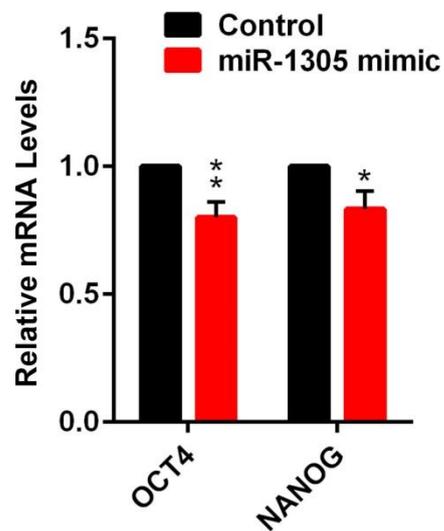
Figure 41. Quantitative RT-PCR analysis of the relative expression levels of pluripotency markers *OCT4* and *NANOG* in H9 hES cells 2 days after transfection with a miRNA-mimic control or miR-1305-mimic.

Quantitative RT-PCR data are represented as the mean ± SD; n = 3. *p < 0.05, **p < 0.01 calculated using the Student-t test. The control was set to 1.0.
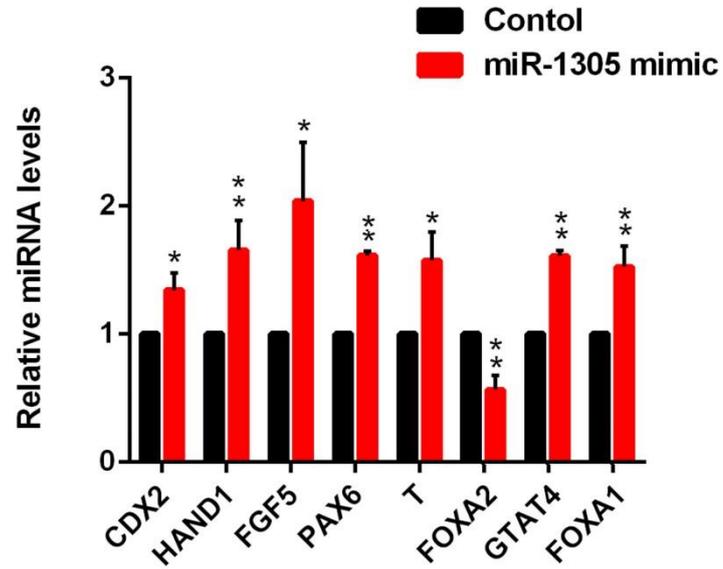
Figure 42. Quantitative RT-PCR analysis of the relative expression levels of differentiation markers in H9 hES cells 2 days after transfection with a miRNA-mimic control or miR-1305-mimic.

Quantitative RT-PCR data are represented as the mean ± SD; n = 3. *p < 0.05, **p < 0.01 calculated using the Student-t test. The control was set to 1.0.

The cells were also analysed by flow cytometry to check the expression of the early differentiation marker SSEA-1 which was significantly increased (~5.6 fold) in the miR-1305 overexpression population of differentiated H9 hES cells (Figure 43).
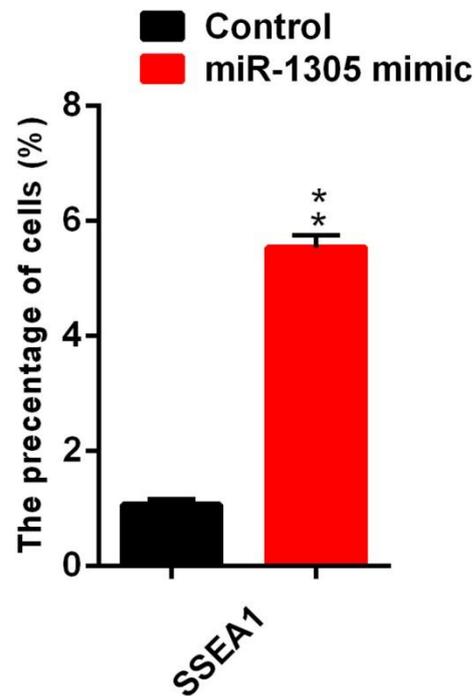
Figure 43. Flow cytometry results showing that 2 days after overexpression of miR-1305 the differentiated-cell population (*SSEA-1* +) population increases.

Data are represented as the mean ± SD; n = 3. *p < 0.05, **p < 0.01 calculated using the Student-t test.

In summary, all results suggest that miR-1305 overexpression could induce the differentiation the hES cells.

4.6.4 Impact of miR-1305 Overexpression on hES Cell Apoptosis and Cell Cycle

Compared with the control cells transfected with miR-1305 mimic generated a lot of small colonies and more cells in suspension in the culture medium. This led us to investigate the impact of miR-1305 overexpression on hES cell apoptosis. To test this hypothesis, 48 hours after miR-1305 mimic transfection, the cells were stained with Annexin V/PI and were further analysed by flow cytometry. There are more late stage apoptosis and dead cells (5%), and more early stage apoptosis cells (2%) in miR-1305-mimic group compare to the control group. The population of surviving cells was much lower in the miR-1305-mimic group indicating that miR-1305 overexpression induces hES cell apoptosis (Figure 44a). This was further confirmed by staining with an apoptosis marker, cleaved-PARP. Our data shows that, miR-1305 mimic significantly increases the cleaved-PARP positive population (Figure 44b).
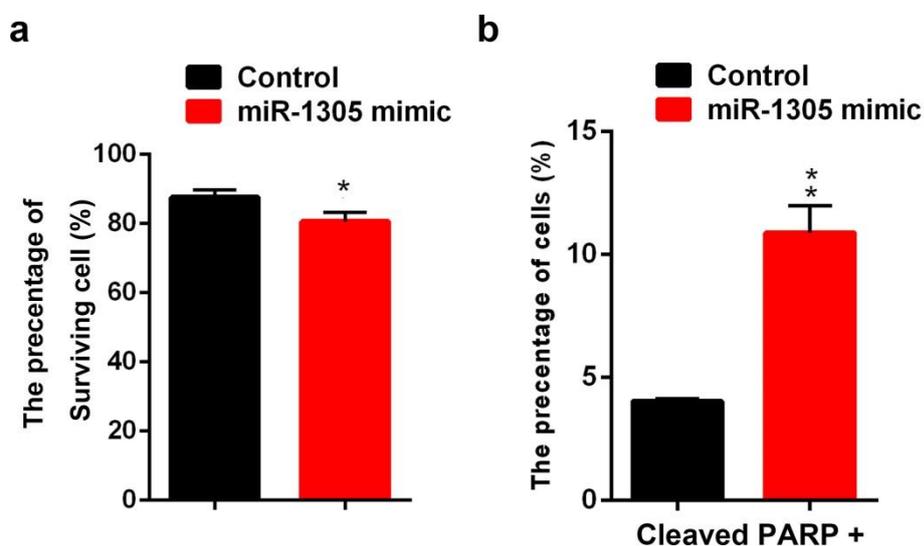
Figure 44. Flow cytometry results showing that miR-1305 overexpression increases cell apoptosis (a) annexin V/PI staining and (b) cleaved PARP staining.
Data are represented as the mean ± SD; n = 3. *$p < 0.05$, **$p < 0.01$ calculated using the Student-t test.

To test the function of miR-1305 in regulating the cell cycle, 24 hours after mimic transfection, the cells were synchronized in the G2/M phase by incubating them with nocodazole for 18 h, as described in Chapter 2.10 (Figure 45) [208].
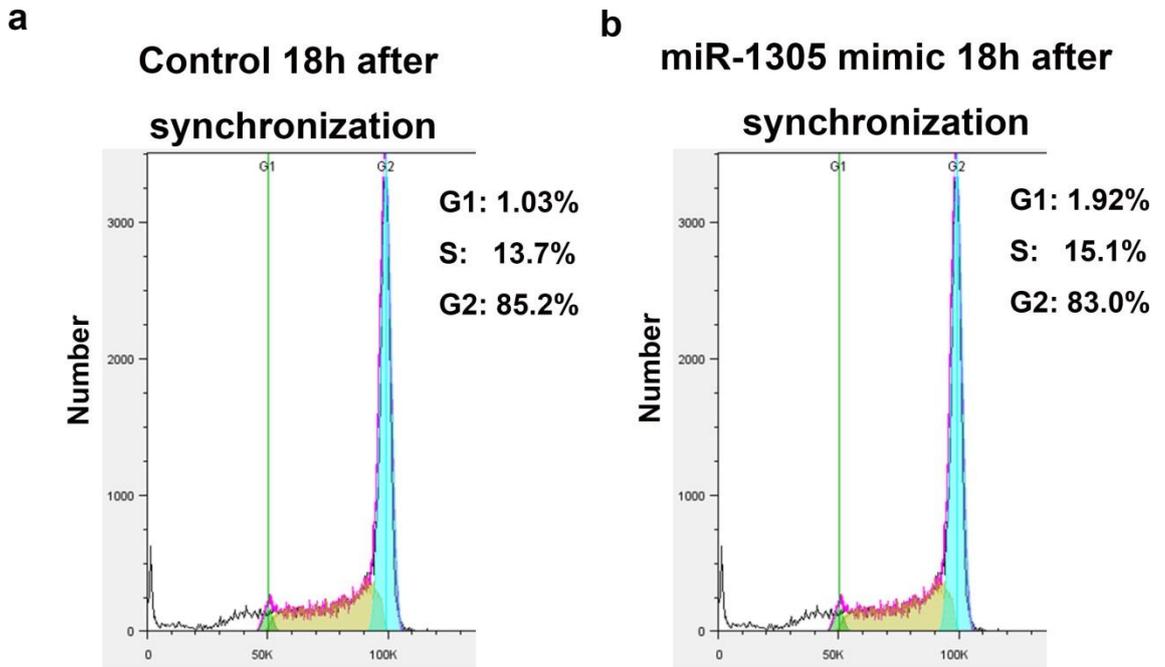
Figure 45. Chart representing the fraction of cells in the G1/S/G2 phase after transfection of (a) miRNA-mimic control or (b) miR-1305 mimic followed by synchronization with nocodazole for 18 h.

Flow cytometry result above shows the percentage of cells in G2 phase after nocodazole treatment for 18 hours. This 18h result represents the state of cells at 0h in time course experiment in Figure 46.

The cell cycle was analysed at different time points after synchronization by flow cytometry. Compared to the control there were more cells in S phase 6 h after synchronization in the cells transfected with miR-1305 mimic, indicating that miR-1305 may speed up the G1/S transition (Figure 46).
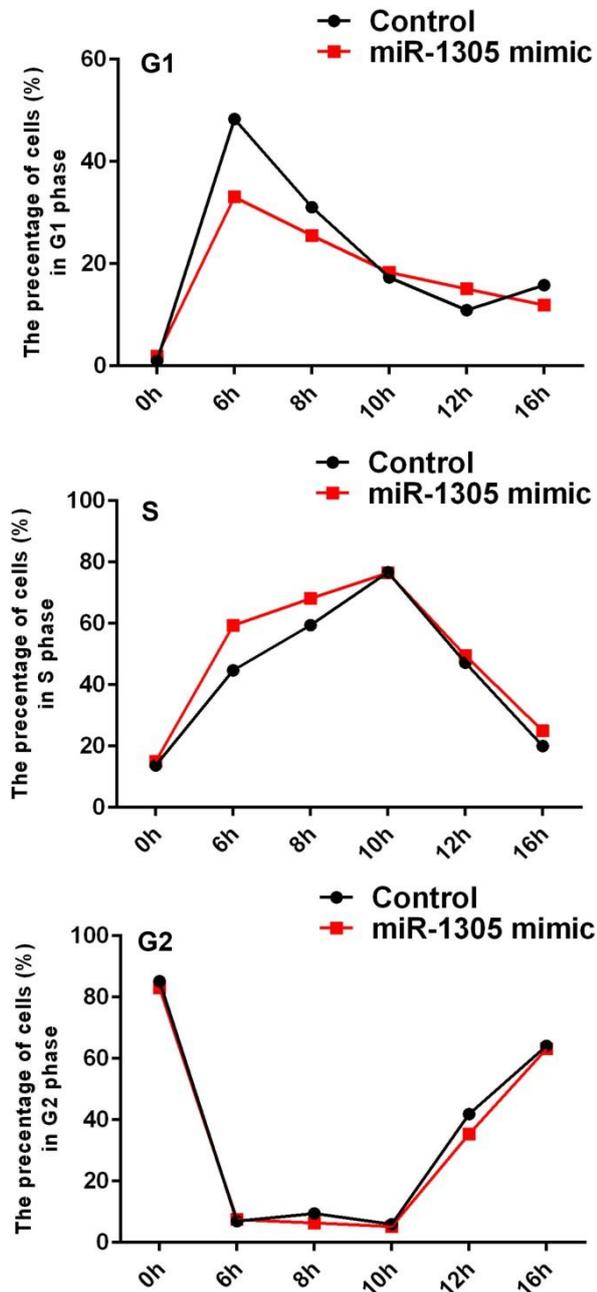
Figure 46. Chart representation of the fraction of cells in G1/S/G2 phase at different time points after transfection with miR-1305 mimic and synchronization with nocodazole for 18 h.

4.6.5 Kinetics of miR-1305 Inhibition

We used miRNA-inhibitors (Invitrogen) to perform loss-of-function tests. hES cells were transfected with a control inhibitor or with a miR-1305 inhibitor using Lipofectamine RNAi max. Quantitative RT-PCR analysis indicated that the miR-1305-inhibitor significantly reduced (~80%) miR-1305 levels which reached their lowest levels 24 hours after transfection, and was still maintained after 96 hours (Figure 47a).

To test the specificity of the miR-1305 inhibitor, we also checked the levels of miR-135a* after miR-1305 inhibitor transfection. After 24 hours after transfection miR-135a* levels did not change, although the levels increased at 48 hours, and decreased at 72 h and 96 h. We attribute these changes to indirect effects induced by miR-1305 knockdown, possibly caused by changes in the cell population (Figure 47b).

These results indicate that the miR-1305 inhibitor specifically and significantly reduces miR-1305 expression and that the transfection method we used worked very well in hES cells.
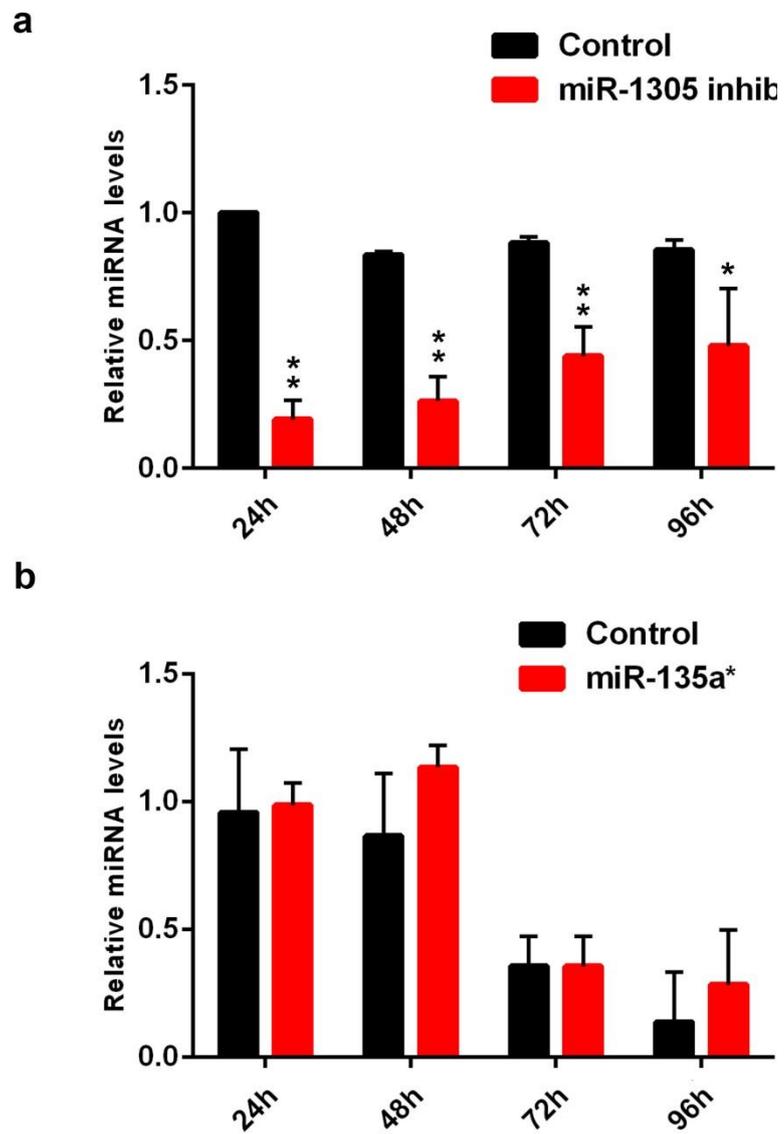
Figure 47. Quantitative RT-PCR analysis of the relative expression levels of miR-1305 and miR-135a* after miR-1305 transfection.

Quantitative RT-PCR data are represented as the mean ± SD; n = 3. *p < 0.05, **p < 0.01 calculated using the Student-t test. The control was set to 1.0.

4.6.6 Impact of miR-1305 Inhibition on hES Cell Pluripotency

We checked the cell morphology 48 hours after transfection of the miR-1305 inhibitor. Both the cells transfected with the control inhibitor or the miR-1305 inhibitor maintained their typical undifferentiated hES cell colony morphology (Figure 48) indicating that miR-1305 inhibition did not induce hES cell differentiation. Furthermore, the colonies in the miR-1305 inhibitor group generally appeared to be bigger than in the control group.
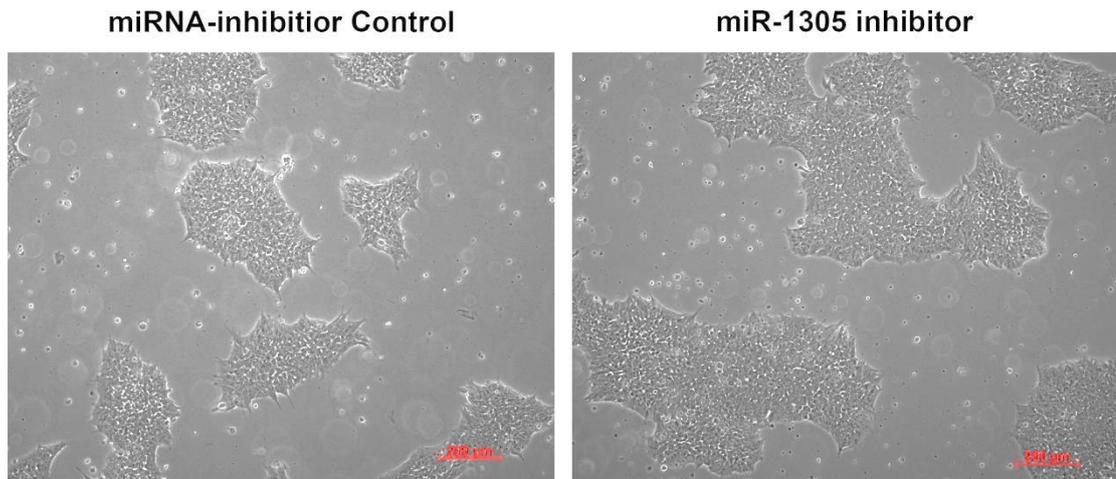
Figure 48. The morphology of H9 hES cells after transfection with the control miRNA-inhibitor or the miR-1305-inhibitor.

This is a representative example of at least three independent experiments.

The cells were collected for qRT-PCR analysis 48 hours after transfection. Consistent with the cell morphology we observed, as shown in Figures 49 and 50, there was a slight but significant increase (10-20%) in the expression of the pluripotency markers *OCT4* and *NANOG* (Figure 49)*,* and a reduction in the expression of ectoderm (*FGF5*), mesoderm (*T* and *MIXL1*), endoderm (*GATA4* and *FOXA1*), and trophectoderm (*HAND1*) markers. The slight change in the expression of pluripotent markers upon miR-1305-inhibit may due to the expression level of miR-1305 in hES cells is relatively low, further reduction miR-1305 may not have obvious effects It is interesting to note that again, unlike any other germ layer makers tested, the expression of *FOXA2*, a definitive endoderm marker, was significantly upregulated (~2.5 fold) upon miR-1305 inhibition (Figure 50).

In brief, miR-1305 inhibition could help hES cell to better maintain the undifferentiated state.
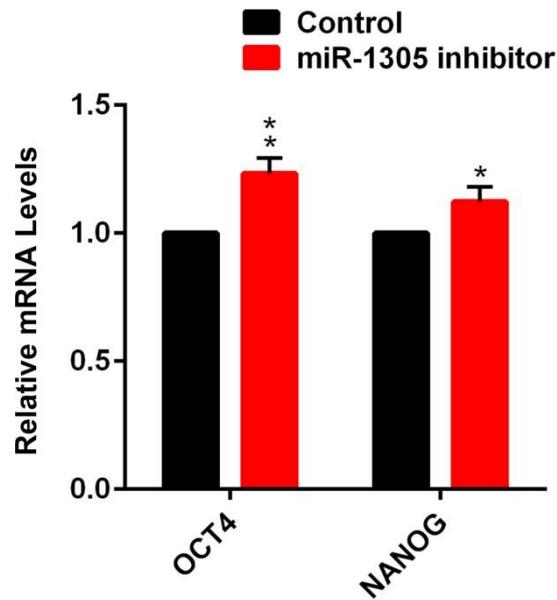
Figure 49. Quantitative RT-PCR analysis of the relative expression levels of pluripotency markers *OCT4* and *NANOG* in H9 hES cells 2 days after transfection with a control inhibitor or a miR-1305-inhibitor.

Quantitative RT-PCR data are represented as the mean ± SD; n = 3. *p < 0.05, **p < 0.01 calculated using the Student-t test. The control was set to 1.0.
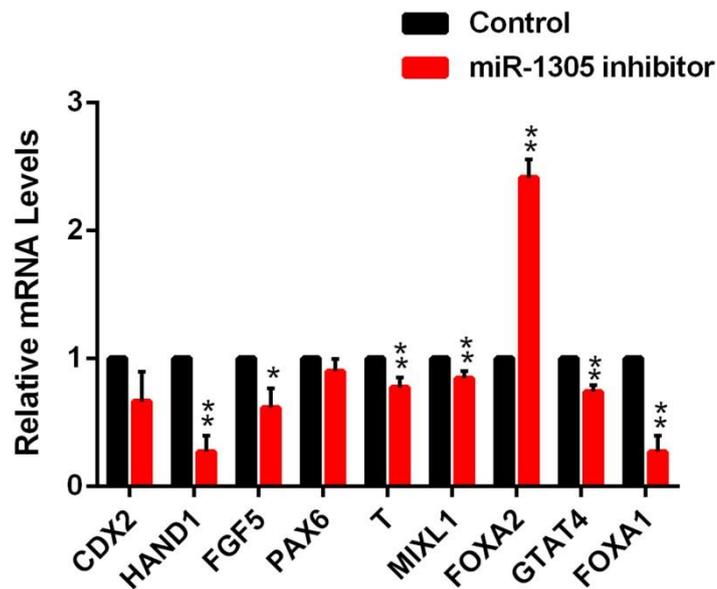
**Figure 50. Quantitative RT-PCR analysis of the relative expression levels of differentiation markers in H9 hES cells 2 days after transfection with a control inhibitor or a miR-1305-inhibitor.**

Quantitative RT-PCR data are represented as the mean ± SD; n = 3. *p < 0.05, **p < 0.01 calculated using the Student-t test. The control was set to 1.0.

4.6.7 Impact of miR-1305 Inhibition on hES Cell Apoptosis and Cell Cycle

Because the cells transfected with the miR-1305 inhibitor generally had better colony morphology we wondered if miR-1305 inhibition affected hES cell apoptosis. To investigate this further we performed flow cytometric analysis on live cells (expressing Annexin V or PI) after transfection. There are less late apoptosis and dead cells (2.5%), and less apoptosis cells in miR-1305-inhibition group compare to the control group (2%). As shown in Figure 51a, miR-1305 inhibition reduced the population of apoptotic cells, which was also confirmed by claved-PAPR1 staining (Figure 51b).
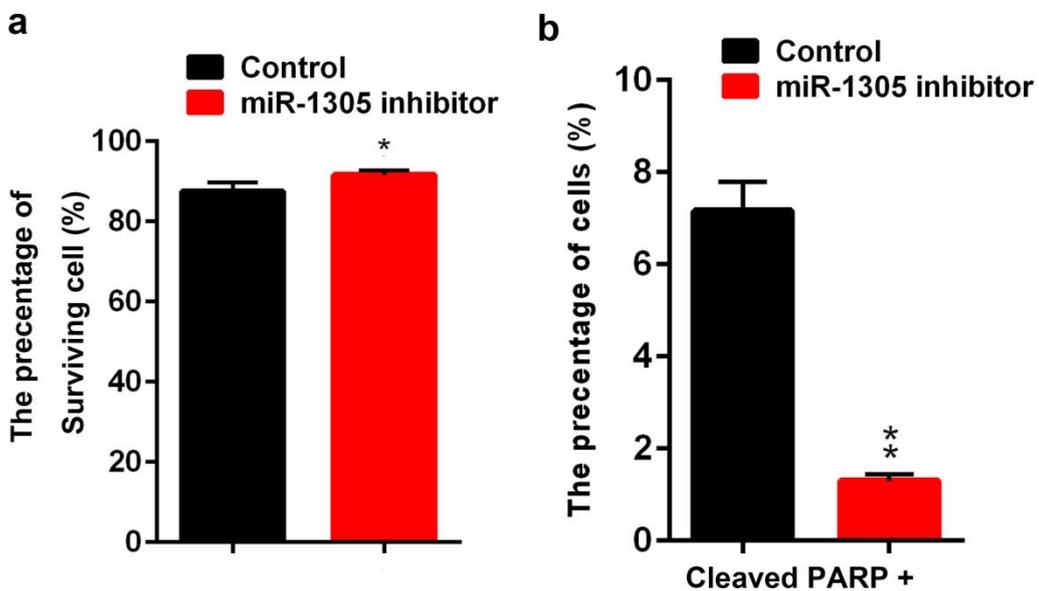
Figure 51. Flow cytometry results showed that inhibition of miR-1305 reduced cell apoptosis.

(a) Annexin V/PI staining (b) Cleaved PARP staining. Data are represented as the mean $\pm$ SD; n = 3. *p < 0.05, **p < 0.01 calculated using the Student-t test.

To test the function of miR-1305 in hES cell cycle regulation, 24 hours after inhibitor transfection the cells were synchronized in the G2/M phase by incubating them with nocodazole for 18 h (Figure 52).
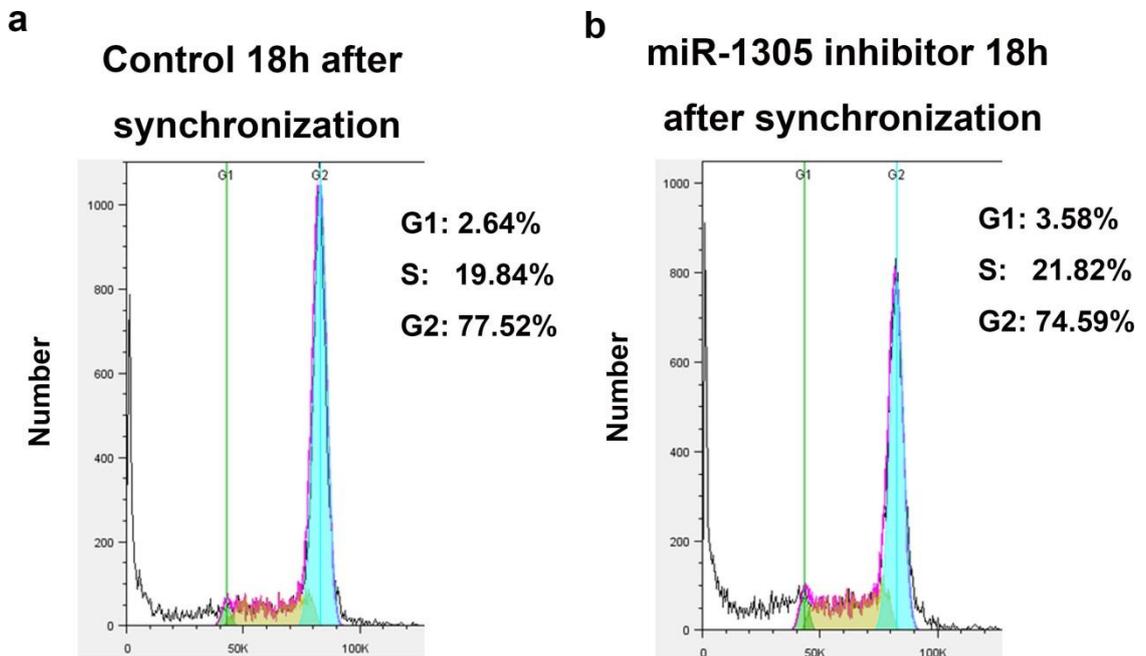
Figure 52. Chart representation of the fraction of cells in the G1/S/G2 phase after transfection of the miR-1305 inhibitor and synchronization by nocodazole for 18 h.

Flow cytometry result above shows the percentage of cells in G2 phase after nocodazole treatment for 18 hours. This 18h result represents the state of cells at 0h in time course experiment in Figure 53.

The cell cycle was analysed at different time points after synchronization by flow cytometry; 10 hours after synchronization, there were fewer miR-1305-inhibitor transfected cells in S phase compared with the control, indicating that miR-1305-inhibition makes the G1/S transition slower (Figure 53).

We are aware that the percentages of cells at G2/M phase (0 h) in two control groups are different (Figure 46 and 53). This may due to the effect of transfected chemical on the cells. When we only compare mimic-control with miR-1305 mimic or inhibit-control with miR-1305 inhibitor, the percentages of cells at G2/M phase is similar after cell synchronization.
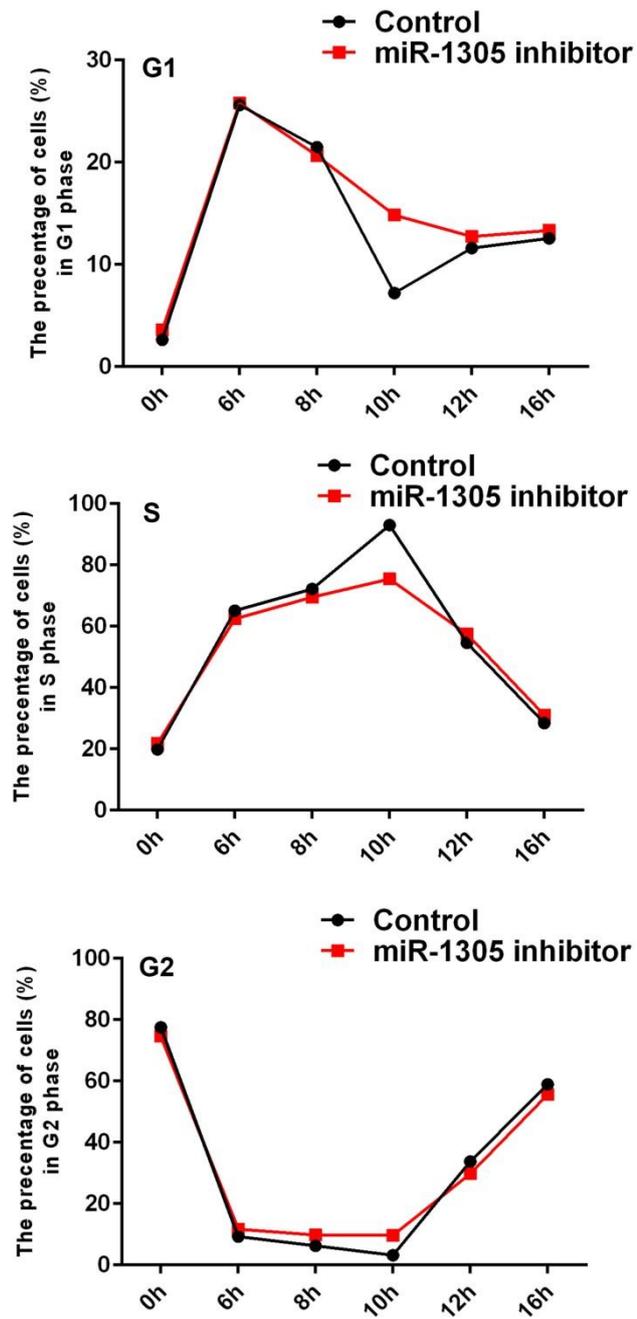
Figure 53. Chart representation of the fraction of cells in the G1/S/G2 phase at different time points after transfection with the miR-1305 inhibitor and synchronization with nocodazole for 18 h.

4.6.8 Impact of miR-1305 Overexpression/Inhibition on hiPS Cell Pluripotency

To test the function of miR-1305 in hiPS cells, we also performed a miRNA mimic/inhibitor transfection in AD3CL1 hiPS cells using same method. AD3CL1 is a well-characterized cell line generated in our lab which we have widely used for other studies. Quantitative RT-PCR analysis indicated similar results to those from the hES cell experiments: miR-1305 overexpression slightly reduced the expression of pluripotency markers *OCT4* and *NANOG* and increased the expression of ectoderm (*FGF5* and *PAX6*), mesoderm (*T* and *MIXL1*), endoderm (*GATA4* and *FOXA1*), and trophectoderm (*CDX2* and *HAND1*) markers. Interestingly, the expression level of *FOXA2* was also reduced in AD3 hiPS cells after miR-1305 mimic transfection (Figure 54).
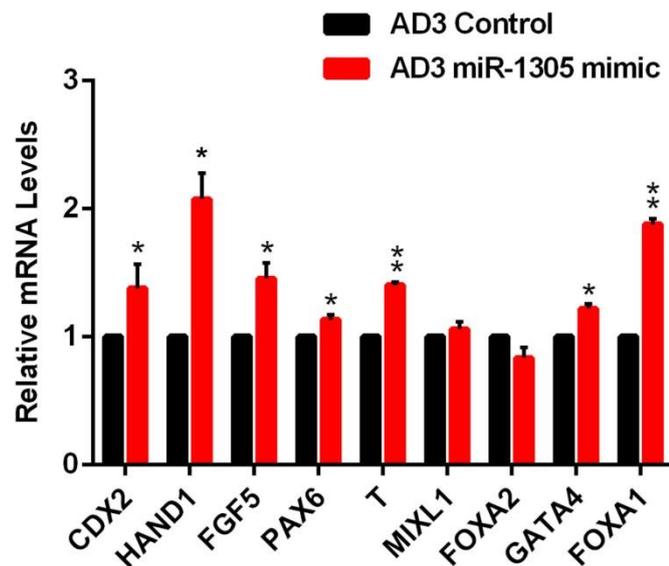
Figure 54. Quantitative RT-PCR analysis of the relative expression levels of differentiation markers in AD3 hiPS cells 2 days after transfection with a control miRNA-mimic or miR-1305-mimic.

Quantitative RT-PCR data are represented as the mean ± SD; n = 3. *p < 0.05, **p < 0.01 calculated using the Student-t test. The control was set to 1.0.

When miR-1305 was inhibited, we could detect a slightly increase in the pluripotency markers *OCT4* and *NANOG* and a reduction in ectoderm (*FGF5* and *PAX6*), mesoderm (*T* and *MIXL1*), endoderm (*GATA4* and *FOXA1*), and trophectoderm (*CDX2* and *HAND1*) markers. Expression of the definitive endoderm marker *FOXA2* was increased upon miR-1305 inhibition on day 2 (Figure 55).
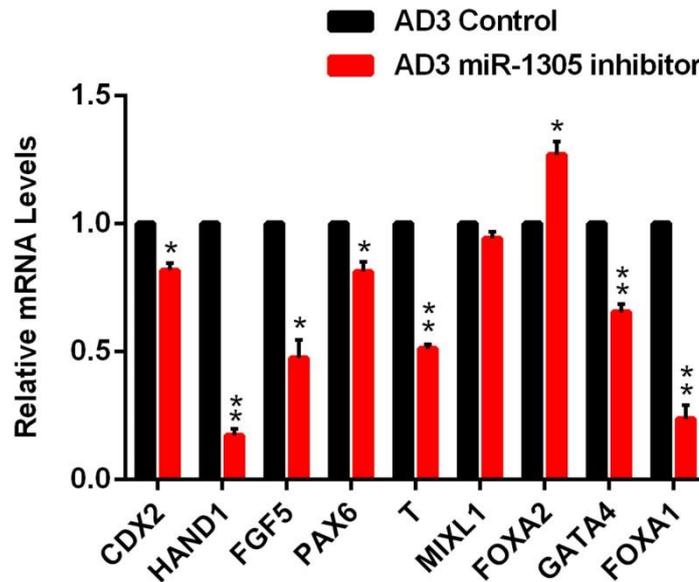
Figure 55. Quantitative RT-PCR analysis of the relative expression levels of differentiation markers in AD3 hiPS cells 2 days after transfection with a control miRNA inhibitor or miR-1305-inhibitor.

Quantitative RT-PCR data are represented as the mean ± SD; n = 3. *p < 0.05, **p < 0.01 calculated using the Student- t test. The control was set to 1.0.

In conclusion, we have confirmed that miR-1305 acts as a cell differentiation, cell cycle, and cell apoptosis regulator in hES/hiPS cells. This microRNA can induce hES/hiPS cell differentiation, speed up the G1/S transition, and increase cell apoptosis.

CHAPTER 5 RESULTS III

Chapter 5. (Result III): Identification of POLR3G as the miRNA-1305 Target in hES Cells

5.1 Microarray-based Expression Profiling of hES Cells with miR-1305 Overexpression or Inhibition

To find potential miR-1305 targets, we studied the global gene expression profiles of H9 hES cells transfected with a miRNA mimic control/miRNA-1305 mimic (2 days after transfection) or a miRNA inhibitor control/miRNA-1305 inhibitor (2 days after transfection) by testing them in a SurePrint G3 Human Gene Expression 8x60K Microarray (Agilent Technologies); the array data was analysed using GeneSpring. The statistical probability of significance was set at $p < 0.05$ and a fold change of greater than 1.3 was used to select the differently-expressed genes after miR-1305 overexpression (miRNA-mimic control vs. miR-1305 mimic) or miR-1305 inhibition (miRNA inhibitor control vs. miR-1305 inhibitor).

The expression level of miRNA target genes should decrease in cells overexpressing miRNA-1305, while it should increase in miRNA-1305-inhibited cells. Therefore Venn analysis (Figure 56) of genes which were downregulated in cells transfected with miR-1305 mimic compared with control, and the genes which were upregulated in miR-1305-inhibited cells compared with control identified 248 potential miR-1305 target genes.
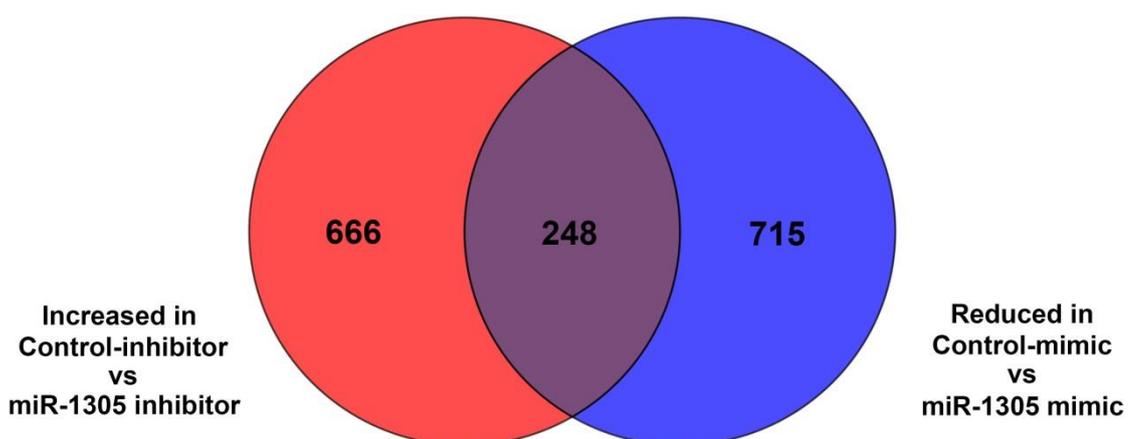
Figure 56. Venn diagram analysis of genes from array data.

The shared area indicates that genes were downregulated in cells transfected with miR-1305 mimic compared with the control and were also upregulated in miR-1305-inhibited cells compared with the control.

5.2 Identification of Gene Expression Signatures Regulated by miR-1305 in hES Cells

In addition to the microarray study, we also used well-known software (TargetScan, miRDB, TargetMINER, RNA22-HAS, and microRNA) to predict miR-1305 targets. To narrow down the candidate miR-1305 target genes, we focused on genes which had been confirmed to function in maintaining pluripotency, and regulating differentiation and cell cycle (Table 26).

Gene name	TargetScan	miRDB	TargetMiner	RNA22-HSA	microRNA
CDK6	+			+	
CYCLIN D2	+		+		
DICER1	+	+			+
LIN28A	+	+	+		+
LIN28B				+	+
POLR3G	+			+	
BCL2	+		+		
MDM2		+			+
MDM4	+				+
ZIC2		+			+

Table 26. List of predicted miR-1305 target genes by TargetScan, miRDB, TargetMINER, RNA22-HAS and microRNA.

By comparing the software prediction results with array data, three potential targets (*LIN28A, POLR3G* and *ZIC2*) which involved in regulating pluripotency and differentiation were choose for further study. *LIN28A* is one of the factors required for pluripotency, which regulates stem cell differentiation and maintenance through targeting let-7. *POLR3G* is a novel pluripotency regulator in hES cells, which is a downstream target of *OCT4* and *NANOG* and can be readily regulated by the ERK1/2 signalling pathway. *ZIC2* is a member of the ZIC family which involved in regulating of Wnt/β-catenin protein signalling [9,308,309].

5.3 Expression Kinetics of Target Gene during miR-1305 Overexpression and Inhibition

We characterized the mRNA expression levels of the predicted target genes in miR-1305-overexpressed or inhibited cells using Quantitative RT-PCR. The results confirmed that *POLR3G, LIN28A,* and *ZIC2* mRNA were decreased upon miR-1305 overexpression and increased upon miR-1305 inhibition (Figure 57).
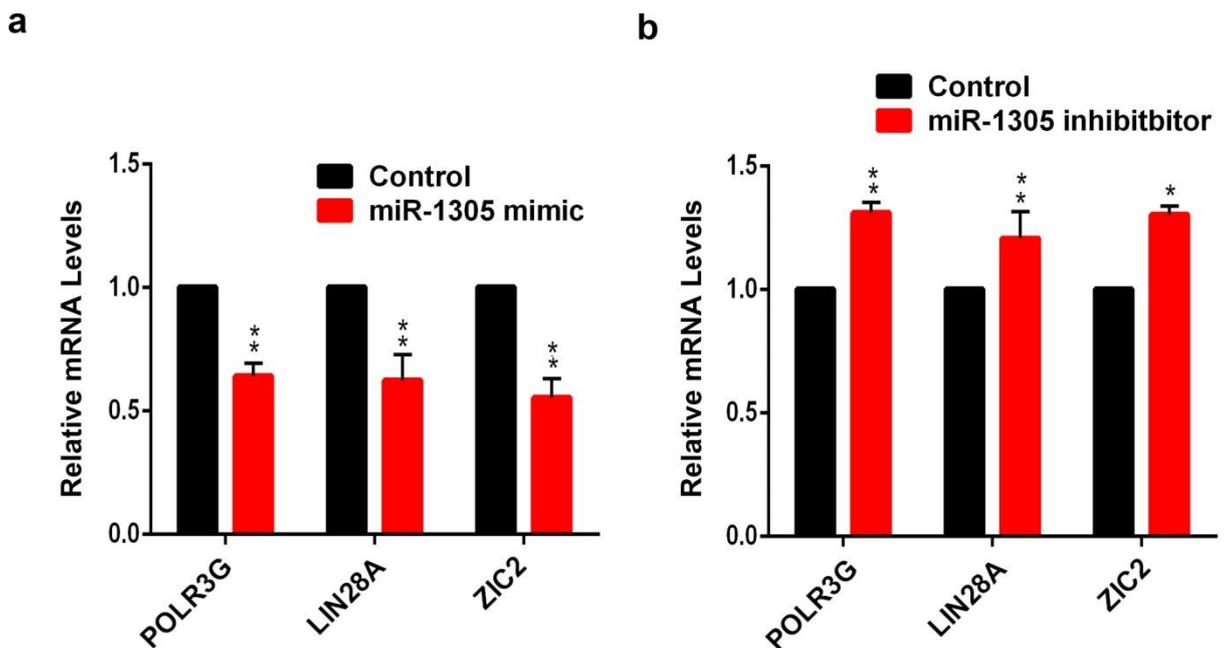
Figure 57. Quantitative RT-PCR analysis of the relative expression levels of the predicted miR-1305 targets.

Quantitative RT-PCR data are represented as the mean ± SD; n = 3. *p < 0.05, **p < 0.01 calculated using the Student-t test. The control was set to 1.0.

Western bolt analysis showed that, the protein level of POLR3G was also reduced when miR-1305 was overexpressed, but was increased when miR-1305 was inhibited (Figure 58). Interestingly, the protein levels of LIN28A and ZIC2 increased upon miR-1305 overexpression, and there was no big difference in their protein levels upon miR-1305 inhibition (Figure 58). Thus, it seems that *POLR3G* is likely to be a direct downstream miR-1305 target.
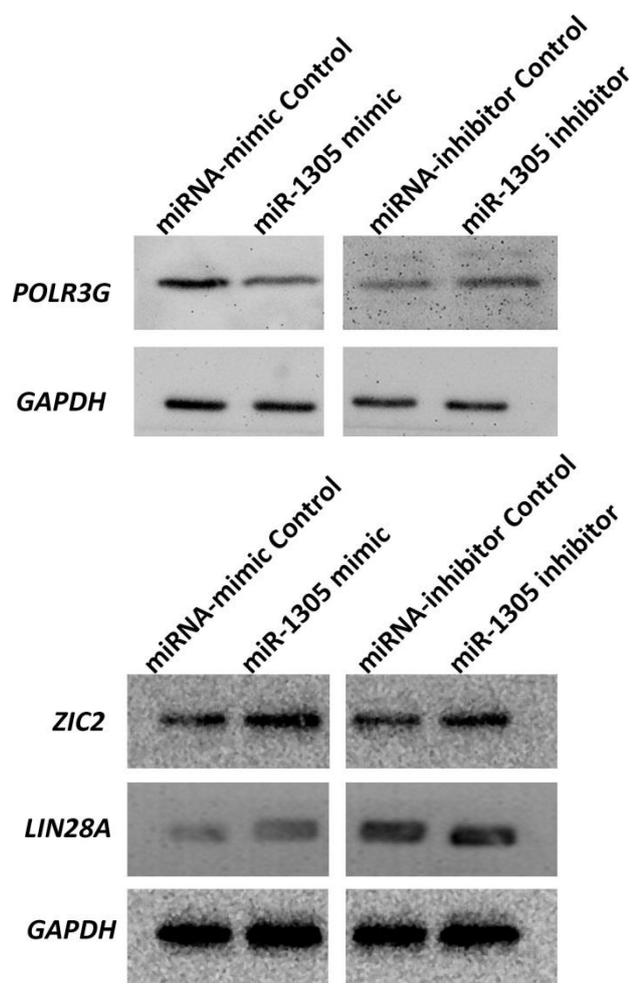
Figure 58. Western blot analysis of the protein levels of the predicted miR-1305 targets.

This is a representative example of at least three independent experiments.

5.4 Confirmation that POLR3G is a Direct miR-1305 Target

Three putative miR-1305 binding sites were identified in the 3'UTR of *POLR3G*. All three predicted binding sites were conserved between different species (Figure 59).
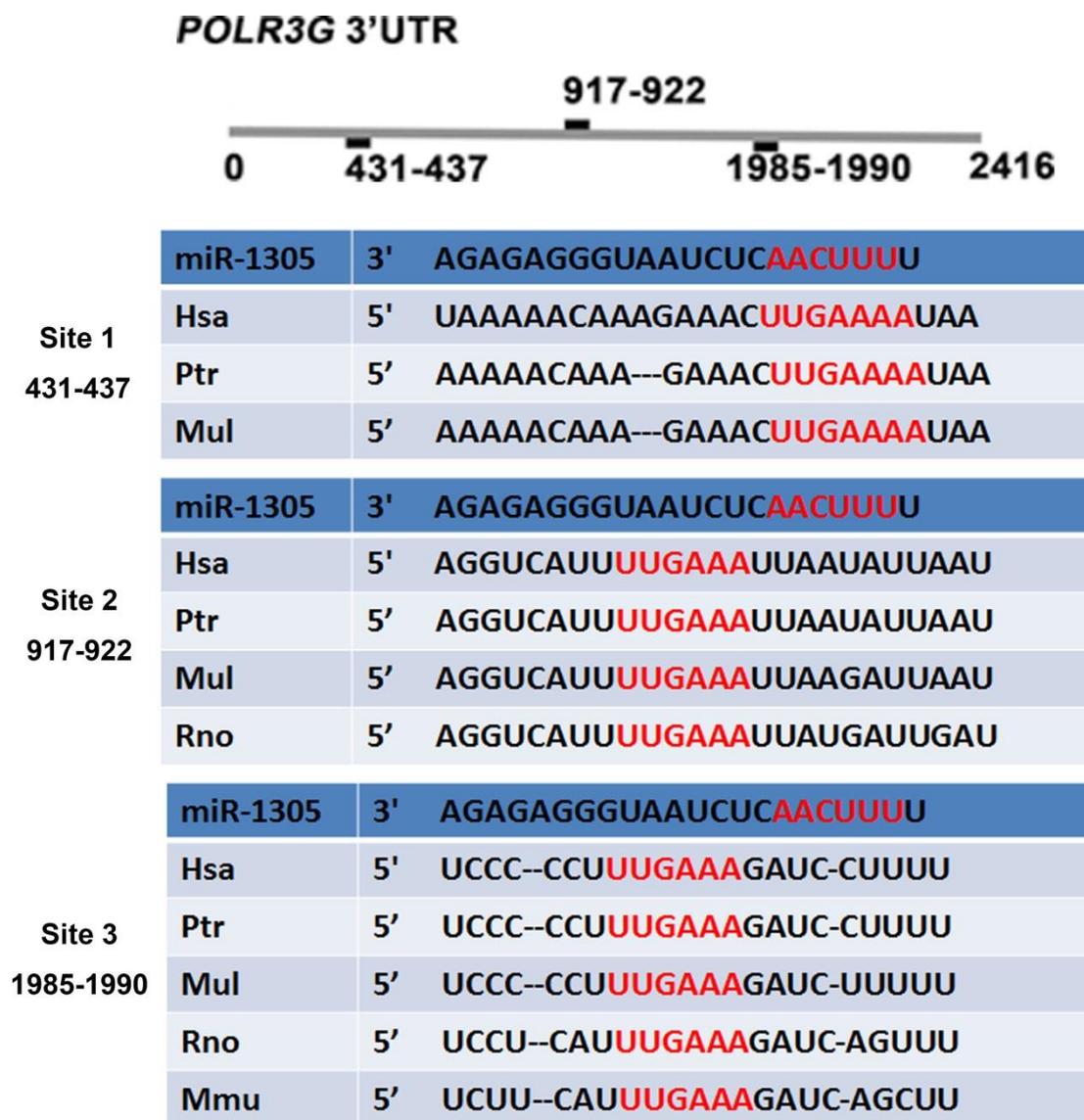
Figure 59. Three putative miR-1305 binding sites in the *POLR3G* 3'-UTR which were identified using TargetScan software.

Next, we investigated the functional interaction between miR-1305 and the *POLR3G* 3'-UTR. We cloned the *POLR3G* 3'-UTR into a psiCHECK™-2 vector (Promega) in order to create a reporter assay. To confirm miR-1305 regulates *POLR3G* by directly binding to its 3'-UTR, all three binding sites were mutated separately or together (Table 27).

Predicated miR-1305 binding sites on *POLR3G* 3'UTR		Sequence
Site 1 431-437	Wild Type	UAAAAACAAAGAAACUUGAAAAUAA
	Mutant	UAAAAACAAAGAAACCCTGGGGUAA
Site 2 917-922	Wild Type	AGGUCAUUUUGAAAUUAAUAUUAAU
	Mutant	AGGUCAUUCCTCCCUUAAUAUUAAU
Site 3 1985-1990	Wild Type	UCCC--CCUUUGAAAGAUC-CUUUU
	Mutant	UCCC--CCUGGTGGGGAUC-CUUUU

Table 27. The wild type and mutated sequences of the predicated miR-1305 binding sites in the *POLR3G* 3'UTR.

All three binding sites were mutated separately or together.

The reporter results showed that ectopic expression of miR-1305 significantly suppressed (~45%) the activity of the 3'UTR *POLR3G* reporter (Figure 60). Moreover, this inhibitory effect could be abolished when all three sites (mu-all) were mutated. Mutation of any single site (mu-1, mu-2, or mu-3) did not disrupt the interaction. Thus, our data shows that miR-1305 can regulate *POLR3G* expression by binding to its 3'UTR.
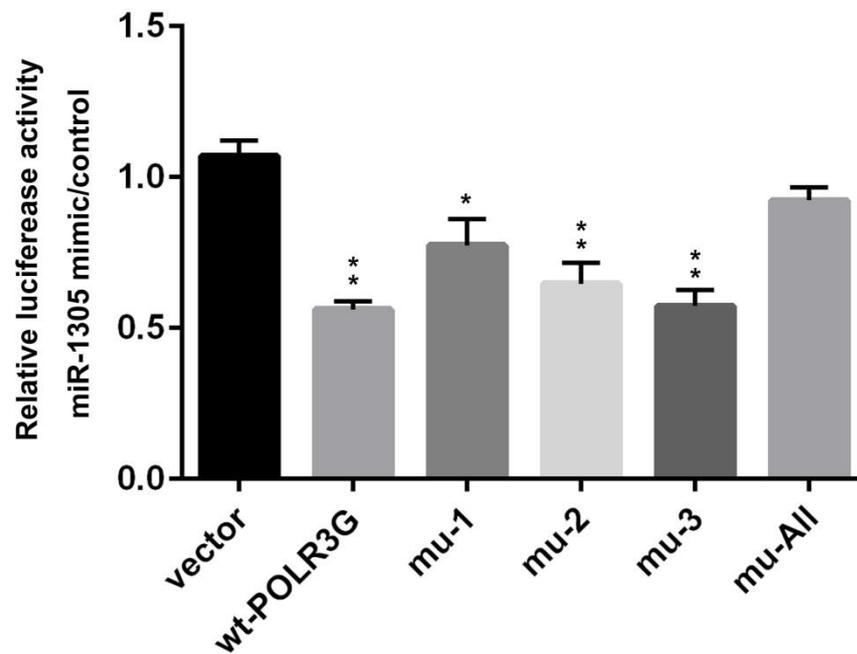
Figure 60. Dual luciferase reporter assays in hES cells co-transfected with dual-luciferase constructs containing wild-type (wt-*POLR3G*) or the *POLR3G* 3'-UTR mutants (mu 1-3) along with the control miR-1305 mimic.

Data are represented as the mean $\pm$ SD; n = 3. *p < 0.05, **p < 0.01 calculated using the Student-t test. The normalised luciferase activity of the miRNA-mimic control-transfected cells was set as 1. Mu-All includes mutations for all three identified miR-1305 binding sites.

5.5 miR-1305 Regulates hES Cell Pluripotency by Targeting POLR3G

POLR3G is an RNA polymerase III (Pol III) subunit [310]. Recent studies show that *POLR3G* is a novel pluripotency regulator in hES cells, and it is a downstream target of *OCT4* and *NANOG* and can be readily regulated by the ERK1/2 signalling pathway [9]. However, the function and regulatory mechanism of *POLR3G* in hES cells remain poorly studied.

To test whether miR-1305 regulates cell differentiation by targeting *POLR3G*, we tried to knockdown *POLR3G* in miR-1305-inhibited hES cells using an siRNA. The experiment was set up as three groups, (1) miRNA-inhibitor control/siRNA control, (2) miR-1305-inhibitor control/siRNA control, (3) miR-1305 inhibitor/*POLR3G* siRNA. The efficiency of siRNA was also tested by qRT-PCR, POLR3G siRNA alone reduced the POLR3G expression about 70% and miRNA/siRNA co-inhibition reduced the POLR3G expression about 50%.

The results indicated that miR-1305 inhibition significantly reduces (10-40%) the expression of all the differentiation markers, while this effect is abolished in the knockdown *POLR3G* scenario where all the differentiation makers were significantly higher (1-1.5 fold) compared with miR-1305 inhibition alone (Figure 61).
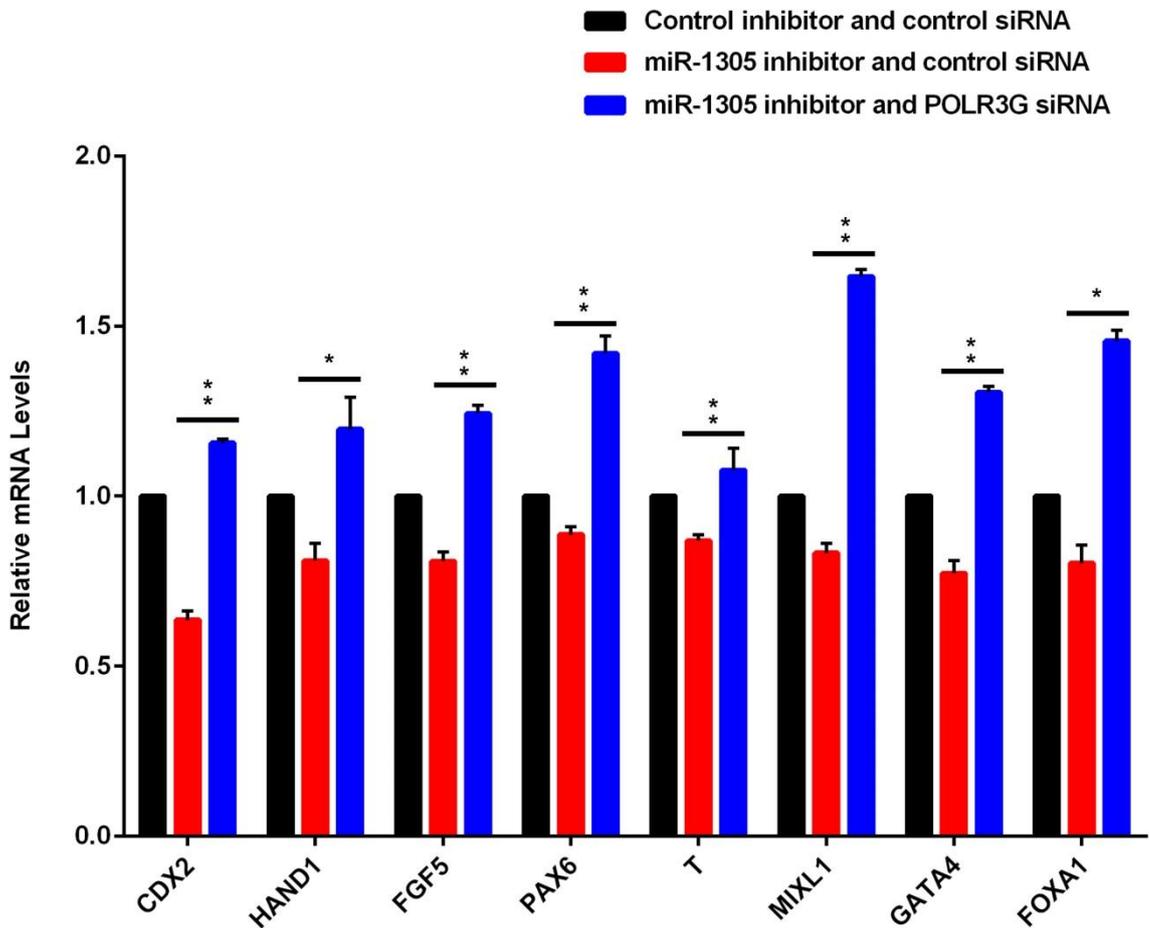

Figure 61. Quantitative RT-PCR analyses of the relative expression levels of differentiation markers in H9 hES cells 2 days after transfection with a control miRNA-inhibitor or miR-1305-inhibitor and control siRNA or *POLR3G* siRNA.

Quantitative RT-PCR data are represented as the mean $\pm$ SD; n = 3. *p < 0.05, **p < 0.01 calculated using the Student-t test. The control was set to 1.0.

Next we studied whether *POLR3G* overexpression could inhibit hES cell differentiation induced by miR-1305. The coding region of *POLR3G* was cloned into a vector with a CAG-promoter and a puromycin expression cassette. We generated a POLR3G-overexpressing stable cell line by transfecting the *POLR3G-CAG* into hES cells and selecting with puromycin (10 μg/mL). Both the mRNA (Figure 62, 2-fold higher) and the protein levels (Figure 63) of POLR3G were increased in the stable cell line compared to the control.
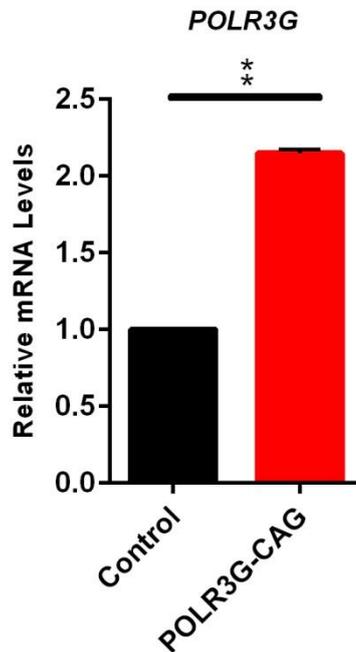
Figure 62. Quantitative RT-PCR analysis of the relative expression levels of *POLR3G* in the control and POLR3G-overexpressing stable cell line.

Quantitative RT-PCR data are represented as the mean $\pm$ SD; n = 3. *p < 0.05, **p < 0.01 calculated using the Student-t test. The control was set to 1.
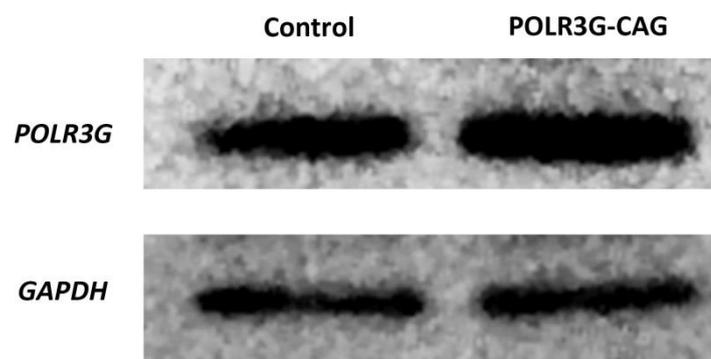
Figure 63. Western blot of the POLR3G protein levels in the control and POLR3G-overexpressing stable cell line.

To test whether *POLR3G* overexpression could inhibit hES cell differentiation induced by miR-1305, a further experiment was set in three groups, (1) control-mimic/control-CAG, (2) miR-1305 mimic/control-CAG, and (3) miRNA-1305 mimic/*POLR3G* and the relative levels of differentiated marker expression were detected by qRT-PCR. As shown in Figure 64, miR-1305 overexpression increased the levels of trophectoderm (*CDX2* and *HAND1*), ectoderm (*FGF5* and *PAX6*), mesoderm (T), and endoderm (*GATA4* and *FOXA1*) markers. While *POLR3G* overexpression abolished the increase of all these differentiation markers, indicating that miR-1305 overexpression induced differentiation by regulating *POLR3G*.
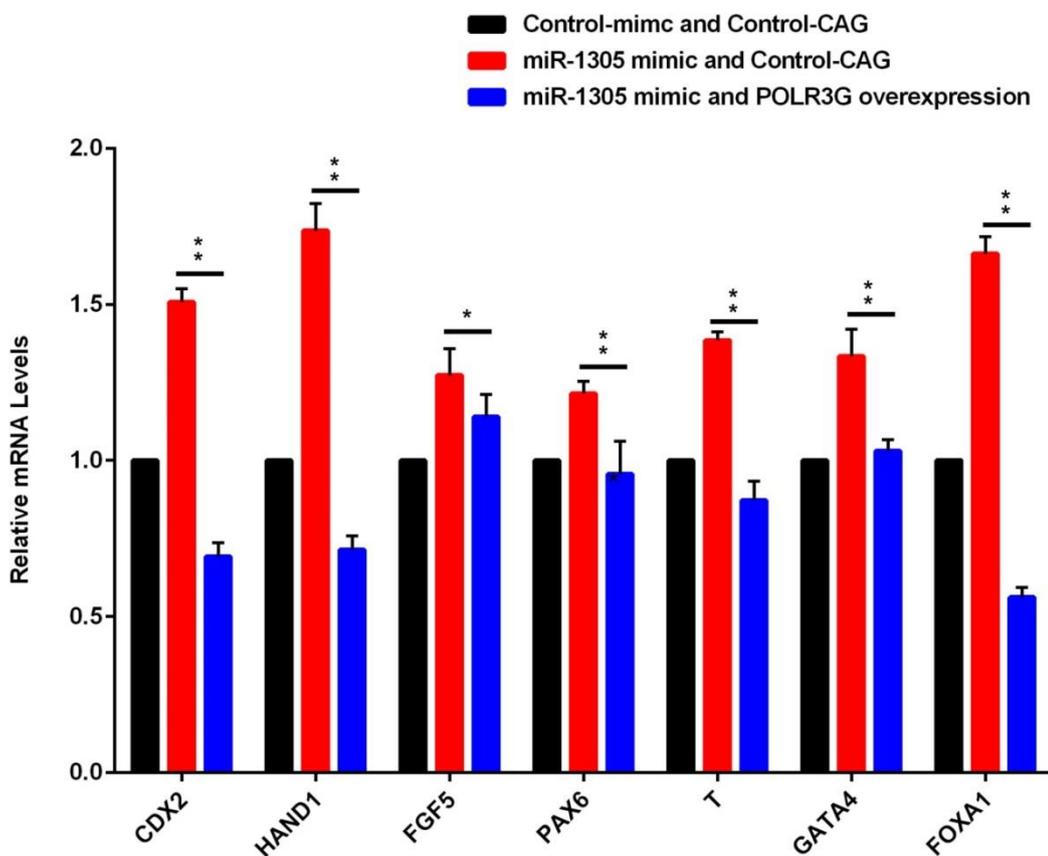
Figure 64. Quantitative RT-PCR analysis of the relative expression levels of differentiation markers in the control-CAG cell line or the POLR3G-CAG cell line 2 days after transfection with a control miRNA-mimic or a miRNA-1305-mimic.

Quantitative RT-PCR data are represented as the mean ± SD; n = 3. *p < 0.05, **p < 0.01 calculated using Student-t test. The control was set to 1.0.

In summary, all these results suggest that the miR-1305 regulates the hES cell pluripotency by directly regulating POLR3G.

CHAPTER 6 DISCUSSION AND FUTURE WORK

Chapter 6. Discussion and Future Work

Pluripotent stem cells, including hES cells and hiPS cells can self-renew indefinitely while also maintaining their full developmental potential to produce all the tissues of the adult body. These remarkable properties hold great potential for modelling early human development and thus represent promising tools for clinical applications in regenerative medicine [44,289]. However, to fully realise their potential and to avoid safety issues, proper strategies must be developed to control their self-renewal and differentiation processes. This requires a good understanding of the molecular details underlying the regulation of hES and hiPS cell cycles, self-renewal, and pluripotency. Along with signalling pathways, transcription factors, and epigenetic regulators, miRNAs are emerging as important regulators in the establishment and maintenance of pluripotency and the cell cycle.

Our study revealed that miR-1305 has a function in regulating pluripotency and the cell cycle in hES cells and hiPS cells. Overexpression of miR-1305 promotes differentiation of hES cells to all three germ layers, increases cell apoptosis, and speeds up the G1/S transition. On the other hand, inhibition of miR-1305 enhances hES pluripotency, decreases apoptosis, and makes the G1/S transition slower. Our results show, for the first time, that *POLR3G*, a regulator of hES cell pluripotency, is a downstream target of miR-1305. This is also the first time that miR-1305 has been shown to have an important role in the regulation of pluripotency and the cell cycle in hES cells. Thus, we have described a link between miRNA (miR-1305) and a pluripotency factor (*POLR3G*), which will help us to better understand the regulatory network in human pluripotent stem cells.

miR-1305 was chosen as the target based on our array screening-experiments which contained samples of undifferentiated hES cells, differentiated cells, and hES cells in different stages of the cell cycle. The array results show that miR-1305 increased expression during the G1/S transition and was highly expressed in hES cells compared to differentiated cells (Table 24). The validity of our array data was further confirmed by checking that the changes in expression of several other well-known miRNAs matched those reported in the literature. For example, in our array, miR-372, which is enriched in hES cells [259] and promotes the G1/S transition [277], was also highly expressed in hES cells in S phase relative to the G1 and G2 phases.

Further study by qRT-PCR confirmed the expression of miR-1305 was higher in S phase and was generally downregulated during hES cell differentiation (it was higher in hES cells compared with adult fibroblast cells). Interestingly, miR-1305 expression significantly increased at the beginning of EB differentiation (EB D1), and its expression decreased from D3 but it was still detectable in D21 EBs and fibroblasts (Figures 20, 21). Besides miR-1305, qRT-PCR experiments also confirmed that miR-367, which is enriched in undifferentiated hES cells and plays role in the G1/S transition [276,299,300], was also highly expressed in the G1 phase relative to the S and G2 phases in our undifferentiated hES cells. These results demonstrate the validity and accuracy of our array and expression profile data, and further indicate that our list of 33 miRNA candidates is likely to represent a valuable resource for future functional studies aimed at comprehensively defining the role of miRNAs in every aspect of hES cell behaviour, as well as in the hES cell cycle process.

Little is known about the function of miR-1305, because most previous studies focus on its expression profile; it is highly expressed in CpG island methylator-phenotype positive or TP53-mutated colon tumours [311], while it expressed at a lower level in systemic lupus erythematosus and rheumatoid arthritis patient cells compared to healthy controls [312]. More recently, another study showed that miR-1305 was significantly upregulated in human periodontal ligament-derived stem cells (PDLSC) derived from smokers, suggesting that it might play an important role in the deleterious effects on stem cells caused by cigarette smoke [313].

Our results reveal a function for miR-1305 in initiating hES cell differentiation. Compared with the control, miR-1305 overexpression induced a 10-20% reduction in the expression of pluripotency markers (*OCT4* and *NANOG*), and a 1.5-2-fold increase in the expression of differentiation markers (*CDX2, HAND1, FGF5, PAX6, T, GATA4, and FOXA1*). hES cells overexpressing miR-1305 still maintained the hES cell colony morphology but there were increased signs of differentiation. These results suggest that miR-1305-induced differentiation occurs at a very early stage. Consistent with this finding, miR-1305 expression increased at the beginning of differentiation (D1) in an EB spontaneous-differentiation model, and then decreased as differentiation progressed (Figure 21), thus indicating that miR-1305 has role in initiating, but not furthering, hES cell differentiation. The function of miR-1305 in hES cells can be further elucidated in future studies by specifically overexpressing miR-1305 at different time points during hES cells differentiation, or by first increasing its expression and then inhibiting it.

This 'first increase, then decrease' expression profile during differentiation has also been found in other genes. For example, transcription factor Snail, which is involved in controlling the epithelial-to-mesenchymal transition (EMT), a process that is essential for initiating and promoting ES cell differentiation. Snail first increases at the beginning of the differentiation, reaching its peak on day 3.5, and then decreases as differentiation continues [314].

We also performed these functional studies with miR-1305 in AD3 hiPS cells, which gave similar results to hES cells. The overexpression of miR-1305 induced cell differentiation and its knockdown helped maintain pluripotency. These results demonstrate that miR-1305 may also have a fundamental role in regulating human pluripotent stem cell biogenesis.

Our study revealed *POLR3G* as an authentic downstream miR-1305 target. Thus we provide the first evidence of a direct link between *POLR3G* and miR-1305 in regulating hES cell pluripotency. POLR3G plays an important role in maintaining hES cell pluripotency, as decreased levels of *POLR3G* results in the loss of pluripotency and promotes hES cell differentiation, while its overexpression makes hES cells more resistant to differentiation. Moreover, *OCT4* and *NANOG* can regulate *POLR3G* levels by binding its promoter region [9], and *POLR3G* overexpression can rescue the hES cell differentiation induced by miR-1305. However, there was only about a 30% change of the *POLR3G* expression level after overexpressing or inhibiting miR-1305.

miRNAs bind to complementary target sites in mRNA 3'UTRs, which results in degradation or translational repression of the target mRNAs [240]. In general, one gene can be repressed by multiple miRNAs and one miRNA may repress multiple target genes, which results in the formation of complex regulatory feedback networks [241]. Many miRNAs have a very 'gentle' regulatory function in regulating the levels of their target genes, like for example, miR-145 which targets *KLF4* in hES cells. Increased miR-145 expression inhibits hES cell self-renewal and represses KLF4 expression, but only reduces *KLF4* mRNA levels by 20% and its protein levels by 50% [270]. Another example are miRNAs belonging to the miR-302 cluster, which are emerging as key players in the control of proliferation and cell fate determination during hES cell differentiation. This miRNA can directly repress NR2F2, but NR2F2 mRNA levels are only reduced by about 20-50% cells overexpressing miR-302 cells compared with the control [315].

Our functional study of miR-1305 is consistent with previous data on *POLR3G*, its knockdown resulted in loss of hES cell morphology and we noted similar observations to the authors, "bulky cells with multiple granules and a spindle-like cell type" [9], in our miR-1305-overexpressing cells (Figure 40). *POLR3G* knockdown in hES cells results in a 2-6-fold upregulation of differentiation markers and a 40% reduction in pluripotent markers (*OCT4* and *NANOG*), which was a more significant change than was induced by miR-1305 overexpression. One possible explanation for this is that the reduction is more effective by directly knocking down *POLR3G* (40-50% reduction) compared to decreasing it indirectly via miR-1305 overexpression (30% reduction) [9]. Knockdown of miR-1305 helps hES cells maintain an undifferentiated state with typical hES morphology, lowers differentiation marker (*HAND1*, *FGF5*, *T*, *MIXL1*, *GATA4,* and *FOXA1*) expression compared to hES cells (by 20-70%), and slightly increases pluripotent marker (*OCT4* and *NANOG*) expression (by 10-15%). This is also consistent with the *POLR3G* study, in which *POLR3G* overexpression had no effect on hES cell morphology but slightly increased (by 15%) pluripotent marker (*OCT4* and *NANOG*) expression and reduced (by 40-70%) differentiation marker expression during EB differentiation [9].

Besides pluripotency marker, *POLR3G*, there are some other genes which are potential miR-1305 targets. For example, *FOXA2* could be potential miR-1305 targets. In *POLR3G* study, expression of *FOXA2* during *POLR3G* ectopic expression was not studied. In this study, unlike other germ layer markers, *FOXA2* decreased when overexpressed miR-1305 and increased when inhibited miR-1305, which indicated that miR-1305 might regulate the *FOXA2* level directly. miR-1305 could target not only pluripotent genes, but also some differentiated genes, this might be the mechanism of why miR-1305 increased at the beginning of differentiation, but need to decrease later for further differentiation (Figure 21).

Cell cycle in hES cells and hiPS cells is rapid: it is estimated at about 15-16 h, with a very short G1 phase [173,187]. Cell-cycle regulation is important for maintaining hES cell self-renewal, as illustrated by experiments that inhibited CDKs in hES cells, thus promoting hES cell G1/S arrest, downregulating the pluripotency marker *OCT4,* and inducing hES cell differentiation [206]. In this study, miR-1305 overexpression in hES cells induced their differentiation and accelerated their entry into S-phase. This is noteworthy because differentiated cells normally enter S-phase more slowly than hES cells [172]. This result indicted that miR-1305 might regulate the cell cycle and

pluripotency independently. There are several cell-cycle related genes on the list of predicted miR-1305 target genes, such as *CDK6* and *CYCLIN D2* (Table 26), which further hints at the potential function of this miRNA in cell cycle regulation. However, our microarray study did not reveal any changes in the expression of these targets, leaving the question of how miR-1305 regulates the G1/S transition process. Previous array analysis of miR-1305 has also indicated that miR-1305 may be involved in cell cycle regulation [316], and so future work in this area will focus on exploring its potential cell cycle targets by further analysis of our array data and other published array data.

Similarly, our study showed that miR-1305 overexpression increased cell apoptosis while its knockdown reduced the population of apoptotic cells, however there was no changes in apoptosis when POLR3G was knocked down [9]. There are also several apoptosis related genes on the list of predicted miR-1305 target genes, such as *BCL2, MDM2,* and *MDM4* (Table 26). These findings indicate that miR-1305 might have potential function in regulating cell apoptosis, but not via *POLR3G*.

Recent study in human periodontal ligament-derived stem cells, RUNX2 was found as one of the miR-1305 target genes [316]. It was showed that upregulation of miR-1305 could be associated with downregulation of RUNX2, which effect stem cell migration and osteogenic differentiation [317,318]. RUNX2 is known as a critical regulator during osteogenic development [319]. Its expression significantly increased during hES cell differentiation [318]. One recent study revealed the role of Runx2 in regulating cell cycle and apoptosis in MCF-10A [320]. They found that ectopic Runx2 expression increases cell cycle G1 stage, and reduced the cell apoptosis [320], which is in a good agreement with our data about knocking down miR-1305 in hES cells. Future work will focus on investigation whether RUNX2 is the target of miR-1305 or the function of RUNX2 in hES cells might help us find the answer for the mechanism of miR-1305 in regulating cell cycle and apoptosis.

Here we report the miR-1305 expression profile during hES cell differentiation, its function in regulating pluripotency, and its downstream targets. However, upstream regulators of miR-1305 in hES cells remains unclear. From the data presented here we can infer that miR-1305 expression is precisely regulated in hES cells, because 1) it is expressed at much higher levels in undifferentiated hES cells compared with fully differentiated cells (fibroblasts), 2) when its level in hES cells goes higher than normal the cells are induced to initiate differentiation.

In future studies, in order to find upstream miR-1305 regulators we could carry out ChIP qPCR analysis of OCT4, SOX2, KLF4, c-MYC, NANOG, TCF3, and SUZ12 binding in hES cells, then use NimbleScan software to link them to histone methylation (especially H3K4me3 which is associated with transcription start sites, even in non-transcribing genes) and acetylation marks, as well as miR-1305 pluripotency factors to regulatory regions. Loss-of-function experiments in hES and hiPS cells using siRNAs could also be performed for the previously mentioned pluripotency factors, followed by miR-1305 expression analysis.

Previous studies on *POLR3G* have shown that it is present in the cytoplasm of fertilized mouse zygotes and two-cell embryos, and that it is located in the nucleus during the 8-16-cell stages and the blastocyst stage, suggesting it may have function during embryo development [9]. Given that previous studies have shown that miRNAs are expressed at specific stages of mammalian embryonic development [321,322], it would be interesting to study the function of miR-1305 in embryonic development, especially in the light that *POLR3G* is a functional miR-1305 target.

In conclusion, we have established a useful platform for studying miRNA expression in hES cells in our lab. Furthermore, our work has revealed a novel role of miR-1305 in regulating pluripotency, cell cycle, and cell apoptosis in hES cells, and we also found that POLR3G is a downstream target of miR-1305. Taken together, our results provide a link between miRNAs (miR-1305) and pluripotency factors (*POLR3G*) which will help us to better understand the regulatory network in hES cells. A schematic summary of the published literature and the data generated from this manuscript is presented in Figure 65.
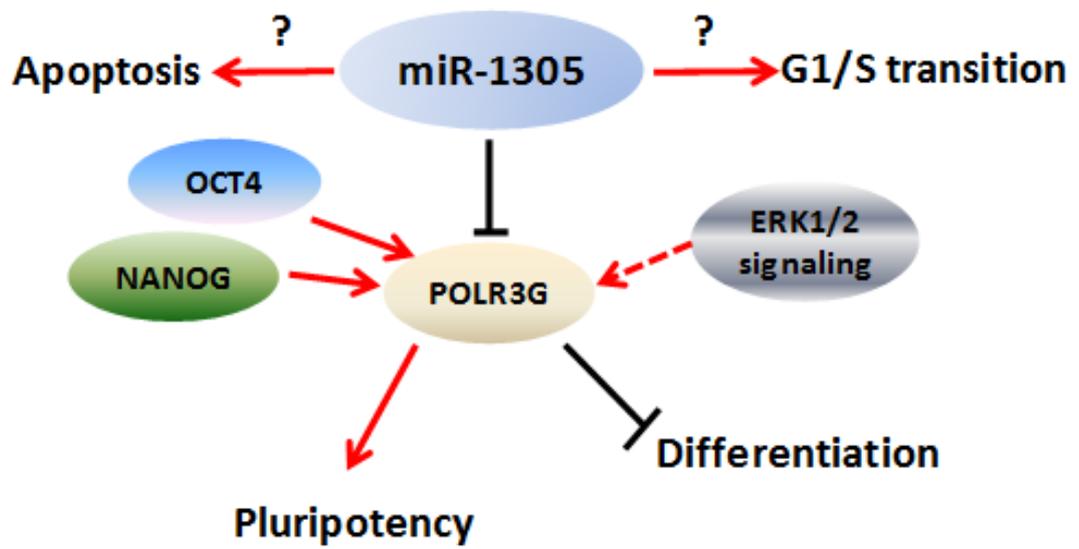
Figure 65. Schematic representation of the function of miR-1305 in regulating pluripotency, cell cycle, and cell apoptosis in hES cells.

Arrows indicate stimulatory modifications and blocked lines show inhibitory modifications. ? indicates scientific questions that have not yet been addressed.

APPENDIX

Primer name	Forward Sequence	Reverse Sequence
GAPDH	TGCACCACCAACTGCTTAGC	GGCATGGACTGTGGTCATGAG
PAX6	GCCTATGCAACCCCCAGT	TCACTTCCGGGAACTTGAAC
SOX2	TTGTTCGATCCCAACTTTCC	ACATGGATTCTCGGCAGACT
MIXL1	GAGACTTGGCACGCCTGT	GGTACCCCGACATCCACTT
T	CAGTGGCAGTCTCAGGTTAAGAAGGA	CGCTACTGCAGGTGTGAGCAA
FOXA2	GCATTCCCAATCTTGACACGGTGA	GCCCTTGCAGCCAGAATACACATT
GATA4	TCCAAACCAGAAAACGGAAG	AAGGCTCTCACTGCCTGAAG
CDX2	CTCGGCAGCCAAGTGAAAAC	CTCCTTTGCTCTGCGGTTCT
HAND1	ACCAGCTACATCGCCTACCTGATG	TCCCTATTAACGCCGCTCCAT
OCT4	GAGAACCGAGTGAGAGGCAACC	CATAGTCGCTGCTTGATCGCTTG
KLF4	TTACCAAGAGCTCATGCCACC	GCGAATTTCCATCCACAGCC
FGF5	CACTGATAGGAACCCTAGAGGC	CAGATGGAAACCGATGCCC
NANOG	AAGGTCCCGGTCAAGAAACAG	CTTCTGCGTCACACCATTGC
FOXA1	AAGGCATACGAACAGGCACTG	TACACACCTTGGTAGTACGCC
TWF1-1	ATGCAGCAACAAGAGCAACTC	TCCTCTGGGCTCTCATTGAT
TWF1-2	CAATGAGAGCCCAGAGGATCATA	AACGAGCTGAATCCTTGGGAA
POLR3G	CGCTTCGAGACTTAGGGAGC	GGGGGTGGTTTCAACACTACA
LIN28	AGCGCAGATCAAAAGGAGACA	CCTCTCGAAAGTAGGTTGGCT
ZIC2	CACCTCCGATAAGCCCTATCT	GGCGTGGACGACTCATAGC

Table 28. List of Quantitative PCR primers used in this study.

Potential targets of miR-1305 (generated from array data)

Probe Name	Gene Symbol	Description
A_21_P0002274	lnc-INSIG2-1	LNCipedia lincRNA
A_21_P0002430	lnc-HAAO-1	Q3X3G3_9ACTN
A_19_P00322705	MIAT	Homo sapiens myocardial infarction associated transcript (non-protein coding) (MIAT), transcript variant 1
A_23_P129174	LRRC49	Homo sapiens leucine rich repeat containing 49 (LRRC49), transcript variant 2
A_21_P0002549	lnc-GPR55-2	LNCipedia lincRNA
A_21_P0007055	lnc-MAP3K8-6	LNCipedia lincRNA
A_21_P0008673	lnc-FURIN-1	LNCipedia lincRNA
A_33_P3233546		
A_23_P306352	RGAG1	Homo sapiens retrotransposon gag domain containing 1
A_23_P86283	LAPTM5	Homo sapiens lysosomal protein transmembrane 5
A_24_P396231	LAMP2	Homo sapiens lysosomal-associated membrane protein 2 (LAMP2), transcript variant A
A_21_P0013316	XLOC_l2_013868	BROAD Institute lincRNA
A_23_P423309	PCDH12	Homo sapiens protocadherin 12
A_33_P3326662	lnc-PDGFB-2	Homo sapiens cDNA FLJ42244 fis, clone TKIDN2005934
A_33_P3344861	LOC389602	Homo sapiens uncharacterized LOC389602
A_24_P293530	CYP4X1	Homo sapiens cytochrome P450, family 4, subfamily X, polypeptide 1
A_33_P3256883		
A_33_P3415623	LRRIQ1	leucine-rich repeats and IQ motif containing 1
A_24_P402779	PARP3	Homo sapiens poly (ADP-ribose) polymerase family, member 3 (PARP3), transcript variant 2
A_32_P116989	ZCCHC18	Homo sapiens zinc finger, CCHC domain containing 18 (ZCCHC18), transcript variant 1

A_21_P0007296	LOC101929497	Homo sapiens uncharacterized LOC101929497
A_21_P0011629	DNAH17-AS1	Homo sapiens DNAH17 antisense RNA 1
A_21_P0014290	LOC100507480	PREDICTED: Homo sapiens uncharacterized LOC100507480
A_33_P3231602	ZNF569	Homo sapiens zinc finger protein 569
A_21_P0001447		PREDICTED: Homo sapiens uncharacterized LOC102724382
A_21_P0007879	CISTR	Homo sapiens chondrogenesis-associated transcript (CISTR), transcript variant 1
A_23_P120794	SLC7A4	Homo sapiens solute carrier family 7, member 4
A_23_P100386	IL34	Homo sapiens interleukin 34 (IL34), transcript variant 1
A_23_P147465	PARK2	Homo sapiens parkin RBR E3 ubiquitin protein ligase (PARK2), transcript variant 1
A_21_P0013827	XLOC_l2_015789	BROAD Institute lincRNA
A_23_P86599	DMBT1	Homo sapiens deleted in malignant brain tumors 1 (DMBT1), transcript variant 2
A_21_P0003563	lnc-STK32B-1	DB207493 TRACH2 Homo sapiens cDNA
A_33_P3328543		
A_33_P3371237	LOC100131514	PREDICTED: Homo sapiens mucin-3A-like
A_23_P373687	PUS10	Homo sapiens pseudouridylate synthase 10
A_33_P3391455	SCN5A	Homo sapiens sodium channel, voltage gated, type V alpha subunit (SCN5A), transcript variant 6
A_33_P3287403		
A_21_P0014166	LOC100506379	AF064804 transcription factor SUPT3H
A_33_P3316169	ZNF705E	Homo sapiens zinc finger protein 705E
A_33_P3362367	RTN3	reticulon 3
A_21_P0003455		BX115251
A_33_P3340802	DHDDS	dehydrodolichyl diphosphate synthase

A_21_P0002066		
A_21_P0006342	lnc-DMRTA1-5	LNCipedia lincRNA
A_23_P140375	NGB	Homo sapiens neuroglobin
A_33_P3213645	ERN2	Homo sapiens endoplasmic reticulum to nucleus signaling 2
A_33_P3388067	ZNF735	Homo sapiens zinc finger protein 735
A_24_P294851	TRIM38	Homo sapiens tripartite motif containing 38
A_24_P147242	RBFOX1	Homo sapiens RNA binding protein, fox-1 homolog (C. elegans) 1 (RBFOX1), transcript variant 3
A_23_P31124	COL21A1	Homo sapiens collagen, type XXI, alpha 1
A_23_P169278	AGTPBP1	Homo sapiens ATP/GTP binding protein 1 (AGTPBP1), transcript variant 2
A_21_P0003235	lnc-GPR27-1	LNCipedia lincRNA
A_23_P300056	CDC42	Homo sapiens cell division cycle 42 (CDC42), transcript variant 2
A_23_P78849	SYT5	Homo sapiens synaptotagmin V (SYT5), transcript variant 1
A_21_P0009969	lnc-ARFGEF2-2	LNCipedia lincRNA
A_33_P3317797	SLC2A5	Homo sapiens solute carrier family 2 (facilitated glucose/fructose transporter), member 5 (SLC2A5), transcript variant 2
A_33_P3241681	CDKL2	Homo sapiens cyclin-dependent kinase-like 2 (CDC2-related kinase)
A_23_P73571	MUM1L1	Homo sapiens melanoma associated antigen (mutated) 1-like 1 (MUM1L1), transcript variant 2
A_23_P98571	PPP1R32	Homo sapiens protein phosphatase 1, regulatory subunit 32 (PPP1R32), transcript variant 1
A_21_P0014088	LOC101929752	PREDICTED: Homo sapiens uncharacterized LOC101929752
A_19_P00320492	lnc-MRPL14-1	Homo sapiens alpha-actinin-like mRNA
A_24_P612446	C6orf89	Homo sapiens chromosome 6 open reading frame 89 (C6orf89), transcript variant 1

A_24_P33508	-March11	Homo sapiens membrane-associated ring finger (C3HC4) 11 (MARCH11)
A_23_P212126	COLQ	Homo sapiens collagen-like tail subunit (single strand of homotrimer) of asymmetric acetylcholinesterase (COLQ), transcript variant II
A_33_P3295991		Homo sapiens cDNA FLJ46084 fis, clone TESTI2006543
A_21_P0004552	LINC01019	Homo sapiens long intergenic non-protein coding RNA 1019
A_21_P0013338	XLOC_l2_013931	BROAD Institute lincRNA
A_23_P308839	TMEM132D	Homo sapiens transmembrane protein 132D
A_21_P0001161	LINC01349	Homo sapiens long intergenic non-protein coding RNA 1349
A_21_P0009175		DB100140 TESTI4 Homo sapiens cDNA clone TESTI4051979
A_24_P263786		immunoglobulin kappa variable 2D-30
A_23_P62709	SPRR3	Homo sapiens small proline-rich protein 3 (SPRR3), transcript variant 1
A_24_P41850	MASP1	Homo sapiens mannan-binding lectin serine peptidase 1 (C4/C2 activating component of Ra-reactive factor) (MASP1), transcript variant 3
A_33_P3388536	LOC728752	Homo sapiens uncharacterized LOC728752
A_33_P3318966	METTL20	Homo sapiens methyltransferase like 20 (METTL20), transcript variant 1
A_33_P3404922	KIAA1217	Homo sapiens KIAA1217 (KIAA1217), transcript variant 7
A_33_P3297853	AKNA	Homo sapiens AT-hook transcription factor
A_23_P419786	ZNF781	Homo sapiens zinc finger protein 781
A_32_P142779	SPPL2C	Homo sapiens signal peptide peptidase like 2C
A_21_P0014674		
A_21_P0012179	XLOC_l2_009134	BROAD Institute lincRNA
A_33_P3241489	CEBPZOS	Homo sapiens CEBPZ opposite strand (CEBPZOS), transcript variant 1

A_33_P3635527	KRTAP24-1	Homo sapiens keratin associated protein 24-1
A_23_P435601	ST8SIA4	Homo sapiens ST8 alpha-N-acetyl-neuraminide alpha-2,8-sialyltransferase 4 (ST8SIA4), transcript variant 2
A_21_P0002196	lnc-TTC27-1	LNCipedia lincRNA
A_21_P0004502	lnc-FBXO4-1	LNCipedia lincRNA
A_33_P3236077	CLRN2	Homo sapiens clarin 2
A_23_P434430	ZNF439	Homo sapiens zinc finger protein 439
A_33_P3421318	NR2F2-AS1	Homo sapiens NR2F2 antisense RNA 1 (NR2F2-AS1), transcript variant 3
A_21_P0011338	LINC00933	Homo sapiens long intergenic non-protein coding RNA 933 (LINC00933), transcript variant 1
A_21_P0012176	XLOC_l2_009096	BROAD Institute lincRNA
A_23_P135486	AHSP	Homo sapiens alpha hemoglobin stabilizing protein
A_21_P0005927	LOC101930275	
A_23_P502336	EMR2	Homo sapiens egf-like module containing, mucin-like, hormone receptor-like 2 (EMR2), transcript variant 1
A_21_P0004716		
A_33_P3354514	SLC2A13	Homo sapiens solute carrier family 2 (facilitated glucose transporter), member 13
A_33_P3260223	TXLNGY	Homo sapiens taxilin gamma pseudogene, Y-linked (TXLNGY), transcript variant 1
A_21_P0002470	lnc-POLR1A-1	LNCipedia lincRNA
A_24_P277657	GMPR	Homo sapiens guanosine monophosphate reductase
A_23_P27229	MYO15A	Homo sapiens myosin XVA
A_33_P3367541	lnc-SEC61G-7	LNCipedia lincRNA
A_21_P0011518		
A_33_P3257683		

A_33_P3286552	NOX1	Homo sapiens NADPH oxidase 1 (NOX1), transcript variant 2
A_21_P0004361	LOC101929261	PREDICTED: Homo sapiens uncharacterized LOC101929261
A_33_P3250018	HCFC2	Homo sapiens host cell factor C2
A_21_P0001158	LOC101928241	Homo sapiens uncharacterized LOC101928241
A_23_P213137	LNX1	Homo sapiens ligand of numb-protein X 1, E3 ubiquitin protein ligase (LNX1), transcript variant 2
A_33_P3301221	MORN1	Homo sapiens MORN repeat containing 1 (MORN1), transcript variant 3
A_33_P3401586	EFCAB10	Homo sapiens EF-hand calcium binding domain 10
A_23_P69637	OTUD4	Homo sapiens OTU deubiquitinase 4 (OTUD4), transcript variant 2
A_23_P87036	APOA4	Homo sapiens apolipoprotein A-IV
A_33_P3306232	PABPC1L2A	Homo sapiens poly(A) binding protein, cytoplasmic 1-like 2A (PABPC1L2A)
A_23_P168130	IP6K3	Homo sapiens inositol hexakisphosphate kinase 3 (IP6K3), transcript variant 1
A_33_P3396527	POLR3G	Homo sapiens polymerase (RNA) III (DNA directed) polypeptide G (32kD)
A_21_P0001016	SRGAP2-AS1	Homo sapiens SRGAP2 antisense RNA 1
A_21_P0000573	CCDC162P	Homo sapiens coiled-coil domain containing 162, pseudogene
A_21_P0000843	LOC100507250	Homo sapiens uncharacterized LOC100507250
A_24_P170395		
A_23_P91636	POM121L9P	Homo sapiens POM121 transmembrane nucleoporin-like 9, pseudogene
A_24_P46130	ACPP	Homo sapiens acid phosphatase, prostate (ACPP), transcript variant 1
A_21_P0001954		RST724 Athersys RAGE Library Homo sapiens cDNA
A_33_P3376954	XLOC_l2_001648	BROAD Institute lincRNA
A_21_P0002334	lnc-OBFC2A-1	LNCipedia lincRNA

A_21_P0006625	lnc-JMJD1C-2	BX358171
A_21_P0004486	lnc-ADCY2-5	LNCipedia lincRNA
A_21_P0014454	LOC100507600	Homo sapiens uncharacterized LOC100507600
A_24_P252945	CXCR5	Homo sapiens chemokine (C-X-C motif) receptor 5 (CXCR5), transcript variant 2
A_24_P29594	HBS1L	Homo sapiens HBS1-like translational GTPase (HBS1L), transcript variant 1
A_24_P203000	IL2RB	Homo sapiens interleukin 2 receptor, beta
A_24_P129834	TPH2	Homo sapiens tryptophan hydroxylase 2
A_21_P0001513	lnc-JUN-6	LNCipedia lincRNA
A_24_P268196	LZIC	leucine zipper and CTNNBIP1 domain containing
A_33_P3226761	SOX18	Homo sapiens SRY (sex determining region Y)-box 18
A_33_P3423853	C20orf166-AS1	Homo sapiens C20orf166 antisense RNA 1
A_24_P193244	SOHLH2	Homo sapiens spermatogenesis and oogenesis specific basic helix-loop-helix 2 (SOHLH2), transcript variant 1
A_21_P0001796	lnc-FAM168B-1	Homo sapiens cDNA FLJ33681 fis, clone BRAWH2002549
A_21_P0013744	LOC101929116	Homo sapiens uncharacterized LOC101929116
A_21_P0005902	lnc-FAM84B-2	LNCipedia lincRNA
A_21_P0010968	WT1-AS	Homo sapiens WT1 antisense RNA (WT1-AS), transcript variant 4
A_33_P3743432	DEFA8P	Homo sapiens defensin, alpha 8 pseudogene
A_33_P3257518	FLJ22447	Homo sapiens uncharacterized LOC400221
A_32_P155826	USP27X-AS1	Homo sapiens USP27X antisense RNA 1
A_33_P3212022	RGS6	Homo sapiens regulator of G-protein signaling 6 (RGS6), transcript variant 4
A_21_P0014300	LOC104613533	Homo sapiens uncharacterized LOC104613533

A_21_P0007460	MIR4454	long intergenic non-protein coding RNA 678
A_32_P170481	LOC100240735	Homo sapiens uncharacterized LOC100240735
A_33_P3262742	DAPL1	Homo sapiens death associated protein-like 1
A_23_P81529	ISL1	Homo sapiens ISL LIM homeobox 1
A_33_P3367062	SWT1	Homo sapiens SWT1 RNA endoribonuclease homolog
A_24_P417935	AGAP2-AS1	Homo sapiens AGAP2 antisense RNA 1
A_21_P0006440		
A_21_P0004031		
A_33_P3879161	PIK3AP1	Homo sapiens phosphoinositide-3-kinase adaptor protein 1
A_33_P3492042	LINC00307	Homo sapiens long intergenic non-protein coding RNA 307
A_21_P0000567	SLC25A5-AS1	Homo sapiens SLC25A5 antisense RNA 1
A_23_P24211	MMP21	Homo sapiens matrix metallopeptidase 21
A_33_P3272668		
A_24_P213950	HEPACAM	Homo sapiens hepatic and glial cell adhesion molecule
A_33_P3319860	IFFO1	Homo sapiens intermediate filament family orphan 1 (IFFO1), transcript variant 7
A_21_P0008821	LOC102725022	PREDICTED: Homo sapiens uncharacterized LOC102725022 (LOC102725022), transcript variant X2
A_33_P3271800	SIRT2	Homo sapiens sirtuin 2 (SIRT2), transcript variant 1
A_33_P3327208		zinc finger protein 114 pseudogene 1
A_23_P420831	TRIM10	Homo sapiens tripartite motif containing 10 (TRIM10), transcript varian 2
A_21_P0007819	lnc-CLEC2D-5	ou35e09.x1
A_32_P347617	APOBEC3H	Homo sapiens apolipoprotein B mRNA editing enzyme, catalytic polypeptide-like 3H (APOBEC3H), transcript variant SV-183

A_23_P211584	SMDT1	Homo sapiens single-pass membrane protein with aspartate-rich tail 1
A_24_P415280	SEC61A2	Homo sapiens Sec61 alpha 2 subunit (S. cerevisiae) (SEC61A2), transcript variant 1
A_33_P3334305	TFF3	Homo sapiens trefoil factor 3 (intestinal)
A_33_P3235562	CAPZB	Homo sapiens capping protein (actin filament) muscle Z-line, beta (CAPZB), transcript variant 2
A_33_P3242713		Homo sapiens cDNA FLJ11996 fis
A_33_P3271711		
A_21_P0013170	ZNF316	Homo sapiens zinc finger protein 316
A_23_P3221	SQRDL	Homo sapiens sulfide quinone reductase-like (yeast) (SQRDL), transcript variant 1
A_19_P00318363	lnc-QPCT-2	LNCipedia lincRNA
A_33_P3380618	HSPG2	Homo sapiens heparan sulfate proteoglycan 2 (HSPG2), transcript variant 1
A_33_P3257609	PPP1R12B	Homo sapiens protein phosphatase 1, regulatory subunit 12B (PPP1R12B), transcript variant 1
A_33_P3264179	LCE3E	Homo sapiens late cornified envelope 3E
A_33_P3402071		
A_21_P0009088	lnc-C16orf95-2	LNCipedia lincRNA
A_33_P3241090	OR6Q1	Homo sapiens olfactory receptor, family 6, subfamily Q, member 1
A_33_P3311740	ZNF774	Homo sapiens zinc finger protein 774
A_23_P256624	DDX4	Homo sapiens DEAD (Asp-Glu-Ala-Asp) box polypeptide 4
A_21_P0014724	LOC100507336	PREDICTED: Homo sapiens uncharacterized LOC100507336 (LOC100507336), transcript variant X1
A_33_P3252479	SETDB1	Homo sapiens SET domain, bifurcated 1 (SETDB1), transcript variant 3
A_21_P0003045	lnc-P2RY1-3	LNCipedia
A_21_P0002655	LOC100505774	PREDICTED: Homo sapiens uncharacterized LOC100505774

A_23_P146294	EFCAB1	Homo sapiens EF-hand calcium binding domain 1 (EFCAB1), transcript variant 1
A_33_P3217958	FCHSD2	Homo sapiens FCH and double SH3 domains 2
A_21_P0001570	lnc-NGF-1	LNCipedia lincRNA
A_24_P381441	LMO3	Homo sapiens LIM domain only 3 (rhombotin-like 2) (LMO3), transcript variant 1
A_33_P3217743	LINC01061	Homo sapiens long intergenic non-protein coding RNA 1061
A_33_P3221403	LOC646743	Homo sapiens clone TESTIS-608 mRNA sequence.
A_21_P0014055	MROH1	Homo sapiens maestro heat-like repeat family member 1 (MROH1), transcript variant 4
A_33_P3302652		chromosome 1 open reading frame 132
A_21_P0010050	lnc-PREX1-4	LNCipedia lincRNA
A_21_P0010375		601671535F1
A_24_P769672	C12orf73	Homo sapiens chromosome 12 open reading frame 73
A_24_P342944	CSPG5	Homo sapiens chondroitin sulfate proteoglycan 5 (neuroglycan C) (CSPG5), transcript variant 1
A_23_P168357	CPA1	carboxypeptidase A1 (pancreatic)
A_21_P0000065	SLC1A3	Homo sapiens solute carrier family 1 (glial high affinity glutamate transporter), member 3 (SLC1A3), transcript variant 3
A_21_P0006220	lnc-RP11-295D22.1.1-6	LNCipedia lincRNA
A_21_P0007670		
A_24_P277673	HIST1H4G	Homo sapiens histone cluster 1, H4g
A_33_P3346083	DCDC1	Homo sapiens doublecortin domain containing 1
A_21_P0004729	LINC00518	long intergenic non-protein coding RNA 518
A_21_P0011368	LOC101928134	Homo sapiens uncharacterized LOC101928134 (LOC101928134), transcript variant 2
A_33_P3326235	HBM	Homo sapiens hemoglobin, mu

A_23_P143526	**S100B**	**Homo sapiens S100 calcium binding protein B**
A_33_P3278714		
A_19_P00316324	**LINC01132**	**Homo sapiens long intergenic non-protein coding RNA 1132**
A_24_P54174	**TNFRSF1B**	**Homo sapiens tumor necrosis factor receptor superfamily, member 1B**
A_33_P3280360	**LOC100133857**	**Homo sapiens cDNA FLJ45691 fis**
A_21_P0008196	**lnc-SLITRK6-1**	**LNCipedia lincRNA**
A_33_P3247342	**ANO7**	**Homo sapiens anoctamin 7 (ANO7), transcript variant NGEP-S**
A_23_P118095	**RPL3L**	**Homo sapiens ribosomal protein L3-like**
A_23_P397937	**SAMD3**	**Homo sapiens sterile alpha motif domain containing 3 (SAMD3), transcript variant 3**
A_23_P201211	**FCRL5**	**Homo sapiens Fc receptor-like 5 (FCRL5), transcript variant 1**
A_33_P3679221	**LOC152578**	**Homo sapiens uncharacterized LOC152578**
A_21_P0003253	**lnc-GYG1-1**	**LNCipedia lincRNA**
A_21_P0003027	**LOC644662**	**PREDICTED: Homo sapiens uncharacterized LOC644662**
A_23_P254896	**FGF16**	**Homo sapiens fibroblast growth factor 16**
A_21_P0006433	**LOC101928495**	**Homo sapiens uncharacterized LOC101928495**
A_23_P34144	**MAGEH1**	**Homo sapiens melanoma antigen family H, 1**
A_33_P3332937	**MIPEPP3**	**Homo sapiens mRNA**
A_23_P216118	**UNC5D**	**Homo sapiens unc-5 homolog D**
A_33_P3237804	**lnc-RP11-351M8.1.1-1**	**LNCipedia lincRNA**
A_21_P0009007	**LINC01569**	**Homo sapiens long intergenic non-protein coding RNA 1569**
A_23_P370544	**ANKAR**	**Homo sapiens ankyrin and armadillo repeat containing**
A_21_P0007875	**lnc-SLC38A2-1**	**LNCipedia lincRNA**

A_21_P0000124	DENND1B	Homo sapiens DENN/MADD domain containing 1B
A_21_P0012466	XLOC_l2_010405	BROAD Institute lincRNA
A_23_P47579	NLRP14	Homo sapiens NLR family, pyrin domain containing 14
A_33_P3283824	SLC39A8	Homo sapiens solute carrier family 39 (zinc transporter), member 8 (SLC39A8), transcript variant 3
A_21_P0014037		
A_32_P159234	KIAA1456	Homo sapiens KIAA1456 (KIAA1456), transcript variant 1
A_21_P0006664		
A_33_P3402993		
A_32_P9986	lnc-PHF10-1	LNCipedia lincRNA
A_19_P00321414	LINC01091	Homo sapiens long intergenic non-protein coding RNA 1091 (LINC01091), transcript variant 2
A_33_P3259457		PREDICTED: Homo sapiens golgin-like
A_23_P313652	AKAP14	Homo sapiens A kinase (PRKA) anchor protein 14 (AKAP14), transcript variant 1
A_33_P3374833	BLOC1S6	Homo sapiens biogenesis of lysosomal organelles complex-1, subunit 6, pallidin
A_21_P0007398		
A_21_P0011878	XLOC_l2_007788	BROAD Institute lincRNA
A_32_P213349	lnc-DPP4-1	Q56A81_HUMAN (Q56A81) TBR1 protein
A_33_P3339731	LOC100131170	Homo sapiens cDNA FLJ25537 fis
A_23_P1320	MYOZ1	Homo sapiens myozenin 1

Table 29. List of 248 potential targets downregulate in miR-1305 overexpression and upregulate in miR-1305 knockdown generated from array data.

REFERENCES

1   Hyslop, L. *et al.* Downregulation of NANOG induces differentiation of human embryonic stem cells to extraembryonic lineages. *Stem Cells* **23**, 1035-1043, doi:10.1634/stemcells.2005-0080 (2005).

2   Singh, A. M. & Dalton, S. The cell cycle and Myc intersect with mechanisms that regulate pluripotency and reprogramming. *Cell stem cell* **5**, 141-149, doi:10.1016/j.stem.2009.07.003 (2009).

3   Yabut, O. & Bernstein, H. S. The promise of human embryonic stem cells in aging-associated diseases. *Aging* **3**, 494-508 (2011).

4   Thomson, J. A. *et al.* Embryonic stem cell lines derived from human blastocysts. *Science* **282**, 1145-1147 (1998).

5   Heins, N. *et al.* Derivation, characterization, and differentiation of human embryonic stem cells. *Stem Cells* **22**, 367-376, doi:10.1634/stemcells.22-3-367 (2004).

6   Amit, M. & Itskovitz-Eldor, J. Derivation and spontaneous differentiation of human embryonic stem cells. *Journal of anatomy* **200**, 225-232 (2002).

7   Li, C. *et al.* Efficient derivation of Chinese human embryonic stem cell lines from frozen embryos. *In vitro cellular & developmental biology. Animal* **46**, 186-191, doi:10.1007/s11626-010-9304-4 (2010).

8   Boyer, L. A. *et al.* Core transcriptional regulatory circuitry in human embryonic stem cells. *Cell* **122**, 947-956, doi:10.1016/j.cell.2005.08.020 (2005).

9   Wong, R. C. *et al.* A novel role for an RNA polymerase III subunit POLR3G in regulating pluripotency in human embryonic stem cells. *Stem Cells* **29**, 1517-1527, doi:10.1002/stem.714 (2011).

10   Richards, M., Tan, S. P., Tan, J. H., Chan, W. K. & Bongso, A. The transcriptome profile of human embryonic stem cells as defined by SAGE. *Stem Cells* **22**, 51-64, doi:DOI 10.1634/stemcells.22-1-51 (2004).

11   Coathup, M. J., Kalia, P., Konan, S., Mirza, K. & Blunn, G. W. A comparison of allogeneic and autologous mesenchymal stromal cells and osteoprogenitor cells in augmenting bone formation around massive bone tumor prostheses. *J Biomed Mater Res A* **101**, 2210-2218, doi:10.1002/jbm.a.34536 (2013).

12   Evans, M. J. & Kaufman, M. H. Establishment in culture of pluripotential cells from mouse embryos. *Nature* **292**, 154-156 (1981).

13   Rossant, J. Stem cells and early lineage development. *Cell* **132**, 527-531, doi:10.1016/j.cell.2008.01.039 (2008).

14   Ying, Q. L. *et al.* The ground state of embryonic stem cell self-renewal. *Nature* **453**, 519-523, doi:10.1038/nature06968 (2008).

15   Bradley, A., Evans, M., Kaufman, M. H. & Robertson, E. Formation of germ-line chimaeras from embryo-derived teratocarcinoma cell lines. *Nature* **309**, 255-256 (1984).

16   Brons, I. G. *et al.* Derivation of pluripotent epiblast stem cells from mammalian embryos. *Nature* **448**, 191-195, doi:10.1038/nature05950 (2007).

17   Tesar, P. J. *et al.* New cell lines from mouse epiblast share defining features with human embryonic stem cells. *Nature* **448**, 196-199, doi:10.1038/nature05972 (2007).

18   Hayashi, K. & Surani, M. A. Self-renewing epiblast stem cells exhibit continual delineation of germ cells with epigenetic reprogramming in vitro. *Development* **136**, 3549-3556, doi:10.1242/dev.037747 (2009).

19   Greber, B. *et al.* Conserved and divergent roles of FGF signaling in mouse epiblast stem cells and human embryonic stem cells. *Cell stem cell* **6**, 215-226, doi:10.1016/j.stem.2010.01.003 (2010).

20   Silva, S. S., Rowntree, R. K., Mekhoubad, S. & Lee, J. T. X-chromosome inactivation and epigenetic fluidity in human embryonic stem cells. *P Natl Acad Sci USA* **105**, 4820-4825, doi:10.1073/pnas.0712136105 (2008).

21   Xu, R. H. *et al.* NANOG is a direct target of TGFbeta/activin-mediated SMAD signaling in human ESCs. *Cell stem cell* **3**, 196-206, doi:10.1016/j.stem.2008.07.001 (2008).

22   Schnerch, A., Cerdan, C. & Bhatia, M. Distinguishing between mouse and human pluripotent stem cell regulation: the best laid plans of mice and men. *Stem Cells* **28**, 419-430, doi:10.1002/stem.298 (2010).

23   Draper, J. S., Pigott, C., Thomson, J. A. & Andrews, P. W. Surface antigens of human embryonic stem cells: changes upon differentiation in culture. *Journal of anatomy* **200**, 249-258 (2002).

24   Pera, M. F. & Tam, P. P. Extrinsic regulation of pluripotent stem cells. *Nature* **465**, 713-720, doi:10.1038/nature09228 (2010).

25   Neganova, I., Zhang, X., Atkinson, S. & Lako, M. Expression and functional analysis of G1 to S regulatory components reveals an important role for CDK2 in cell cycle regulation in human embryonic stem cells. *Oncogene* **28**, 20-30, doi:10.1038/onc.2008.358 (2009).

26   Neganova, I. *et al.* CDK1 plays an important role in the maintenance of pluripotency and genomic stability in human pluripotent stem cells. *Cell death & disease* **5**, e1508, doi:10.1038/cddis.2014.464 (2014).

27   Guo, W. T., Wang, X. W. & Wang, Y. Micro-management of pluripotent stem cells. *Protein & cell* **5**, 36-47, doi:10.1007/s13238-013-0014-z (2014).

28   Buecker, C. *et al.* A murine ESC-like state facilitates transgenesis and homologous recombination in human pluripotent stem cells. *Cell stem cell* **6**, 535-546, doi:10.1016/j.stem.2010.05.003 (2010).

29   Dunn, S. J., Martello, G., Yordanov, B., Emmott, S. & Smith, A. G. Defining an essential transcription factor program for naive pluripotency. *Science* **344**, 1156-1160, doi:10.1126/science.1248882 (2014).

30   Hackett, J. A. & Surani, M. A. Regulatory principles of pluripotency: from the ground state up. *Cell stem cell* **15**, 416-430, doi:10.1016/j.stem.2014.09.015 (2014).

31   Niwa, H. The pluripotency transcription factor network at work in reprogramming. *Current opinion in genetics & development* **28**, 25-31, doi:10.1016/j.gde.2014.08.004 (2014).

32   Yang, S. H. *et al.* Otx2 and Oct4 drive early enhancer activation during embryonic stem cell transition from naive pluripotency. *Cell reports* **7**, 1968-1981, doi:10.1016/j.celrep.2014.05.037 (2014).

33   Chan, Y. S. *et al.* Induction of a human pluripotent state with distinct regulatory circuitry that resembles preimplantation epiblast. *Cell stem cell* **13**, 663-675, doi:10.1016/j.stem.2013.11.015 (2013).

34   Duggal, G. *et al.* Alternative Routes to Induce Naive Pluripotency in Human Embryonic Stem Cells. *Stem cells* **33**, 2686-2698, doi:10.1002/stem.2071 (2015).

35   Gafni, O. *et al.* Derivation of novel human ground state naive pluripotent stem cells. *Nature* **504**, 282-286, doi:10.1038/nature12745 (2013).

36   Takashima, Y. *et al.* Resetting transcription factor control circuitry toward ground-state pluripotency in human. *Cell* **158**, 1254-1269, doi:10.1016/j.cell.2014.08.029 (2014).

37   Theunissen, T. W. *et al.* Systematic identification of culture conditions for induction and maintenance of naive human pluripotency. *Cell stem cell* **15**, 471-487, doi:10.1016/j.stem.2014.07.002 (2014).

38   Valamehr, B. *et al.* Platform for induction and maintenance of transgene-free hiPSCs resembling ground state pluripotent stem cells. *Stem Cell Rep* **2**, 366-381, doi:10.1016/j.stemcr.2014.01.014 (2014).

39   Van der Jeught, M. *et al.* Application Of Small Molecules Favoring Naive Pluripotency during Human Embryonic Stem Cell Derivation. *Cellular reprogramming* **17**, 170-180, doi:10.1089/cell.2014.0085 (2015).

40   Ware, C. B. Naive embryonic stem cells: the future of stem cell research? *Regenerative medicine* **9**, 401-403, doi:10.2217/rme.14.31 (2014).

41   Ware, C. B. *et al.* Derivation of naive human embryonic stem cells. *P Natl Acad Sci USA* **111**, 4484-4489, doi:10.1073/pnas.1319738111 (2014).

42   Takahashi, K. & Yamanaka, S. Induction of pluripotent stem cells from mouse embryonic and adult fibroblast cultures by defined factors. *Cell* **126**, 663-676, doi:10.1016/j.cell.2006.07.024 (2006).

43   Takahashi, K. *et al.* Induction of pluripotent stem cells from adult human fibroblasts by defined factors. *Cell* **131**, 861-872, doi:10.1016/j.cell.2007.11.019 (2007).

44   Buganim, Y., Faddah, D. A. & Jaenisch, R. Mechanisms and models of somatic cell reprogramming. *Nature reviews. Genetics* **14**, 427-439, doi:10.1038/nrg3473 (2013).

45   Wu, Y. L. *et al.* Clinical grade iPS cells: need for versatile small molecules and optimal cell sources. *Chemistry & biology* **20**, 1311-1322, doi:10.1016/j.chembiol.2013.09.016 (2013).

46   Wang, T., Warren, S. T. & Jin, P. Toward pluripotency by reprogramming: mechanisms and application. *Protein & cell* **4**, 820-832, doi:10.1007/s13238-013-3074-1 (2013).

47   Li, X. *et al.* Small-Molecule-Driven Direct Reprogramming of Mouse Fibroblasts into Functional Neurons. *Cell stem cell* **17**, 195-203, doi:10.1016/j.stem.2015.06.003 (2015).

48   Giorgetti, A. *et al.* Generation of induced pluripotent stem cells from human cord blood using OCT4 and SOX2. *Cell stem cell* **5**, 353-357, doi:10.1016/j.stem.2009.09.008 (2009).

49   Aasen, T. *et al.* Efficient and rapid generation of induced pluripotent stem cells from human keratinocytes. *Nature biotechnology* **26**, 1276-1284, doi:10.1038/nbt.1503 (2008).

50   Hou, P. *et al.* Pluripotent stem cells induced from mouse somatic cells by small-molecule compounds. *Science* **341**, 651-654, doi:10.1126/science.1239278 (2013).

51   Ban, H. *et al.* Efficient generation of transgene-free human induced pluripotent stem cells (iPSCs) by temperature-sensitive Sendai virus vectors. *Proceedings of the National Academy of Sciences of the United States of America* **108**, 14234-14239, doi:10.1073/pnas.1103509108 (2011).

52   Yu, J. *et al.* Human induced pluripotent stem cells free of vector and transgene sequences. *Science* **324**, 797-801, doi:10.1126/science.1172482 (2009).

53   Okita, K. *et al.* A more efficient method to generate integration-free human iPS cells. *Nature methods* **8**, 409-412, doi:10.1038/nmeth.1591 (2011).

54   Warren, L. *et al.* Highly efficient reprogramming to pluripotency and directed differentiation of human cells with synthetic modified mRNA. *Cell stem cell* **7**, 618-630, doi:10.1016/j.stem.2010.08.012 (2010).

55   Anokye-Danso, F. *et al.* Highly efficient miRNA-mediated reprogramming of mouse and human somatic cells to pluripotency. *Cell stem cell* **8**, 376-388, doi:10.1016/j.stem.2011.03.001 (2011).

56   Kim, D. *et al.* Generation of human induced pluripotent stem cells by direct delivery of reprogramming proteins. *Cell stem cell* **4**, 472-476, doi:10.1016/j.stem.2009.05.005 (2009).

57   Yu, J. *et al.* Induced pluripotent stem cell lines derived from human somatic cells. *Science* **318**, 1917-1920, doi:10.1126/science.1151526 (2007).

58   Hotta, A. *et al.* Isolation of human iPS cells using EOS lentiviral vectors to select for pluripotency. *Nature methods* **6**, 370-376, doi:10.1038/nmeth.1325 (2009).

59   Woltjen, K. & Stanford, W. L. Preview. Inhibition of Tgf-beta signaling improves mouse fibroblast reprogramming. *Cell stem cell* **5**, 457-458, doi:10.1016/j.stem.2009.10.007 (2009).

60   Stadtfeld, M., Nagaya, M., Utikal, J., Weir, G. & Hochedlinger, K. Induced Pluripotent Stem Cells Generated Without Viral Integration. *Science* **322**, 945-949, doi:10.1126/science.1162494 (2008).

61 Silva, J. *et al.* Promotion of reprogramming to ground state pluripotency by signal inhibition. *PLoS biology* **6**, e253, doi:10.1371/journal.pbio.0060253 (2008).

62 Zhu, S. *et al.* Reprogramming of human primary somatic cells by OCT4 and chemical compounds. *Cell stem cell* **7**, 651-655, doi:10.1016/j.stem.2010.11.015 (2010).

63 Yuan, X. *et al.* Brief report: combined chemical treatment enables Oct4-induced reprogramming from mouse embryonic fibroblasts. *Stem Cells* **29**, 549-553, doi:10.1002/stem.594 (2011).

64 Huangfu, D. *et al.* Induction of pluripotent stem cells by defined factors is greatly improved by small-molecule compounds. *Nature biotechnology* **26**, 795-797, doi:10.1038/nbt1418 (2008).

65 Wang, A. *et al.* Functional modules distinguish human induced pluripotent stem cells from embryonic stem cells. *Stem cells and development* **20**, 1937-1950, doi:10.1089/scd.2010.0574 (2011).

66 Newman, A. M. & Cooper, J. B. Lab-specific gene expression signatures in pluripotent stem cells. *Cell stem cell* **7**, 258-262, doi:10.1016/j.stem.2010.06.016 (2010).

67 Guenther, M. G. *et al.* Chromatin structure and gene expression programs of human embryonic and induced pluripotent stem cells. *Cell stem cell* **7**, 249-257, doi:10.1016/j.stem.2010.06.015 (2010).

68 Ruiz, S. *et al.* Identification of a specific reprogramming-associated epigenetic signature in human induced pluripotent stem cells. *Proceedings of the National Academy of Sciences of the United States of America* **109**, 16196-16201, doi:10.1073/pnas.1202352109 (2012).

69 Hu, B. Y. *et al.* Neural differentiation of human induced pluripotent stem cells follows developmental principles but with variable potency. *Proceedings of the National Academy of Sciences of the United States of America* **107**, 4335-4340, doi:10.1073/pnas.0910012107 (2010).

70 Narsinh, K. H. *et al.* Single cell transcriptional profiling reveals heterogeneity of human induced pluripotent stem cells. *The Journal of clinical investigation* **121**, 1217-1221, doi:10.1172/JCI44635 (2011).

71 Wilson, V., Olivera-Martinez, I. & Storey, K. G. Stem cells, signals and vertebrate body axis extension. *Development* **136**, 1591-1604, doi:10.1242/dev.021246 (2009).

72 Chin, M. H. *et al.* Induced pluripotent stem cells and embryonic stem cells are distinguished by gene expression signatures. *Cell stem cell* **5**, 111-123, doi:10.1016/j.stem.2009.06.008 (2009).

73 Ghosh, R. *et al.* Transcriptional regulation of VEGF-A by the unfolded protein response pathway. *PloS one* **5**, e9575, doi:10.1371/journal.pone.0009575 (2010).

74 Kim, K. *et al.* Epigenetic memory in induced pluripotent stem cells. *Nature* **467**, 285-290, doi:10.1038/nature09342 (2010).

75 Polo, J. M. *et al.* Cell type of origin influences the molecular and functional properties of mouse induced pluripotent stem cells. *Nature biotechnology* **28**, 848-855, doi:10.1038/nbt.1667 (2010).

76   Huang, K. *et al.* A panel of CpG methylation sites distinguishes human embryonic stem cells and induced pluripotent stem cells. *Stem cell reports* **2**, 36-43, doi:10.1016/j.stemcr.2013.11.003 (2014).

77   Feng, Q. *et al.* Hemangioblastic derivatives from human induced pluripotent stem cells exhibit limited expansion and early senescence. *Stem Cells* **28**, 704-712, doi:10.1002/stem.321 (2010).

78   Dvash, T., Ben-Yosef, D. & Eiges, R. Human embryonic stem cells as a powerful tool for studying human embryogenesis. *Pediatr Res* **60**, 111-117, doi:10.1203/01.pdr.0000228349.24676.17 (2006).

79   Dvash, T. *et al.* Temporal gene expression during differentiation of human embryonic stem cells and embryoid bodies. *Hum Reprod* **19**, 2875-2883, doi:10.1093/humrep/deh529 (2004).

80   Eiges, R. *et al.* Developmental study of fragile X syndrome using human embryonic stem cells derived from preimplantation genetically diagnosed embryos. *Cell stem cell* **1**, 568-577, doi:10.1016/j.stem.2007.09.001 (2007).

81   Niclis, J. C. *et al.* Characterization of forebrain neurons derived from late-onset Huntington's disease human embryonic stem cell lines. *Frontiers in cellular neuroscience* **7**, 37, doi:10.3389/fncel.2013.00037 (2013).

82   Biancotti, J. C. *et al.* Human embryonic stem cells as models for aneuploid chromosomal syndromes. *Stem cells* **28**, 1530-1540, doi:10.1002/stem.483 (2010).

83   Mateizel, I. *et al.* Derivation of human embryonic stem cell lines from embryos obtained after IVF and after PGD for monogenic disorders. *Hum Reprod* **21**, 503-511, doi:10.1093/humrep/dei345 (2006).

84   Di Giorgio, F. P., Boulting, G. L., Bobrowicz, S. & Eggan, K. C. Human embryonic stem cell-derived motor neurons are sensitive to the toxic effect of glial cells carrying an ALS-causing mutation. *Cell stem cell* **3**, 637-648, doi:10.1016/j.stem.2008.09.017 (2008).

85   Marchetto, M. C. *et al.* Non-cell-autonomous effect of human SOD1 G37R astrocytes on motor neurons derived from human embryonic stem cells. *Cell stem cell* **3**, 649-657, doi:10.1016/j.stem.2008.10.001 (2008).

86   Urnov, F. D., Rebar, E. J., Holmes, M. C., Zhang, H. S. & Gregory, P. D. Genome editing with engineered zinc finger nucleases. *Nature reviews. Genetics* **11**, 636-646, doi:10.1038/nrg2842 (2010).

87   Ding, Q. *et al.* A TALEN genome-editing system for generating human stem cell-based disease models. *Cell stem cell* **12**, 238-251, doi:10.1016/j.stem.2012.11.011 (2013).

88   Mali, P. *et al.* RNA-guided human genome engineering via Cas9. *Science* **339**, 823-826, doi:10.1126/science.1232033 (2013).

89   Cong, L. *et al.* Multiplex genome engineering using CRISPR/Cas systems. *Science* **339**, 819-823, doi:10.1126/science.1231143 (2013).

90   Bellin, M., Marchetto, M. C., Gage, F. H. & Mummery, C. L. Induced pluripotent stem cells: the new patient? *Nature reviews. Molecular cell biology* **13**, 713-726, doi:10.1038/nrm3448 (2012).

91   Malan, D., Friedrichs, S., Fleischmann, B. K. & Sasse, P. Cardiomyocytes obtained from induced pluripotent stem cells with long-QT syndrome 3 recapitulate typical disease-specific features in vitro. *Circulation research* **109**, 841-847, doi:10.1161/CIRCRESAHA.111.243139 (2011).

92   Sinnecker, D. *et al.* Modeling long-QT syndromes with iPS cells. *Journal of cardiovascular translational research* **6**, 31-36, doi:10.1007/s12265-012-9416-1 (2013).

93   Song, B. *et al.* Neural differentiation of patient specific iPS cells as a novel approach to study the pathophysiology of multiple sclerosis. *Stem Cell Res* **8**, 259-273, doi:10.1016/j.scr.2011.12.001 (2012).

94   Yahata, N. *et al.* Anti-Abeta drug screening platform using human iPS cell-derived neurons for the treatment of Alzheimer's disease. *PloS one* **6**, e25788, doi:10.1371/journal.pone.0025788 (2011).

95   Lee, G. *et al.* Modelling pathogenesis and treatment of familial dysautonomia using patient-specific iPSCs. *Nature* **461**, 402-406, doi:10.1038/nature08320 (2009).

96   Yoshida, Y. & Yamanaka, S. iPS cells: a source of cardiac regeneration. *Journal of molecular and cellular cardiology* **50**, 327-332, doi:10.1016/j.yjmcc.2010.10.026 (2011).

97   Takahashi, K. & Yamanaka, S. Induced pluripotent stem cells in medicine and biology. *Development* **140**, 2457-2461, doi:10.1242/dev.092551 (2013).

98   Shen, H. F. *et al.* Induced Pluripotent Stem Cells (iPS Cells): Current Status and Future Prospect. *Prog Biochem Biophys* **36**, 950-960, doi:10.3724/Sp.J.1206.2008.00794 (2009).

99   Carr, A. J. *et al.* Development of human embryonic stem cell therapies for age-related macular degeneration. *Trends in neurosciences* **36**, 385-395, doi:10.1016/j.tins.2013.03.006 (2013).

100   Lu, B. *et al.* Long-term safety and function of RPE from human embryonic stem cells in preclinical models of macular degeneration. *Stem cells* **27**, 2126-2135, doi:10.1002/stem.149 (2009).

101   Schwartz, S. D. *et al.* Embryonic stem cell trials for macular degeneration: a preliminary report. *Lancet* **379**, 713-720, doi:10.1016/S0140-6736(12)60028-2 (2012).

102   Hanna, J. *et al.* Treatment of sickle cell anemia mouse model with iPS cells generated from autologous skin. *Science* **318**, 1920-1923, doi:10.1126/science.1152092 (2007).

103   Wernig, M. *et al.* Neurons derived from reprogrammed fibroblasts functionally integrate into the fetal brain and improve symptoms of rats with Parkinson's disease. *Proceedings of the National Academy of Sciences of the United States of America* **105**, 5856-5861, doi:10.1073/pnas.0801677105 (2008).

104   Vallier, L. *et al.* Activin/Nodal signalling maintains pluripotency by controlling Nanog expression. *Development* **136**, 1339-1349, doi:10.1242/dev.033951 (2009).

105   Greber, B., Lehrach, H. & Adjaye, J. Fibroblast growth factor 2 modulates transforming growth factor beta signaling in mouse embryonic fibroblasts and human ESCs (hESCs) to support hESC self-renewal. *Stem Cells* **25**, 455-464, doi:10.1634/stemcells.2006-0476 (2007).

106   Sato, N. *et al.* Molecular signature of human embryonic stem cells and its comparison with the mouse. *Developmental biology* **260**, 404-413 (2003).

107   James, D., Levine, A. J., Besser, D. & Hemmati-Brivanlou, A. TGFbeta/activin/nodal signaling is necessary for the maintenance of pluripotency in human embryonic stem cells. *Development* **132**, 1273-1282, doi:10.1242/dev.01706 (2005).

108   Xiao, L., Yuan, X. & Sharkis, S. J. Activin A maintains self-renewal and regulates fibroblast growth factor, Wnt, and bone morphogenic protein pathways in human embryonic stem cells. *Stem Cells* **24**, 1476-1486, doi:10.1634/stemcells.2005-0299 (2006).

109   Vallier, L., Alexander, M. & Pedersen, R. A. Activin/Nodal and FGF pathways cooperate to maintain pluripotency of human embryonic stem cells. *Journal of cell science* **118**, 4495-4509, doi:10.1242/jcs.02553 (2005).

110   Itsykson, P. *et al.* Derivation of neural precursors from human embryonic stem cells in the presence of noggin. *Molecular and cellular neurosciences* **30**, 24-36, doi:10.1016/j.mcn.2005.05.004 (2005).

111   Pera, M. F. *et al.* Regulation of human embryonic stem cell differentiation by BMP-2 and its antagonist noggin. *Journal of cell science* **117**, 1269-1280, doi:10.1242/jcs.00970 (2004).

112   Xu, R. H. *et al.* Basic FGF and suppression of BMP signaling sustain undifferentiated proliferation of human ES cells. *Nature methods* **2**, 185-190, doi:10.1038/nmeth744 (2005).

113   Levine, A. J. & Brivanlou, A. H. GDF3, a BMP inhibitor, regulates cell fate in stem cells and early embryos. *Development* **133**, 209-216, doi:10.1242/dev.02192 (2006).

114   Peerani, R. *et al.* Niche-mediated control of human embryonic stem cell self-renewal and differentiation. *The EMBO journal* **26**, 4744-4755, doi:10.1038/sj.emboj.7601896 (2007).

115   Teven, C. M. *et al.* Differentiation of osteoprogenitor cells is induced by high-frequency pulsed electromagnetic fields. *The Journal of craniofacial surgery* **23**, 586-593, doi:10.1097/SCS.0b013e31824cd6de (2012).

116   Lee, S. S. *et al.* The effect of TNFalpha secreted from macrophages activated by titanium particles on osteogenic activity regulated by WNT/BMP signaling in osteoprogenitor cells. *Biomaterials* **33**, 4251-4263, doi:10.1016/j.biomaterials.2012.03.005 (2012).

117   Dvorak, P. *et al.* Expression and potential role of fibroblast growth factor 2 and its receptors in human embryonic stem cells. *Stem Cells* **23**, 1200-1211, doi:10.1634/stemcells.2004-0303 (2005).

118   Kang, H. B. *et al.* Basic fibroblast growth factor activates ERK and induces c-fos in human embryonic stem cell line MizhES1. *Stem cells and development* **14**, 395-401, doi:10.1089/scd.2005.14.395 (2005).

119   Li, J. *et al.* MEK/ERK signaling contributes to the maintenance of human embryonic stem cell self-renewal. *Differentiation; research in biological diversity* **75**, 299-307, doi:10.1111/j.1432-0436.2006.00143.x (2007).

120   Esposito, M. *et al.* Differentiation of human osteoprogenitor cells increases after treatment with pulsed electromagnetic fields. *In Vivo* **26**, 299-304 (2012).

121   Gopinathan, L., Ratnacaram, C. K. & Kaldis, P. Established and novel Cdk/cyclin complexes regulating the cell cycle and development. *Results and problems in cell differentiation* **53**, 365-389, doi:10.1007/978-3-642-19065-0_16 (2011).

122   Bhattacharya, B. *et al.* Gene expression in human embryonic stem cell lines: unique molecular signature. *Blood* **103**, 2956-2964, doi:10.1182/blood-2003-09-3314 (2004).

123   Bresky, G. *et al.* Endoscopic findings in a biennial follow-up program in patients with pernicious anemia. *Hepato-gastroenterology* **50**, 2264-2266 (2003).

124   Williams, R. L. *et al.* Myeloid leukaemia inhibitory factor maintains the developmental potential of embryonic stem cells. *Nature* **336**, 684-687, doi:10.1038/336684a0 (1988).

125   Ginis, H. S., Katsanevaki, V. J. & Pallikaris, I. G. Influence of ablation parameters on refractive changes after phototherapeutic keratectomy. *J Refract Surg* **19**, 443-448 (2003).

126   Orlando, R. *et al.* IDAWG: Metabolic incorporation of stable isotope labels for quantitative glycomics of cultured cells. *Journal of proteome research* **8**, 3816-3823, doi:10.1021/pr8010028 (2009).

127   Davidson, K. C. *et al.* Wnt/beta-catenin signaling promotes differentiation, not self-renewal, of human embryonic stem cells and is repressed by Oct4. *Proceedings of the National Academy of Sciences of the United States of America* **109**, 4485-4490, doi:10.1073/pnas.1118777109 (2012).

128   Vivanco, I. & Sawyers, C. L. The phosphatidylinositol 3-Kinase AKT pathway in human cancer. *Nature reviews. Cancer* **2**, 489-501, doi:10.1038/nrc839 (2002).

129   Singh, A. M. *et al.* Signaling network crosstalk in human pluripotent cells: a Smad2/3-regulated switch that controls the balance between self-renewal and differentiation. *Cell stem cell* **10**, 312-326, doi:10.1016/j.stem.2012.01.014 (2012).

130   Nichols, J. *et al.* Formation of pluripotent stem cells in the mammalian embryo depends on the POU transcription factor Oct4. *Cell* **95**, 379-391 (1998).

131   Rosner, M. H. *et al.* A POU-domain transcription factor in early stem cells and germ cells of the mammalian embryo. *Nature* **345**, 686-692, doi:10.1038/345686a0 (1990).

132   Reubinoff, B. E., Pera, M. F., Fong, C. Y., Trounson, A. & Bongso, A. Embryonic stem cell lines from human blastocysts: somatic differentiation in vitro. *Nature biotechnology* **18**, 399-404, doi:10.1038/74447 (2000).

133   Hay, D. C., Sutherland, L., Clark, J. & Burdon, T. Oct-4 knockdown induces similar patterns of endoderm and trophoblast differentiation markers in human and mouse embryonic stem cells. *Stem Cells* **22**, 225-235, doi:10.1634/stemcells.22-2-225 (2004).

134   Matin, M. M. *et al.* Specific knockdown of Oct4 and beta2-microglobulin expression by RNA interference in human embryonic stem cells and embryonic carcinoma cells. *Stem Cells* **22**, 659-668, doi:10.1634/stemcells.22-5-659 (2004).

135   Yeom, Y. I. *et al.* Germline regulatory element of Oct-4 specific for the totipotent cycle of embryonal cells. *Development* **122**, 881-894 (1996).

136   Niwa, H. Molecular mechanism to maintain stem cell renewal of ES cells. *Cell structure and function* **26**, 137-148 (2001).

137   Nishimoto, M., Fukushima, A., Okuda, A. & Muramatsu, M. The gene for the embryonic stem cell coactivator UTF1 carries a regulatory element which selectively interacts with a complex composed of Oct-3/4 and Sox-2. *Molecular and cellular biology* **19**, 5453-5465 (1999).

138   Tomioka, M. *et al.* Identification of Sox-2 regulatory region which is under the control of Oct-3/4-Sox-2 complex. *Nucleic acids research* **30**, 3202-3213 (2002).

139   Li, M., Pevny, L., Lovell-Badge, R. & Smith, A. Generation of purified neural precursors from embryonic stem cells by lineage selection. *Current biology : CB* **8**, 971-974 (1998).

140   Avilion, A. A. *et al.* Multipotent cell lineages in early mouse development depend on SOX2 function. *Genes & development* **17**, 126-140, doi:10.1101/gad.224503 (2003).

141   Okumura-Nakanishi, S., Saito, M., Niwa, H. & Ishikawa, F. Oct-3/4 and Sox2 regulate Oct-3/4 gene in embryonic stem cells. *The Journal of biological chemistry* **280**, 5307-5317, doi:10.1074/jbc.M410015200 (2005).

142   Rodda, D. J. *et al.* Transcriptional regulation of nanog by OCT4 and SOX2. *The Journal of biological chemistry* **280**, 24731-24737, doi:10.1074/jbc.M502573200 (2005).

143   Kuroda, T. *et al.* Octamer and Sox elements are required for transcriptional cis regulation of Nanog gene expression. *Molecular and cellular biology* **25**, 2475-2485, doi:10.1128/MCB.25.6.2475-2485.2005 (2005).

144   Chambers, I. *et al.* Functional expression cloning of Nanog, a pluripotency sustaining factor in embryonic stem cells. *Cell* **113**, 643-655 (2003).

145   Mitsui, K. *et al.* The homeoprotein Nanog is required for maintenance of pluripotency in mouse epiblast and ES cells. *Cell* **113**, 631-642 (2003).

146   Darr, H., Mayshar, Y. & Benvenisty, N. Overexpression of NANOG in human ES cells enables feeder-free growth while inducing primitive ectoderm features. *Development* **133**, 1193-1201, doi:10.1242/dev.02286 (2006).

147   Babaie, Y. *et al.* Analysis of Oct4-dependent transcriptional networks regulating self-renewal and pluripotency in human embryonic stem cells. *Stem Cells* **25**, 500-510, doi:10.1634/stemcells.2006-0426 (2007).

148   Adachi, K., Suemori, H., Yasuda, S. Y., Nakatsuji, N. & Kawase, E. Role of SOX2 in maintaining pluripotency of human embryonic stem cells. *Genes to cells : devoted to*

molecular & cellular mechanisms **15**, 455-470, doi:10.1111/j.1365-2443.2010.01400.x (2010).

149   Wang, Z., Oron, E., Nelson, B., Razis, S. & Ivanova, N. Distinct lineage specification roles for NANOG, OCT4, and SOX2 in human embryonic stem cells. *Cell stem cell* **10**, 440-454, doi:10.1016/j.stem.2012.02.016 (2012).

150   Kim, J., Chu, J., Shen, X., Wang, J. & Orkin, S. H. An extended transcriptional network for pluripotency of embryonic stem cells. *Cell* **132**, 1049-1061, doi:10.1016/j.cell.2008.02.039 (2008).

151   Orkin, S. H. *et al.* The transcriptional network controlling pluripotency in ES cells. *Cold Spring Harbor symposia on quantitative biology* **73**, 195-202, doi:10.1101/sqb.2008.72.001 (2008).

152   Momcilovic, O., Navara, C. & Schatten, G. Cell cycle adaptations and maintenance of genomic integrity in embryonic stem cells and induced pluripotent stem cells. *Results and problems in cell differentiation* **53**, 415-458, doi:10.1007/978-3-642-19065-0_18 (2011).

153   Edgar, B. A. & Lehner, C. F. Developmental control of cell cycle regulators: a fly's perspective. *Science* **274**, 1646-1652 (1996).

154   Abubakar, M. B., Abdullah, W. Z., Sulaiman, S. A. & Suen, A. B. A review of molecular mechanisms of the anti-leukemic effects of phenolic compounds in honey. *International journal of molecular sciences* **13**, 15054-15073, doi:10.3390/ijms131115054 (2012).

155   Swali, A. *et al.* Cell cycle regulation and cytoskeletal remodelling are critical processes in the nutritional programming of embryonic development. *PloS one* **6**, e23189, doi:10.1371/journal.pone.0023189 (2011).

156   Aleem, E., Kiyokawa, H. & Kaldis, P. Cdc2-cyclin E complexes regulate the G1/S phase transition. *Nature cell biology* **7**, 831-836, doi:10.1038/ncb1284 (2005).

157   Stein, G. S. *et al.* An architectural perspective of cell-cycle control at the G1/S phase cell-cycle transition. *Journal of cellular physiology* **209**, 706-710, doi:10.1002/jcp.20843 (2006).

158   Branzei, D. & Foiani, M. The DNA damage response during DNA replication. *Curr Opin Cell Biol* **17**, 568-575, doi:10.1016/j.ceb.2005.09.003 (2005).

159   Avni, D. *et al.* Active localization of the retinoblastoma protein in chromatin and its response to S phase DNA damage. *Molecular cell* **12**, 735-746 (2003).

160   Kieserman, E. K. & Heald, R. Mitotic chromosome size scaling in Xenopus. *Cell Cycle* **10**, 3863-3870, doi:10.4161/cc.10.22.17975 (2011).

161   Liskay, R. M. & Meiss, H. K. Complementation between two temperature-sensitive mammalian cell mutants, each defective in the G1 phase of the cell cycle. *Somatic cell genetics* **3**, 343-347 (1977).

162   Hermeking, H. *et al.* 14-3-3 sigma is a p53-regulated inhibitor of G2/M progression. *Molecular cell* **1**, 3-11 (1997).

163   Chae, H. D., Yun, J., Bang, Y. J. & Shin, D. Y. Cdk2-dependent phosphorylation of the NF-Y transcription factor is essential for the expression of the cell cycle-regulatory genes and cell cycle G1/S and G2/M transitions. *Oncogene* **23**, 4084-4088, doi:10.1038/sj.onc.1207482 (2004).

164   Bravo, R., Fey, S. J., Bellatin, J., Larsen, P. M. & Celis, J. E. Identification of a nuclear polypeptide ("cyclin") whose relative proportion is sensitive to changes in the rate of cell proliferation and to transformation. *Progress in clinical and biological research* **85 Pt A**, 235-248 (1982).

165   Woodbury, E. L. & Morgan, D. O. Cdk and APC activities limit the spindle-stabilizing function of Fin1 to anaphase. *Nature cell biology* **9**, 106-112, doi:10.1038/ncb1523 (2007).

166   Falck, J., Mailand, N., Syljuasen, R. G., Bartek, J. & Lukas, J. The ATM-Chk2-Cdc25A checkpoint pathway guards against radioresistant DNA synthesis. *Nature* **410**, 842-847, doi:10.1038/35071124 (2001).

167   Ma, Y., Pannicke, U., Schwarz, K. & Lieber, M. R. Hairpin opening and overhang processing by an Artemis/DNA-dependent protein kinase complex in nonhomologous end joining and V(D)J recombination. *Cell* **108**, 781-794 (2002).

168   Ohtsubo, M. & Roberts, J. M. Cyclin-dependent regulation of G1 in mammalian fibroblasts. *Science* **259**, 1908-1912 (1993).

169   Savatier, P., Huang, S., Szekely, L., Wiman, K. G. & Samarut, J. Contrasting patterns of retinoblastoma protein expression in mouse embryonic stem cells and embryonic fibroblasts. *Oncogene* **9**, 809-818 (1994).

170   Hoffmann, I., Clarke, P. R., Marcote, M. J., Karsenti, E. & Draetta, G. Phosphorylation and activation of human cdc25-C by cdc2--cyclin B and its involvement in the self-amplification of MPF at mitosis. *The EMBO journal* **12**, 53-63 (1993).

171   Neganova, I. & Lako, M. G1 to S phase cell cycle transition in somatic and embryonic stem cells. *Journal of anatomy* **213**, 30-44, doi:10.1111/j.1469-7580.2008.00931.x (2008).

172   Lange, C. & Calegari, F. Cdks and cyclins link G1 length and differentiation of embryonic, neural and hematopoietic stem cells. *Cell Cycle* **9**, 1893-1900 (2010).

173   Becker, S., de Angelis, M. H. & Beckers, J. Use of chemical mutagenesis in mouse embryonic stem cells. *Methods Mol Biol* **329**, 397-407, doi:10.1385/1-59745-037-5:397 (2006).

174   Gostjeva, E. V. *et al.* Metakaryotic stem cell lineages in organogenesis of humans and other metazoans. *Organogenesis* **5**, 191-200 (2009).

175   Calegari, F. & Huttner, W. B. An inhibition of cyclin-dependent kinases that lengthens, but does not arrest, neuroepithelial cell cycle induces premature neurogenesis. *Journal of cell science* **116**, 4947-4955, doi:10.1242/jcs.00825 (2003).

176   Kozar, K. *et al.* Mouse development and cell proliferation in the absence of D-cyclins. *Cell* **118**, 477-491, doi:10.1016/j.cell.2004.07.025 (2004).

177   Coronado, D. *et al.* A short G1 phase is an intrinsic determinant of naive embryonic stem cell pluripotency. *Stem Cell Res* **10**, 118-131, doi:10.1016/j.scr.2012.10.004 (2013).

178   Pauklin, S. & Vallier, L. The cell-cycle state of stem cells determines cell fate propensity. *Cell* **155**, 135-147, doi:10.1016/j.cell.2013.08.031 (2013).

179   White, J. *et al.* Developmental activation of the Rb-E2F pathway and establishment of cell cycle-regulated cyclin-dependent kinase activity during embryonic stem cell differentiation. *Molecular biology of the cell* **16**, 2018-2027, doi:10.1091/mbc.E04-12-1056 (2005).

180   Pardee, A. B. A restriction point for control of normal animal cell proliferation. *Proceedings of the National Academy of Sciences of the United States of America* **71**, 1286-1290 (1974).

181   Macleod, K. F. *et al.* p53-dependent and independent expression of p21 during cell growth, differentiation, and DNA damage. *Genes & development* **9**, 935-944 (1995).

182   Cartwright, P. *et al.* LIF/STAT3 controls ES cell self-renewal and pluripotency by a Myc-dependent mechanism. *Development* **132**, 885-896, doi:10.1242/dev.01670 (2005).

183   Collado, M., Blasco, M. A. & Serrano, M. Cellular senescence in cancer and aging. *Cell* **130**, 223-233, doi:10.1016/j.cell.2007.07.003 (2007).

184   Toledo, F. & Wahl, G. M. MDM2 and MDM4: p53 regulators as targets in anticancer therapy. *The international journal of biochemistry & cell biology* **39**, 1476-1482, doi:10.1016/j.biocel.2007.03.022 (2007).

185   Stead, E. *et al.* Pluripotent cell division cycles are driven by ectopic Cdk2, cyclin A/E and E2F activities. *Oncogene* **21**, 8320-8333, doi:10.1038/sj.onc.1206015 (2002).

186   Savatier, P., Lapillonne, H., van Grunsven, L. A., Rudkin, B. B. & Samarut, J. Withdrawal of differentiation inhibitory activity/leukemia inhibitory factor up-regulates D-type cyclins and cyclin-dependent kinase inhibitors in mouse embryonic stem cells. *Oncogene* **12**, 309-322 (1996).

187   Becker, K. A. *et al.* Self-renewal of human embryonic stem cells is supported by a shortened G1 cell cycle phase. *Journal of cellular physiology* **209**, 883-893, doi:10.1002/jcp.20776 (2006).

188   Goodhead, D. T. The initial physical damage produced by ionizing radiations. *International journal of radiation biology* **56**, 623-634 (1989).

189   Hutchinson, F. Chemical changes induced in DNA by ionizing radiation. *Progress in nucleic acid research and molecular biology* **32**, 115-154 (1985).

190   Abraham, R. T. Cell cycle checkpoint signaling through the ATM and ATR kinases. *Genes & development* **15**, 2177-2196, doi:Doi 10.1101/Gad.914401 (2001).

191   Bakkenist, C. J. & Kastan, M. B. DNA damage activates ATM through intermolecular autophosphorylation and dimer dissociation. *Nature* **421**, 499-506, doi:10.1038/nature01368 (2003).

192   Kitagawa, R. & Rose, A. M. Components of the spindle-assembly checkpoint are essential in Caenorhabditis elegans. *Nature cell biology* **1**, 514-521, doi:10.1038/70309 (1999).

193   Tibbetts, R. S. *et al.* A role for ATR in the DNA damage-induced phosphorylation of p53. *Genes & development* **13**, 152-157 (1999).

194   Serrano, M., Lin, A. W., McCurrach, M. E., Beach, D. & Lowe, S. W. Oncogenic ras provokes premature cell senescence associated with accumulation of p53 and p16INK4a. *Cell* **88**, 593-602 (1997).

195   Sharpless, N. E. INK4a/ARF: a multifunctional tumor suppressor locus. *Mutation research* **576**, 22-38, doi:10.1016/j.mrfmmm.2004.08.021 (2005).

196   Acquaviva, C. & Pines, J. The anaphase-promoting complex/cyclosome: APC/C. *Journal of cell science* **119**, 2401-2404, doi:10.1242/jcs.02937 (2006).

197   el-Deiry, W. S. *et al.* WAF1, a potential mediator of p53 tumor suppression. *Cell* **75**, 817-825 (1993).

198   Momcilovic, O. *et al.* Ionizing radiation induces ataxia telangiectasia mutated-dependent checkpoint signaling and G(2) but not G(1) cell cycle arrest in pluripotent human embryonic stem cells. *Stem Cells* **27**, 1822-1835, doi:10.1002/stem.123 (2009).

199   Fluckiger, A. C. *et al.* Cell cycle features of primate embryonic stem cells. *Stem Cells* **24**, 547-556, doi:10.1634/stemcells.2005-0194 (2006).

200   Hong, Y. & Stambrook, P. J. Restoration of an absent G1 arrest and protection from apoptosis in embryonic stem cells after ionizing radiation. *Proceedings of the National Academy of Sciences of the United States of America* **101**, 14443-14448, doi:10.1073/pnas.0401346101 (2004).

201   Chuykin, I. A., Lianguzova, M. S., Pospelova, T. V. & Pospelov, V. A. Activation of DNA damage response signaling in mouse embryonic stem cells. *Cell Cycle* **7**, 2922-2928 (2008).

202   Barta, T. *et al.* Human embryonic stem cells are capable of executing G1/S checkpoint activation. *Stem Cells* **28**, 1143-1152, doi:10.1002/stem.451 (2010).

203   Neganova, I. *et al.* An important role for CDK2 in G1 to S checkpoint activation and DNA damage response in human embryonic stem cells. *Stem Cells* **29**, 651-659, doi:10.1002/stem.620 (2011).

204   Ruiz, S. *et al.* A high proliferation rate is required for cell reprogramming and maintenance of human embryonic stem cell identity. *Current biology : CB* **21**, 45-52, doi:10.1016/j.cub.2010.11.049 (2011).

205   Van Hoof, D. *et al.* Phosphorylation dynamics during early differentiation of human embryonic stem cells. *Cell stem cell* **5**, 214-226, doi:10.1016/j.stem.2009.05.021 (2009).

206   Maimets, T., Neganova, I., Armstrong, L. & Lako, M. Activation of p53 by nutlin leads to rapid differentiation of human embryonic stem cells. *Oncogene* **27**, 5277-5287, doi:10.1038/onc.2008.166 (2008).

207   Menchon, C., Edel, M. J. & Izpisua Belmonte, J. C. The cell cycle inhibitor p27Kip(1) controls self-renewal and pluripotency of human embryonic stem cells by regulating the cell cycle, Brachyury and Twist. *Cell Cycle* **10**, 1435-1447 (2011).

208   Zhang, X. *et al.* A role for NANOG in G1 to S transition in human embryonic stem cells through direct binding of CDK6 and CDC25A. *The Journal of cell biology* **184**, 67-82, doi:10.1083/jcb.200801009 (2009).

209   Yang, V. S. *et al.* Geminin escapes degradation in G1 of mouse pluripotent cells and mediates the expression of Oct4, Sox2, and Nanog. *Current biology : CB* **21**, 692-699, doi:10.1016/j.cub.2011.03.026 (2011).

210   Card, D. A. *et al.* Oct4/Sox2-regulated miR-302 targets cyclin D1 in human embryonic stem cells. *Molecular and cellular biology* **28**, 6426-6438, doi:10.1128/MCB.00359-08 (2008).

211   Liu, H. *et al.* Oct4 regulates the miR-302 cluster in P19 mouse embryonic carcinoma cells. *Molecular biology reports* **38**, 2155-2160, doi:10.1007/s11033-010-0343-4 (2011).

212   Wang, Q. *et al.* miR-17-92 cluster accelerates adipocyte differentiation by negatively regulating tumor-suppressor Rb2/p130. *Proceedings of the National Academy of Sciences of the United States of America* **105**, 2889-2894, doi:10.1073/pnas.0800178105 (2008).

213   Melton, C., Judson, R. L. & Blelloch, R. Opposing microRNA families regulate self-renewal in mouse embryonic stem cells. *Nature* **463**, 621-626, doi:10.1038/nature08725 (2010).

214   Smith, K. N., Singh, A. M. & Dalton, S. Myc represses primitive endoderm differentiation in pluripotent stem cells. *Cell stem cell* **7**, 343-354, doi:10.1016/j.stem.2010.06.023 (2010).

215   Hindley, C. & Philpott, A. The cell cycle and pluripotency. *The Biochemical journal* **451**, 135-143, doi:10.1042/BJ20121627 (2013).

216   Ganier, O. *et al.* Synergic reprogramming of mammalian cells by combined exposure to mitotic Xenopus egg extracts and transcription factors. *Proceedings of the National Academy of Sciences of the United States of America* **108**, 17331-17336, doi:10.1073/pnas.1100733108 (2011).

217   Li, H. *et al.* The Ink4/Arf locus is a barrier for iPS cell reprogramming. *Nature* **460**, 1136-1139, doi:10.1038/nature08290 (2009).

218   Kawamura, T. *et al.* Linking the p53 tumour suppressor pathway to somatic cell reprogramming. *Nature* **460**, 1140-1144, doi:10.1038/nature08311 (2009).

219   Subramanyam, D. *et al.* Multiple targets of miR-302 and miR-372 promote reprogramming of human fibroblasts to induced pluripotent stem cells. *Nature biotechnology* **29**, 443-448, doi:10.1038/nbt.1862 (2011).

220   Lee, R. C., Feinbaum, R. L. & Ambros, V. The C. elegans heterochronic gene lin-4 encodes small RNAs with antisense complementarity to lin-14. *Cell* **75**, 843-854 (1993).

221   Creighton, C. J. *et al.* Discovery of novel microRNAs in female reproductive tract using next generation sequencing. *PloS one* **5**, e9637, doi:10.1371/journal.pone.0009637 (2010).

222   Rodriguez, A., Griffiths-Jones, S., Ashurst, J. L. & Bradley, A. Identification of mammalian microRNA host genes and transcription units. *Genome research* **14**, 1902-1910, doi:10.1101/gr.2722704 (2004).

223   Baskerville, S. & Bartel, D. P. Microarray profiling of microRNAs reveals frequent coexpression with neighboring miRNAs and host genes. *RNA* **11**, 241-247, doi:10.1261/rna.7240905 (2005).

224   Wienholds, E. *et al.* MicroRNA expression in zebrafish embryonic development. *Science* **309**, 310-311, doi:10.1126/science.1114519 (2005).

225   Cai, X., Hagedorn, C. H. & Cullen, B. R. Human microRNAs are processed from capped, polyadenylated transcripts that can also function as mRNAs. *RNA* **10**, 1957-1966, doi:10.1261/rna.7135204 (2004).

226   Gregory, R. I. *et al.* The Microprocessor complex mediates the genesis of microRNAs. *Nature* **432**, 235-240, doi:10.1038/nature03120 (2004).

227   Han, J. *et al.* The Drosha-DGCR8 complex in primary microRNA processing. *Genes & development* **18**, 3016-3027, doi:10.1101/gad.1262504 (2004).

228   Han, J. *et al.* Molecular basis for the recognition of primary microRNAs by the Drosha-DGCR8 complex. *Cell* **125**, 887-901, doi:10.1016/j.cell.2006.03.043 (2006).

229   Bohnsack, M. T., Czaplinski, K. & Gorlich, D. Exportin 5 is a RanGTP-dependent dsRNA-binding protein that mediates nuclear export of pre-miRNAs. *RNA* **10**, 185-191 (2004).

230   Lund, E., Guttinger, S., Calado, A., Dahlberg, J. E. & Kutay, U. Nuclear export of microRNA precursors. *Science* **303**, 95-98, doi:10.1126/science.1090599 (2004).

231   Yi, R., Qin, Y., Macara, I. G. & Cullen, B. R. Exportin-5 mediates the nuclear export of pre-microRNAs and short hairpin RNAs. *Genes & development* **17**, 3011-3016, doi:10.1101/gad.1158803 (2003).

232   Hutvagner, G. *et al.* A cellular function for the RNA-interference enzyme Dicer in the maturation of the let-7 small temporal RNA. *Science* **293**, 834-838, doi:10.1126/science.1062961 (2001).

233   Bartel, D. P. MicroRNAs: target recognition and regulatory functions. *Cell* **136**, 215-233, doi:10.1016/j.cell.2009.01.002 (2009).

234   Winter, J., Jung, S., Keller, S., Gregory, R. I. & Diederichs, S. Many roads to maturity: microRNA biogenesis pathways and their regulation. *Nature cell biology* **11**, 228-234, doi:10.1038/ncb0309-228 (2009).

235   Wu, L., Fan, J. & Belasco, J. G. MicroRNAs direct rapid deadenylation of mRNA. *Proceedings of the National Academy of Sciences of the United States of America* **103**, 4034-4039, doi:10.1073/pnas.0510928103 (2006).

236   Eulalio, A. *et al.* Deadenylation is a widespread effect of miRNA regulation. *RNA* **15**, 21-32, doi:10.1261/rna.1399509 (2009).

237   Selbach, M. *et al.* Widespread changes in protein synthesis induced by microRNAs. *Nature* **455**, 58-63, doi:10.1038/nature07228 (2008).

238   Chekulaeva, M., Filipowicz, W. & Parker, R. Multiple independent domains of dGW182 function in miRNA-mediated repression in Drosophila. *RNA* **15**, 794-803, doi:10.1261/rna.1364909 (2009).

239   Place, R. F., Li, L. C., Pookot, D., Noonan, E. J. & Dahiya, R. MicroRNA-373 induces expression of genes with complementary promoter sequences. *Proceedings of the National Academy of Sciences of the United States of America* **105**, 1608-1613, doi:10.1073/pnas.0707594105 (2008).

240   Bartel, D. P. MicroRNAs: genomics, biogenesis, mechanism, and function. *Cell* **116**, 281-297 (2004).

241   Pritchard, C. C., Cheng, H. H. & Tewari, M. MicroRNA profiling: approaches and considerations. *Nature reviews. Genetics* **13**, 358-369, doi:10.1038/nrg3198 (2012).

242   Poy, M. N. *et al.* A pancreatic islet-specific microRNA regulates insulin secretion. *Nature* **432**, 226-230, doi:10.1038/nature03076 (2004).

243   Greco, S. J. & Rameshwar, P. MicroRNAs regulate synthesis of the neurotransmitter substance P in human mesenchymal stem cell-derived neuronal cells. *Proceedings of the National Academy of Sciences of the United States of America* **104**, 15484-15489, doi:10.1073/pnas.0703037104 (2007).

244   O'Connell, R. M., Rao, D. S., Chaudhuri, A. A. & Baltimore, D. Physiological and pathological roles for microRNAs in the immune system. *Nature reviews. Immunology* **10**, 111-122, doi:10.1038/nri2708 (2010).

245   Cheng, H. Y. *et al.* microRNA modulation of circadian-clock period and entrainment. *Neuron* **54**, 813-829, doi:10.1016/j.neuron.2007.05.017 (2007).

246   Jopling, C. L., Yi, M., Lancaster, A. M., Lemon, S. M. & Sarnow, P. Modulation of hepatitis C virus RNA abundance by a liver-specific MicroRNA. *Science* **309**, 1577-1581, doi:10.1126/science.1113329 (2005).

247   Lee, Y. S. & Dutta, A. MicroRNAs in cancer. *Annual review of pathology* **4**, 199-227, doi:10.1146/annurev.pathol.4.110807.092222 (2009).

248   Di Leva, G. & Croce, C. M. Roles of small RNAs in tumor formation. *Trends in molecular medicine* **16**, 257-267, doi:10.1016/j.molmed.2010.04.001 (2010).

249   Wienholds, E. & Plasterk, R. H. MicroRNA function in animal development. *FEBS letters* **579**, 5911-5922, doi:10.1016/j.febslet.2005.07.070 (2005).

250   Fabbri, M. *et al.* Association of a microRNA/TP53 feedback circuitry with pathogenesis and outcome of B-cell chronic lymphocytic leukemia. *Jama* **305**, 59-67, doi:10.1001/jama.2010.1919 (2011).

251   Tsang, J. S., Ebert, M. S. & van Oudenaarden, A. Genome-wide dissection of microRNA functions and cotargeting networks using gene set signatures. *Molecular cell* **38**, 140-153, doi:10.1016/j.molcel.2010.03.007 (2010).

252   Stadler, B. *et al.* Characterization of microRNAs involved in embryonic stem cell states. *Stem cells and development* **19**, 935-950, doi:10.1089/scd.2009.0426 (2010).

253   Kanellopoulou, C. *et al.* Dicer-deficient mouse embryonic stem cells are defective in differentiation and centromeric silencing. *Genes & development* **19**, 489-501, doi:10.1101/gad.1248505 (2005).

254   Murchison, E. P., Partridge, J. F., Tam, O. H., Cheloufi, S. & Hannon, G. J. Characterization of Dicer-deficient murine embryonic stem cells. *Proceedings of the National Academy of Sciences of the United States of America* **102**, 12135-12140, doi:10.1073/pnas.0505479102 (2005).

255   Qi, J. *et al.* microRNAs regulate human embryonic stem cell division. *Cell Cycle* **8**, 3729-3741 (2009).

256   Wang, Y. *et al.* Embryonic stem cell-specific microRNAs regulate the G1-S transition and promote rapid proliferation. *Nature genetics* **40**, 1478-1483, doi:10.1038/ng.250 (2008).

257   Marson, A. *et al.* Connecting microRNA genes to the core transcriptional regulatory circuitry of embryonic stem cells. *Cell* **134**, 521-533, doi:10.1016/j.cell.2008.07.020 (2008).

258   Benetti, R. *et al.* A mammalian microRNA cluster controls DNA methylation and telomere recombination via Rbl2-dependent regulation of DNA methyltransferases. *Nature structural & molecular biology* **15**, 998, doi:10.1038/nsmb0908-998b (2008).

259   Suh, M. R. *et al.* Human embryonic stem cells express a unique set of microRNAs. *Developmental biology* **270**, 488-498, doi:10.1016/j.ydbio.2004.02.019 (2004).

260   Judson, R. L., Babiarz, J. E., Venere, M. & Blelloch, R. Embryonic stem cell-specific microRNAs promote induced pluripotency. *Nature biotechnology* **27**, 459-461, doi:10.1038/nbt.1535 (2009).

261   Miyoshi, N. *et al.* Reprogramming of mouse and human cells to pluripotency using mature microRNAs. *Cell stem cell* **8**, 633-638, doi:10.1016/j.stem.2011.05.001 (2011).

262   Yang, C. S., Li, Z. & Rana, T. M. microRNAs modulate iPS cell generation. *RNA* **17**, 1451-1460, doi:10.1261/rna.2664111 (2011).

263   Choi, Y. J. *et al.* miR-34 miRNAs provide a barrier for somatic cell reprogramming. *Nature cell biology* **13**, 1353-1360, doi:10.1038/ncb2366 (2011).

264   Ambasudhan, R. *et al.* Direct reprogramming of adult human fibroblasts to functional neurons under defined conditions. *Cell stem cell* **9**, 113-118, doi:10.1016/j.stem.2011.07.002 (2011).

265   Jayawardena, T. M. *et al.* MicroRNA-mediated in vitro and in vivo direct reprogramming of cardiac fibroblasts to cardiomyocytes. *Circulation research* **110**, 1465-1473, doi:10.1161/CIRCRESAHA.112.269035 (2012).

266   Ong, S. G., Lee, W. H., Kodo, K. & Wu, J. C. MicroRNA-mediated regulation of differentiation and trans-differentiation in stem cells. *Advanced drug delivery reviews* **88**, 3-15, doi:10.1016/j.addr.2015.04.004 (2015).

267 Tay, Y. M. *et al.* MicroRNA-134 modulates the differentiation of mouse embryonic stem cells, where it causes post-transcriptional attenuation of Nanog and LRH1. *Stem Cells* **26**, 17-29, doi:10.1634/stemcells.2007-0295 (2008).

268 Tay, Y., Zhang, J., Thomson, A. M., Lim, B. & Rigoutsos, I. MicroRNAs to Nanog, Oct4 and Sox2 coding regions modulate embryonic stem cell differentiation. *Nature* **455**, 1124-1128, doi:10.1038/nature07299 (2008).

269 Wellner, U. *et al.* The EMT-activator ZEB1 promotes tumorigenicity by repressing stemness-inhibiting microRNAs. *Nature cell biology* **11**, 1487-1495, doi:10.1038/ncb1998 (2009).

270 Xu, N., Papagiannakopoulos, T., Pan, G., Thomson, J. A. & Kosik, K. S. MicroRNA-145 regulates OCT4, SOX2, and KLF4 and represses pluripotency in human embryonic stem cells. *Cell* **137**, 647-658, doi:10.1016/j.cell.2009.02.038 (2009).

271 Worringer, K. A. *et al.* The let-7/LIN-41 pathway regulates reprogramming to human induced pluripotent stem cells by controlling expression of prodifferentiation genes. *Cell stem cell* **14**, 40-52, doi:10.1016/j.stem.2013.11.001 (2014).

272 Wang, Y. M., Medvid, R., Melton, C., Jaenisch, R. & Blelloch, R. DGCR8 is essential for microRNA biogenesis and silencing of embryonic stem cell self-renewal. *Nature genetics* **39**, 380-385, doi:10.1038/ng1969 (2007).

273 Miska, E. A. *et al.* Most Caenorhabditis elegans microRNAs are individually not essential for development or viability. *PLoS genetics* **3**, e215, doi:10.1371/journal.pgen.0030215 (2007).

274 Wang, Y. *et al.* miR-294/miR-302 promotes proliferation, suppresses G1-S restriction point, and inhibits ESC differentiation through separable mechanisms. *Cell reports* **4**, 99-109, doi:10.1016/j.celrep.2013.05.027 (2013).

275 Wang, Y. & Blelloch, R. Cell cycle regulation by MicroRNAs in embryonic stem cells. *Cancer research* **69**, 4093-4096, doi:10.1158/0008-5472.CAN-09-0309 (2009).

276 Lipchina, I. *et al.* Genome-wide identification of microRNA targets in human ES cells reveals a role for miR-302 in modulating BMP response. *Genes & development* **25**, 2173-2186, doi:10.1101/gad.17221311 (2011).

277 Qi, J. L. *et al.* microRNAs regulate human embryonic stem cell division. *Cell Cycle* **8**, 3729-3741 (2009).

278 Sengupta, S. *et al.* MicroRNA 92b controls the G1/S checkpoint gene p57 in human embryonic stem cells. *Stem Cells* **27**, 1524-1528, doi:10.1002/stem.84 (2009).

279 Jain, A. K. *et al.* p53 regulates cell cycle and microRNAs to promote differentiation of human embryonic stem cells. *PLoS biology* **10**, e1001268, doi:10.1371/journal.pbio.1001268 (2012).

280 Feng, Z., Zhang, C., Wu, R. & Hu, W. Tumor suppressor p53 meets microRNAs. *Journal of molecular cell biology* **3**, 44-50, doi:10.1093/jmcb/mjq040 (2011).

281 Holley, A. K., Dhar, S. K. & St Clair, D. K. Manganese superoxide dismutase versus p53: the mitochondrial center. *Annals of the New York Academy of Sciences* **1201**, 72-78, doi:10.1111/j.1749-6632.2010.05612.x (2010).

282   Hu, W. *et al.* Negative regulation of tumor suppressor p53 by microRNA miR-504. *Molecular cell* **38**, 689-699, doi:10.1016/j.molcel.2010.05.027 (2010).

283   Corney, D. C., Flesken-Nikitin, A., Godwin, A. K., Wang, W. & Nikitin, A. Y. MicroRNA-34b and MicroRNA-34c are targets of p53 and cooperate in control of cell proliferation and adhesion-independent growth. *Cancer research* **67**, 8433-8438, doi:10.1158/0008-5472.CAN-07-1585 (2007).

284   He, L. *et al.* A microRNA component of the p53 tumour suppressor network. *Nature* **447**, 1130-1134, doi:10.1038/nature05939 (2007).

285   Afanasyeva, E. A. *et al.* MicroRNA miR-885-5p targets CDK2 and MCM5, activates p53 and inhibits proliferation and survival. *Cell death and differentiation* **18**, 974-984, doi:10.1038/cdd.2010.164 (2011).

286   Xiao, J., Lin, H., Luo, X. & Wang, Z. miR-605 joins p53 network to form a p53:miR-605:Mdm2 positive feedback loop in response to stress. *The EMBO journal* **30**, 5021, doi:10.1038/emboj.2011.463 (2011).

287   Pichiorri, F. *et al.* Downregulation of p53-inducible microRNAs 192, 194, and 215 impairs the p53/MDM2 autoregulatory loop in multiple myeloma development. *Cancer cell* **18**, 367-381, doi:10.1016/j.ccr.2010.09.005 (2010).

288   Hunten, S., Siemens, H., Kaller, M. & Hermeking, H. The p53/microRNA network in cancer: experimental and bioinformatics approaches. *Advances in experimental medicine and biology* **774**, 77-101, doi:10.1007/978-94-007-5590-1_5 (2013).

289   Spagnoli, F. M. & Hemmati-Brivanlou, A. Guiding embryonic stem cells towards differentiation: lessons from molecular embryology. *Current opinion in genetics & development* **16**, 469-475, doi:10.1016/j.gde.2006.08.004 (2006).

290   Lin, S. L. *et al.* Regulation of somatic cell reprogramming through inducible mir-302 expression. *Nucleic acids research* **39**, 1054-1065, doi:10.1093/nar/gkq850 (2011).

291   Wang, J., Park, J. W., Drissi, H., Wang, X. & Xu, R. H. Epigenetic regulation of miR-302 by JMJD1C inhibits neural differentiation of human embryonic stem cells. *The Journal of biological chemistry* **289**, 2384-2395, doi:10.1074/jbc.M113.535799 (2014).

292   Zhang, Z. *et al.* Dissecting the roles of miR-302/367 cluster in cellular reprogramming using TALE-based repressor and TALEN. *Stem cell reports* **1**, 218-225, doi:10.1016/j.stemcr.2013.07.002 (2013).

293   Zhang, Z. *et al.* MicroRNA-302/367 cluster governs hESC self-renewal by dually regulating cell cycle and apoptosis pathways. *Stem cell reports* **4**, 645-657, doi:10.1016/j.stemcr.2015.02.009 (2015).

294   Bolstad, B. M., Irizarry, R. A., Astrand, M. & Speed, T. P. A comparison of normalization methods for high density oligonucleotide array data based on variance and bias. *Bioinformatics (Oxford, England)* **19**, 185-193 (2003).

295   Smyth, G. K. Linear models and empirical bayes methods for assessing differential expression in microarray experiments. *Statistical applications in genetics and molecular biology* **3**, Article3, doi:10.2202/1544-6115.1027 (2004).

296   Garcia, D. M. *et al.* Weak seed-pairing stability and high target-site abundance decrease the proficiency of lsy-6 and other microRNAs. *Nature structural & molecular biology* **18**, 1139-1146, doi:10.1038/nsmb.2115 (2011).

297   Friedman, R. C., Farh, K. K. H., Burge, C. B. & Bartel, D. P. Most mammalian mRNAs are conserved targets of microRNAs. *Genome research* **19**, 92-105, doi:10.1101/gr.082701.108 (2009).

298   Agarwal, V., Bell, G. W., Nam, J. W. & Bartel, D. P. Predicting effective microRNA target sites in mammalian mRNAs. *eLife* **4**, doi:10.7554/eLife.05005 (2015).

299   Li, S. S. *et al.* Target identification of microRNAs expressed highly in human embryonic stem cells. *Journal of cellular biochemistry* **106**, 1020-1030, doi:10.1002/jcb.22084 (2009).

300   Kuo, C. H., Deng, J. H., Deng, Q. & Ying, S. Y. A novel role of miR-302/367 in reprogramming. *Biochemical and biophysical research communications* **417**, 11-16, doi:10.1016/j.bbrc.2011.11.058 (2012).

301   Sokolov, M. V., Panyutin, I. V. & Neumann, R. D. Unraveling the global microRNAome responses to ionizing radiation in human embryonic stem cells. *PloS one* **7**, e31028, doi:10.1371/journal.pone.0031028 (2012).

302   Migliore, C. *et al.* MiR-1 downregulation cooperates with MACC1 in promoting MET overexpression in human colon cancer. *Clinical cancer research : an official journal of the American Association for Cancer Research* **18**, 737-747, doi:10.1158/1078-0432.CCR-11-1699 (2012).

303   Li, Y., Shelat, H. & Geng, Y. J. IGF-1 prevents oxidative stress induced-apoptosis in induced pluripotent stem cells which is mediated by microRNA-1. *Biochemical and biophysical research communications* **426**, 615-619, doi:10.1016/j.bbrc.2012.08.139 (2012).

304   Wu, C. D., Kuo, Y. S., Wu, H. C. & Lin, C. T. MicroRNA-1 induces apoptosis by targeting prothymosin alpha in nasopharyngeal carcinoma cells. *Journal of biomedical science* **18**, 80, doi:10.1186/1423-0127-18-80 (2011).

305   Xu, C. *et al.* The muscle-specific microRNAs miR-1 and miR-133 produce opposing effects on apoptosis by targeting HSP60, HSP70 and caspase-9 in cardiomyocytes. *Journal of cell science* **120**, 3045-3052, doi:10.1242/jcs.010728 (2007).

306   Xie, C. *et al.* MicroRNA-1 regulates smooth muscle cell differentiation by repressing Kruppel-like factor 4. *Stem cells and development* **20**, 205-210, doi:10.1089/scd.2010.0283 (2011).

307   Fleming, J. L. *et al.* Differential expression of miR-1, a putative tumor suppressing microRNA, in cancer resistant and cancer susceptible mice. *PeerJ* **1**, e68, doi:10.7717/peerj.68 (2013).

308   Qiu, C., Ma, Y., Wang, J., Peng, S. & Huang, Y. Lin28-mediated post-transcriptional regulation of Oct4 expression in human embryonic stem cells. *Nucleic acids research* **38**, 1240-1248, doi:10.1093/nar/gkp1071 (2010).

309   Pourebrahim, R. *et al.* Transcription factor Zic2 inhibits Wnt/beta-catenin protein signaling. *The Journal of biological chemistry* **286**, 37732-37740, doi:10.1074/jbc.M111.242826 (2011).

310   Wang, Z. & Roeder, R. G. Three human RNA polymerase III-specific subunits form a subcomplex with a selective function in specific transcription initiation. *Genes & development* **11**, 1315-1326 (1997).

311   Slattery, M. L. *et al.* MicroRNAs and colon and rectal cancer: differential expression by tumor location and subtype. *Genes, chromosomes & cancer* **50**, 196-206, doi:10.1002/gcc.20844 (2011).

312   Wang, H. L., Peng, W. J., Ouyang, X., Li, W. X. & Dai, Y. Circulating microRNAs as candidate biomarkers in patients with systemic lupus erythematosus. *Transl Res* **160**, 198-206, doi:10.1016/j.trsl.2012.04.002 (2012).

313   Ng, T. K. *et al.* Cigarette smoking hinders human periodontal ligament-derived stem cell proliferation, migration and differentiation potentials. *Scientific reports* **5**, 7828, doi:10.1038/srep07828 (2015).

314   Eastham, A. M. *et al.* Epithelial-mesenchymal transition events during human embryonic stem cell differentiation. *Cancer research* **67**, 11254-11262, doi:10.1158/0008-5472.CAN-07-2253 (2007).

315   Rosa, A. & Brivanlou, A. H. A regulatory circuitry comprised of miR-302 and the transcription factors OCT4 and NR2F2 regulates human embryonic stem cell differentiation. *The EMBO journal* **30**, 237-248, doi:10.1038/emboj.2010.319 (2011).

316   Ng, T. K. *et al.* Nicotine alters MicroRNA expression and hinders human adult stem cell regenerative potential. *Stem cells and development* **22**, 781-790, doi:10.1089/scd.2012.0434 (2013).

317   Gibon, E. *et al.* MC3T3-E1 osteoprogenitor cells systemically migrate to a bone defect and enhance bone healing. *Tissue engineering. Part A* **18**, 968-973, doi:10.1089/ten.TEA.2011.0545 (2012).

318   Zou, L. *et al.* Use of RUNX2 Expression to Identify Osteogenic Progenitor Cells Derived from Human Embryonic Stem Cells. *Stem cell reports* **4**, 190-198, doi:10.1016/j.stemcr.2015.01.008 (2015).

319   Basile, M. A. *et al.* Development of innovative biopolymers and related composites for bone tissue regeneration: study of their interaction with human osteoprogenitor cells. *Journal of applied biomaterials & functional materials* **10**, 210-214, doi:10.5301/JABFM.2012.10374 (2012).

320   Tandon, M., Chen, Z. J. & Pratap, J. Role of Runx2 in Crosstalk Between Mek/Erk and PI3K/Akt Signaling in MCF-10A Cells. *Journal of cellular biochemistry* **115**, 2208-2217, doi:10.1002/jcb.24939 (2014).

321   Mineno, J. *et al.* The expression profile of microRNAs in mouse embryos. *Nucleic acids research* **34**, 1765-1771, doi:10.1093/nar/gkl096 (2006).

322   Zhang, J. *et al.* Expression and potential role of microRNA-29b in mouse early embryo development. *Cellular physiology and biochemistry : international journal of*

experimental cellular physiology, biochemistry, and pharmacology **35**, 1178-1187, doi:10.1159/000373942 (2015).